2011-8

Mathematical Methods for Biosensor Models

Qi Wang
Technological University Dublin

Mathematical Methods for Biosensor Models

by

Qi Wang, B.Sc. M.Sc.

A thesis submitted for the degree of

Doctor of Philosophy (Ph.D.)

in the School of Mathematical Sciences,

Dublin Institute of Technology.

Supervisor: Dr. Dana Mackey

August 2011

Abstract

A biosensor is defined as a compact analytical device incorporating a biological sensing element integrated within a physico-chemical transducer whose aim is to produce optical or electronic signals proportional to the concentration of an analyte in a sample. Biosensors offer enormous potential to detect a wide range of analytes in health care, the food industry, environmental monitoring, security and defense. The beneficial impact on society as a result of the availability of such systems is immense, therefore investigating any strategy that could reduce development times and costs and reveal alternative designs is of utmost importance. In particular, mathematical modelling and simulation, the so-called "virtual experimentation", is a relatively inexpensive and yet powerful tool for scientific analysis and prediction.

Biosensor modelling is a rich source of mathematical challenges. The main components of biosensors are based on well-understood physical processes (such as diffusion, convective flow, energy and mass transfer) as well as chemical and biological reactions, all of which are amenable to mathematical modelling using ordinary and partial differential equations. The objective of this project is to provide a foundation for mathematical and computational modelling of biosensors, through identifying analytical and numerical methods applicable to the study of electrochemical and optical biosensors, with a view to optimising their design process. The models will be relevant to ongoing experimental work in the National Centre for Sensor Research (NCSR) and the Biomedical Diagnostics Institute (BDI) at Dublin City University.

Declaration

I certify that this thesis which I now submit for examination for the award of degree of Doctor of Philosophy (Ph.D.), is entirely my own work and has not been taken from the work of others, save and to the extent that such work has been cited and acknowledged within the text of my work.

This thesis was prepared according to the regulations for postgraduate study by research of the Dublin Institute of Technology and has not been submitted in whole or in part for another award in any other Institute.

The work reported on in this thesis conforms to the principles and requirements of the Institute's guidelines for ethics in research.

The Institute has permission to keep, lend or copy this thesis in whole or in part, on condition that any such use of the material of the thesis be duly acknowledged.

Signature: ..... Date: .....

Qi Wang

Acknowledgments

First and foremost, I would like to state my deepest gratitude to my supervisor Dr. Dana Mackey - thank you for your encouragement, guidance and support throughout my studies. I am grateful for the support of Head of School of Mathematical Sciences Dr. Chris Hills; Prof. Daphne Gilbert and Dr. Brendan Redmond. My sincere thanks to the Head of Department of Statistics and Commercial Mathematics, Ms. Maev Maguire, for her support, friendship and confidence in me over the past years - she is like family to me. I would also like to acknowledge the Irish Research Council for Science, Engineering and Technology (IRCSET), Dublin Institute of Technology and Mathematics Applications Consortium for Science and Industry (MACSI) for their financial support of my doctoral research.

Special thanks to my parents, Shuyun Yin and Changlai Wang, for their understanding and endless love. Most importantly, I thank Yupeng, for his eternal confidence and love.

Lastly, I thank all of those who supported me in any respect during the completion of my research.

Table of contents

Abstract **2**

Declaration **3**

Acknowledgments **4**

Table of contents **i**

Table of figures **iv**

1 Introduction and Background Material **1**

1.1 Why study biosensors? 1

1.1.1 Immunoassays 4

1.1.2 Enzyme biosensors 7

1.2 Elementary biochemistry concepts 11

1.2.1 Measuring concentrations 11

1.2.2 Basic chemical kinetics 12

1.3 Mathematical modelling 15

1.4 Outline of thesis 19

2 Enzyme-Substrate Kinetics: A Mathematical Analysis of The Michaelis-Menten Model **21**

2.1 Standard Michaelis-Menten kinetics 22

2.1.1 Introduction 22

2.1.2 Equilibrium and stability analysis 25

2.1.3 The quasi-steady-state approximation 29

2.1.4 Perturbation analysis 36

2.2 Reversible Michaelis-Menten kinetics 39

2.2.1 Equilibrium and stability analysis 40

2.2.2 Non-dimensional model and approximate values of the equilibrium solution 42

2.2.3 Boundary layer analysis 46

2.3 Cascade reactions 51

2.4 Summary 57

3 Modelling Antibody-Antigen Interactions **58**

3.1 The direct assay 58

3.1.1 Simplified model for the direct assay 59

3.1.2 Diffusion model for the direct assay 68

3.2 The competitive assay 77

3.2.1 Simplified model for the competitive assay 78

3.2.2 Diffusion model for the competitive assay 91

3.3 The sandwich assay 97

3.4 Summary 104

4 Mathematical Models for Optimising Bi-enzyme Biosensors 106

4.1 Experimental problem and modelling strategies 107

4.2 The comprehensive model 113

4.2.1 Review of the comprehensive model 113

4.2.2 Steady-state analysis 118

4.3 Simplified model 122

4.3.1 Formation of the model 122

4.3.2 Slow-fast dynamics 127

4.3.3 Slow invariant manifold 130

4.3.4 Dynamical systems analysis 134

4.3.5 Results 145

4.4 Intermediate model 147

4.5 Summary and comparisons 152

Conclusions and Future Work 157

Bibliography 161

A 167

Table of figures

1.1 Antibody structure. 5

1.2 Enzyme-substrate interactions. 9

2.1 Relative concentrations of reactants and product of the standard Michaelis-Menten kinetics. Typical values for constants used in this simulation are: $k_1 = 10^2\ m^3/mol \cdot s$, $k_{-1} = 10^{-1}\ m^3/mol \cdot s$, $k_2 = 10\ m^3/mol \cdot s$, $e_0 = 1\ mol/m^2$ and $s_0 = 1\ mol/m^3$. 26

2.2 Numerical solution of the Michaelis-Menten model (2.4) (continuous green line) versus the exact solution of the quasi-steady-state approximation of equation (2.21) (red points). 35

2.3 Relative concentrations of reactants and product of the reversible Michaelis-Menten kinetics. Typical values for constants used in this simulation are: $k_1 = 10^2\ m^3/mol \cdot s$, $k_{-1} = 10^{-1}\ m^3/mol \cdot s$, $k_2 = 10\ m^3/mol \cdot s$, $k_{-2} = 10^{-2}\ m^3/mol \cdot s$, $e_0 = 1\ mol/m^2$ and $s_0 = 1\ mol/m^3$. 41

2.4 Inner, outer and exact solution of reversible Michaelis-Menten kinetics. Typical values for constants used in this simulation are: $k_1 = 4 \times 10^2\ m^3/mol \cdot s$, $k_{-1} = 10\ m^3/mol \cdot s$, $k_2 = 3.2 \times 10^2\ m^3/mol \cdot s$, $k_{-2} = 75\ m^3/mol \cdot s$, $e_0 = 1\ mol/m^2$ and $s_0 = 1\ mol/m^3$. 52

2.5 Enzyme immobilisation. 54

2.6 Relative concentrations of reactants and product of the cascade reactions. Typical values for constants used in this simulation are: $k_1 = 10^2\ m^3/mol \cdot s$, $k_{-1} = 10^{-1}\ m^3/mol \cdot s$, $k_2 = 10\ m^3/mol \cdot s$, $k_3 = 10^2\ m^3/mol \cdot s$, $k_{-3} = 10^{-1}\ m^3/mol \cdot s$, $k_4 = 10\ m^3/mol \cdot s$, $e_0 = 1\ mol/m^2$ and $s_0 = 1\ mol/m^3$. 55

3.1 Antibody-antigen interactions. 59

3.2 Product concentration as a function of the initial (non-dimensional) antigen concentration ψ. Black curve correspond to the exact solution of c given by equation (3.8), red curves and the blue dot correspond to the approximate solution of c given by equations (3.18). Typical values for constants used in this simulation are: $b_0 = 2$, $k = 100$, $k_- = 8$ in (a) and $k_- = 0$ in (b). 67

3.3 Exact value (black) and asymptotic approximation (red) for the labelled product as functions of ψ in Case I. Typical values for constants used in this simulation are: $b_0 = 1$, $a_0^{'} = 1$, $k = 100$ and $k_- = 8$. . . . 90

3.4 Exact value (black) and asymptotic approximation (red) for the labelled product as functions of ψ in Case II. Typical values for constants used in this simulation are: $b_0 = 2$, $a_0^{'} = 1$, $k = 100$, $k_- = 8$ in (a) and $k_- = 0$ in (b). 91

3.5 Immunometric immunoassay. 98

3.6 Sandwich product c_2 (red), combined product $c_2 + d$ (blue), and unbound tracer b_2 (green) as functions of initial antigen concentration α. Typical values for constants used in this simulation are: $k_1 = 100$, $k_{-1} = 10$, $k_2 = 100$, $k_{-2} = 10$, $\beta_1 = 2$ and $\beta_2 = 2$. 102

4.1 Amperometric responses of a HRP/GOX bi-enzyme electrode to a range of glucose concentrations between 0.5 and 20 mM. 109

4.2 Comparison of HRP/GOX ratio and sensitivity to glucose. The electrode prepared immobilising HRP and GOX at the molar ratio 1:1 yields the highest catalytic signals and the highest sensitivity. The glucose concentration used in this experiment was 20 mM. 109

4.3 Dependence of current on ζ for different initial concentrations of s_1. The curves correspond to $s_0 = 1, 5, 10$ and 20 mM from bottom to top. The maximum value of current is indicated on each curve. 117

4.4 Dependence of current on ζ (electrode GOX:HRP ratio) for different k_4/k_2 values. The lower curve corresponds to $k_4/k_2 = 0.5$ and the upper curve corresponds to $k_4/k_2 = 8$. 118

4.5 Dependence of current on ζ as given by system (4.8). The curves correspond to $s_0 = 1, 5, 10$ and 20 mM from the bottom to top. Typical values for constants used in this simulation are: $k_1 = 10^2$, $k_{-1} = 10^{-1}$, $k_2 = 10$, $k_3 = 10^2$, $k_{-3} = 10^{-1}$, $k_4 = 10$, $e_0 = 10^{-5}$, $l = 2 \times 10^{-4}$, $D_1 = 6.7 \times 10^{-10}$ and $D_2 = 8.8 \times 10^{-10}$. 121

4.6 Dependence of current on ζ as given by system (4.8). The curves correspond to $k_4/k_2 = 0.2, 0.5, 1$ and 2 from the bottom to top. Typical values for constants used in this simulation are the same as in Figure 4.5. 121

4.7 Phase portrait of system (4.9) showing c_2 against s_2 in the cases of: (a) $\zeta < \zeta^*$, (b) $\zeta \geq \zeta^*$. 135

4.8 Dependence of current on ζ for different initial concentrations of s_0. The curves correspond to $s_0 = 0.03, 0.09, 0.2$ and 5 mM from the bottom to top. Typical values for constants used in this simulation are: $k_1 = 10^2$, $k_{-1} = 10^{-1}$, $k_2 = 10$ and $k_4 = 10$. 146

4.9 Dependence of current on ζ for different values of k_4/k_2. The curves correspond to $k_4/k_2 = 0.2, 0.5, 1$ and 2 from the bottom to top. Typical values for constants used in this simulation are the same as in Figure 4.8. 146

4.10 Dependence of current on ζ for different initial concentrations of s_0. The curves correspond to $s_0 = 0.03, 0.09, 0.2$ and 5 mM from the bottom to top. Typical values for constants used in this simulation are: $k_1 = 10^2$, $k_{-1} = 10^{-1}$, $k_2 = 10$, $k_3 = 10^2$, $k_{-3} = 10^{-1}$, $k_4 = 10$, $e_0 = 10^{-5}$, $l = 2 \times 10^{-4}$ and $D_1 = 6.7 \times 10^{-10}$. 151

4.11 Dependence of current on ζ for different values of k_4/k_2. The curves correspond to $k_4/k_2 = 0.2, 0.5, 1$ and 2 from the bottom to top. Typical values for constants used in this simulation are the same as in Figure 4.10. 151

4.12 Dependence of current on ζ for different initial concentrations of s_0. Steady-state analysis of (a) and (b) comprehensive model, (c) simplified model, and (d) intermediate model. 153

4.13 Dependence of current on ζ for different values of k_4/k_2. Steady-state analysis of (a) and (b) comprehensive model, (c) simplified model, and (d) intermediate model. 154

4.14 Dependence of optimal ratio (GOX:HRP) on s_0 (glucose concentration). (a) Steady-state analysis of intermediate model, (b) Numerical analysis of comprehensive model, (c) Steady-state analysis of comprehensive model, and (d) Steady-state analysis of simplified model. . . . 155

4.15 Dependence of optimal ratio (GOX:HRP) on k_4/k_2 ratio. (a) Steady-state analysis of intermediate model, (b) Numerical analysis of comprehensive model, (c) Steady-state analysis of comprehensive model, and (d) Steady-state analysis of simplified model. 156

Chapter 1

Introduction and Background Material

1.1 Why study biosensors?

Biosensor design underpins the development of a range of next-generation biomedical diagnostic tools which will directly affect the quality of life worldwide over the next few decades. The level of commercial development in this area is significant, with many international diagnostics companies wishing to develop point-of-care and at-home testing devices for many diseases and disorders. Other important applications of biosensors are in measuring water quality, detecting biological and chemical warfare agents or the presence of toxins or harmful microorganisms in food. The beneficial impact on society as a result of the availability of such systems to both personal health and environmental quality is immense. Therefore, investigating any strategy that could reduce development times and costs, reveal alternative system designs and

subsequently increase the rate at which new devices are brought to the market, is of utmost importance. In particular, mathematical modelling and simulation, the so-called "virtual experimentation" is a relatively inexpensive and yet powerful tool for scientific analysis and prediction.

Biosensors are analytical devices which convert biochemical reactions into measurable signals, using optical or electrical transducers. They involve a biological (recognition) element and a transduction element. The biological or recognition element may be an antibody, an enzyme, DNA, RNA, a whole cell, or a whole organ or system. The transduction element, wherein the biological event or signal is converted to a measurable signal, may include any one of the following forms: chemical, electrical, magnetic, mechanical, optical, or thermal. Biosensor performance parameters may be improved significantly by providing (a) the proper interface between the biological and the transduction element and (b) by manipulating the structure of the interface. One needs to combine these in an optimum manner to suit one's application so as to obtain, ideally a simple, rapid, and label-free application (refer to [1]).

For example, the first and still the most widely used commercial biosensor is the glucose biosensor which was developed by Leland C. Clark in 1962. The glucose biosensor uses an enzyme to break down blood glucose and transfer an electron to an electrode, which can be schematically represented as

$$\text{Glucose} + O_2 \xrightarrow{k_1} \text{gluconic acid} + H_2O_2,$$

$$H_2O_2 \longrightarrow O_2 + 2H^+ + 2e^-.$$

This is an example of an electrochemical biosensor.

Biosensor characteristics

Biosensors are usually characterised by the following parameters (refer to, for example [1]):

- **Sensitivity** is the response of the sensor to changes in analyte concentration.
- **Selectivity** is the ability of the sensor to respond only to the target analyte. That is, lack of response to other interfering chemicals is the desired feature.
- **Range** is the concentration range over which the sensitivity of the sensor is good. Sometimes this is called dynamic range or linearity.
- **Response time** is the time required for the sensor to indicate 63% of its final response due to a step change in analyte concentration.
- **Reproducibility** is the accuracy with which the sensor's output can be obtained.
- **Detection limit** is the lowest concentration of the analyte to which there is a measurable response.
- **Life time** is the time period over which the sensor can be used without significant deterioration in performance characteristics.
- **Stability** characterises the change in its baseline or sensitivity over a fixed period of time.

Biosensors can be broadly categorised as either bioaffinity devices (which are analysed in Chapter 3 of this thesis) or biocatalytic devices (considered in Chapter 2 and 4). In the bioaffinity devices, the analyte in the solution binds selectively to a receptor immobilised on the biosensor surface. In the biocatalytic devices, an enzyme immobilised on the biosensor surface catalyses the target substance (refer to [2]).

1.1.1 Immunoassays

An example of bioaffinity sensors is provided by **immunoassays**, which are a group of sensitive analytical tests that utilise very specific antibody-antigen complexes to produce a signal that can be measured and related to the concentration of a compound in solution (refer to [3]). Immunoassays also produce qualitative data in terms of the presence or absence of a compound in the body. An **antigen** is a substance with the ability to induce an immunological response, such as, for example, bacteria, viruses, allergens, etc. An **epitope**, or antigenic determinant, is the part of the antigen that is recognised by the immune system, specifically by antibodies (B-cells or T-cells). **Antibodies** are the soluble proteins that circulate freely and exhibit properties that contribute specifically to immunity and protection against foreign material (refer to [4]). The part of an antibody that recognises an epitope is called a **paratope**. Each antibody consists of four polypeptides - two heavy chains and two light chains joined to form a **Y** shaped molecule as shown in Figure 1.1. The amino acid sequence in the tips of the **Y** varies greatly among different antibodies and gives each antibody its specificity for binding antigen.

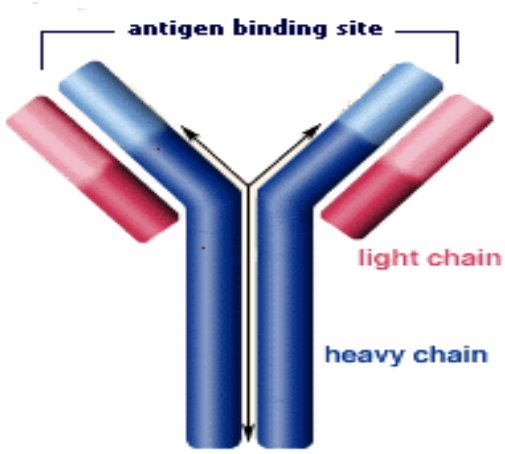

Figure 1.1 – Antibody structure.

The production of antibodies is an important process in the use of immunoassays because it is the antibody-antigen complexes that the device uses for its results. Immunoassays require the use of labelled materials in order to measure the amount of antigen or antibody present. A **label** is a molecule that will react as part of the assay, and in doing so produces a signal that can be measured in the solution. Examples of labels include radioactive compounds or enzymes that cause a change of colour in a solution or its fluorescence (refer to [3]).

The measurement of the analyte using labels is broadly categorised into **competitive** and **non-competitive** methods. In competitive formats, unlabelled analyte in the test sample is measured by its ability to compete with labelled antigen for a limited number of antibody binding sites (refer to [5]). The unlabelled antigen blocks the ability of the labelled antigen to bind because that binding site on the antibody

is already occupied. Thus, in a competitive immunoassay, less label measured in the assay means more of the unlabelled (test sample) antigen is present. The amount of antigen in the test sample is inversely related to the amount of label measured in the competitive format: i.e., as one increases, the other decreases. Competitive assays will be studied in Section 3.2 of this thesis. Non-competitive (sandwich) immunoassays generally provide the highest level of assay sensitivity and specificity. This format is referred to as a "sandwich" assay because the analyte is bound (sandwiched) between two highly specific antibody reagents. The reaction mixture typically includes an excess of labelled antibody, so that all drug/metabolite is bound. The amount of antibody-antigen complex is then measured to determine the amount of drug present in the sample. The measurement of labelled analyte, usually antibody, is directly proportional to the amount of antigen present in the sample. An analysis of simple non-competitive assays is given in Section 3.1 and sandwich assays in Section 3.3.

Results can be either **qualitative** (for example, the pregnancy test provides a "positive" or "negative" result), but most often, in mathematical modelling we will be concerned with **quantitative** results, which are provided as numerical results which give the compound concentration as a function of the (unlabelled) analyte in the sample taking into consideration the competitive/non-competitive nature of the device.

These results are compared with experimental measurements which are often presented in the form of **calibration curves** (also known as **dose-response** curves). A calibration curve is constructed by measuring and plotting the biosensor response

against a wide range of initial analyte concentrations and used for future estimations of the "dose" once the "response" is known.

In constructing mathematical models for antibody-antigen interactions, the following simplifying assumptions are usually made (refer to [3]):

- The antigen is present in a homogeneous form consisting of only one chemical species.
- The antibody should be homogeneous.
- The antigen possesses one epitope for binding.
- The antibody has a single binding site that recognises one epitope of the antigen with one affinity.
- Binding should be uniform with no positive or negative allosteric effects (the binding of one antibody binding site should not influence the binding of the other site).
- The separation of bound from free antigen must be complete.
- There should be no non-specific binding, such as to the walls of the reaction vessel.

1.1.2 Enzyme biosensors

Enzymes are biocatalysts that, like all other catalysts, greatly enhance the rate of specific chemical reactions, without being consumed in the process. These reactions

would still take place without enzymes - but it would take years rather than milliseconds! In the context of living organisms, enzymes perform a wide variety of vital functions. For example, in the digestive systems of animals, enzymes known as ***amylases*** and ***proteases*** break down large molecules (such as starch or proteins) into smaller ones (such as maltose or glucose) so they can be more easily absorbed by intestines.

Enzymes can often work together in a specific order creating so-called **metabolic pathways**, where one enzyme catalyses a substrate and then passes the product on to another enzyme for another catalytic reaction. A similar concept, the **cascade reaction** is studied in Section 2.3 and Chapter 4. An interesting example of a metabolic pathway in the human body is provided by alcohol metabolism. Most of the ethyl alcohol ingested by a person is oxidised to acetaldehyde (a highly toxic substance) by an enzyme called **alcohol dehydrogenase** (ADH). The product, acetaldehyde, is then catalysed by a second enzyme, acetaldehyde dehydrogenase, to acetic acid, which can then be more easily eliminated by the body. It has been conjectured that genetic factors that might speed up the first reaction or slow down the second, could make a person less likely to develop alcoholism since such factors would cause a large buildup of acetaldehyde and make drinking very uncomfortable.

An enzyme has a specific three-dimensional shape, it is a large molecule, usually much bigger than its corresponding binding substrate. Only a relatively small part of the enzyme called its **active site** actually comes into contact with the substrate. Part of the substrate fits into the active site and forms a temporary structure called

an **enzyme-substrate complex**. The substrate molecule is like the key that fits the enzyme's lock. The reaction takes place at the active site and this is where the products are formed. As the products have a different shape from the substrate, they no longer fit the active site and are repelled. The active site is then free to react with more substrates. The active site of the enzyme may not exactly correspond to the shape of the substrate, as the active site has a more flexible shape and therefore it is able to mould itself around the substrate. This mechanism is referred to the **induced fit theory** which is based on the lock and key theory shown in Figure 1.2. Refer to [6] and [7] for a detailed explanation of the lock and key model and the induced fit model.

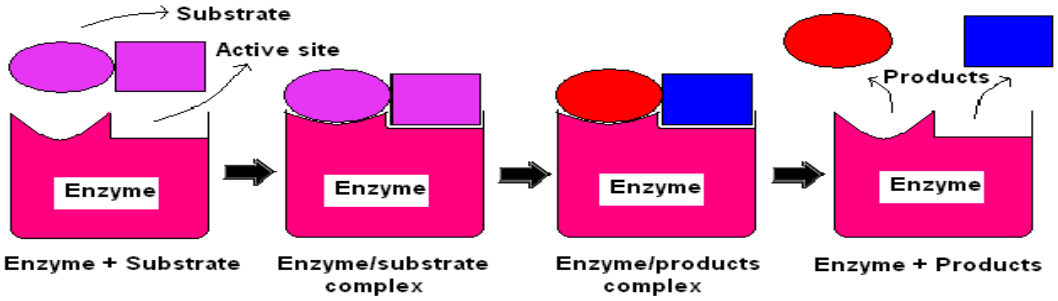

Figure 1.2 – Enzyme-substrate interactions.

An enzyme biosensor consists of an enzyme as a biological sensing element and a transducer, which may be amperometric, potentiometric, conductimetric, optical, calorimetric, etc. Enzyme biosensors have been applied to detecting various substrates, which are selectively oxidised or reduced in enzyme-catalysed processes depending on the nature of the substrates and enzymes used (oxidases or reductases) to

construct a sensor. Most enzyme biosensors modelled in this thesis use amperometric techniques (refer to [8]). Amperometry is the determination of the intensity of the current crossing an electrochemical cell under an imposed potential. This intensity is a function of the concentration of the electrochemically active species in the sample. Oxidation or reduction of a species is generally performed by a working electrode, and a second electrode acts as a reference. For example, a glucose-sensitive biosensor that uses glucose oxidase could detect either the H_2O_2 produced by the enzymatic reaction, or the amount of oxygen consumed during the oxidation of glucose (refer to [9]). For the repeated use of enzymes, cells, antibodies, and other biologically active agents in analytical devices, numerous techniques for fixing them to carrier materials have been developed. **Immobilisation**, particularly of enzymes, brings about a number of further advantages for their application in analytical chemistry:

1. In many cases the enzyme is stabilised.

2. The enzyme-carrier complex may be easily separated from the sample, i.e., the latter is not contaminated by the enzyme preparation.

3. The stable and largely constant enzyme activity renders the enzyme an integral part of the analytical instrument (refer to [10]).

A mathematical study of a biosensor employing two immobilised enzymes is presented in Chapter 4.

1.2 Elementary biochemistry concepts

1.2.1 Measuring concentrations

Any quantitative study of solutions requires that we know the amount of solute dissolved in a solvent or the concentration of the solution. Chemists employ several different concentration measures, each one having advantages and limitations. The use of the solution generally determines how we express its concentration. There are four concentration units defined: percent by weight, mole fraction, molarity, and molality. The concentration unit used in this thesis is molarity (M) (refer to [11]).

A **mole** is the amount of substance that contains as many atoms, molecules, ions, or any other entities as there are atoms in exactly 12g of carbon-12. It has been determined experimentally that the number of atoms per mole of carbon-12 is

$$N_A = 6.0221367 \times 10^{23}\ mol^{-1},$$

which is known as the **Avogadro constant**. The **molar mass** of a substance is the mass in grams or kilograms of one mole of the substance. In many calculations, molar masses are more conveniently expressed as kg mol^{-1} (refer to [11]).

Molar concentration or **molarity** is defined as the number of moles of solute dissolved in one litre (L) of solution; that is,

$$molarity = \frac{number\ of\ moles\ of\ solute}{L\ solution}$$

Thus, molarity has the units moles per litre ($mol\ L^{-1}$). By convention, we use square brackets [ ] to represent molarity. It is one of the most commonly employed concen-

tration measures. The advantage of using molarity is that it is generally easier to measure the volume of a solution using precisely calibrated volumetric flasks than to weigh the solvent. Its main drawback is that it is temperature dependent, because the volume of a solution usually increases with increasing temperature. Another drawback is that molarity does not tell one the amount of solvent present (refer to [11]).

A solution of concentration 1 mol/L is also denoted as 1 molar ($1M$). In numerical simulations throughout this thesis we often use the International System units of $moles/m^3$ and note that

$$1\ mol/m^3 = 10^{-3}\ M = 1\ mM.$$

1.2.2 Basic chemical kinetics

The **rate** of a reaction is expressed as the change in reactant concentration with time. Consider a simple reaction of

$$X \longrightarrow Y. \tag{1.1}$$

If we denote the concentrations of reactant X at time t_0 and t_1 by X_0 and X_1 respectively, then the rate of the reaction (1.1) over the time interval $t_1 - t_0$ can be expressed as

$$\frac{X_1 - X_0}{t_1 - t_0} = \frac{\Delta X}{\Delta t},$$

however, since $X_1 < X_0$, in order to keep the reaction rate as a positive quantity, we introduce a minus sign which gives

$$\text{rate of reaction} = -\frac{\Delta X}{\Delta t}.$$

The reaction rate can also be expressed in terms of the appearance of the product, Y, as

$$\text{rate of reaction} = \frac{Y_1 - Y_0}{t_1 - t_0} = \frac{\Delta Y}{\Delta t} = -\frac{\Delta X}{\Delta t}.$$

The rates of chemical reactions almost always obey the **Law of Mass Action**. Although the direct proportionality to concentration is sometimes modified, this law states that

The rate of reaction is directly proportional to the product of the concentrations of the reactants.

The proportionality constant is known as the rate constant for the reaction in question. For particular sorts of reaction this constant may be given a rather more descriptive name, for example, the association rate constant for a reaction involving association of two molecules, the dissociation rate constant for the reverse reaction. The rate constant is a measure of how fast a reaction takes place (for a specified concentration), or, more precisely, it indicates how frequently the reaction occurs (hence it has the units s^{-1}). At the level of single molecules the rate constant is a measure of the probability (per unit time) that the reaction will happen in the next time interval. Throughout this thesis it is assumed that rate "constants" are indeed constant in the sense that they change neither with time nor with reactant concentration. However, in practice, the value of a rate constant may depend on variables such as temperature, pressure, or electric field (e.g., on membrane potential) (refer to [12]).

In what follows, mathematical descriptions in the form of differential equations are given for the law of mass action in the context of several simple reactions.

First-order reactions

The simplest possible reaction involves the irreversible conversion of a substance X to Y as seen in (1.1). The law of mass action can be written as

$$\frac{dx}{dt} = -kx,$$

where k is the rate constant of the reaction, and x denotes the concentration of the reactant X. This is a first-order reaction since its rate only depends on the first power of the concentration. In reality, most reactions are not as simple as irreversible reactions since, with accumulation of product, the reverse reaction becomes important. These reactions are named reversible reactions, where the equilibrium does not lie far to one side. For example,

$$X \underset{k_{-1}}{\overset{k_1}{\rightleftarrows}} Y, \tag{1.2}$$

where k_{-1} is the dissociation rate constant of the reaction (1.2). It has the rate equation of

$$\frac{dx}{dt} = -k_1 x + k_{-1} y = -\frac{dy}{dt},$$

where y denotes the concentration of Y.

Second-order reactions

Many biochemical reactions are not of first-order, but are of second or higher order. Simple examples of second-order irreversible reactions are

$$2X \xrightarrow{k} Y$$

and

$$X + Y \xrightarrow{k} Z.$$

The rate of such reactions is proportional to the second power of the concentration, or product of concentrations, given by

$$\frac{dy}{dt} = -\frac{1}{2}\frac{dx}{dt} = kx^2$$

and

$$\frac{dz}{dt} = -\frac{dx}{dt} = -\frac{dy}{dt} = kxy$$

respectively, where z denotes the concentration of Z. Similarly, a simple example of second-order reversible reactions is

$$X + Y \underset{k_{-1}}{\overset{k_1}{\rightleftarrows}} Z,$$

which has the corresponding rate equation of

$$\frac{dz}{dt} = -\frac{dx}{dt} = -\frac{dy}{dt} = k_1xy - k_{-1}z.$$

Note that, reaction rates are expressed in mole/liter/second (Ms^{-1}). The first-order rate constants have the dimension of $time^{-1}$ (s^{-1}) and the second-order rate constants have the dimension of $concentration^{-1} \times time^{-1}$ ($M^{-1}s^{-1}$); zero-order rate constants have the dimension of $concentration \times time^{-1}$ (Ms^{-1}) (refer to [13]).

1.3 Mathematical modelling

A **mathematical model** of a physical law is a description of that law in the language of mathematics. Such models make it possible to use mathematical methods

to deduce results about the physical world that are not evident or have never been observed. For example, the possibility of placing a satellite in orbit around the Earth was deduced mathematically from Issac Newton's model of mechanics nearly 200 years before the launching of Sputnik, and Albert Einstein (1879-1955) gave a relativistic model of mechanics in 1915 that explained a precession in the perihelion of the planet Mercury that was not confirmed by physical measurement until 1967 (refer to [14]).

We often need to develop the quantitative context for a particular problem and it can involve the formation of a mathematical model. Mathematical models enable one to furnish an abstract analytical structure for a real world problem. This abstraction of the specific situation and a means to generalise to a broader range of problems. These models of reality constitute an important part of mathematical analysis. Thus, the development and application of mathematical models that reflect real world situations connects to various scientific areas. Analysis of real world problems often requires application of the relevant data to a mathematical model.

Mathematical modelling is a technique which builds on a firm understanding of the basic terminology, notation, and methodology of mathematics. It involves the following steps. First, the problem or objective of the study must be stated in a way that reflects accurately the needs of the organisation. The second step includes finding data relevant to the problem which can be applied to the model, and often includes the scaling of these measurements. This process often yields a more realistic model, the results of which are more easily comprehended. The third step in the modelling process is the development of a mathematical model that addresses the concerns

of the organisation. In developing the mathematical model, the primary goal is to provide a quantitative structure for analysing a large group of possible situations. Model formulation frequently includes the selection of the appropriate mathematical functions to explain the phenomenon. In the fourth step, the data collected at the second step are applied to the mathematical model to obtain quantitative results. Step five involves the interpretation of the analysis completed in the previous step. It is very important that the results are interpreted in a clear and comprehensible way. Next, the results of the analysis are verified as to their applicability to a wide range of possibilities for the organisation. The ability of a model to predict accurately is fundamental to verification. If the model is verified as useful to the organisation, then it will be implemented. After implementation, use of the model may lead to additional applications for similar models, adjustments and refinements of the model, or eventual rejection of the model if it is found inapplicable to function.

Mathematical models and the modelling process serve as learning aids by emphasising the applied aspects of mathematical analysis.

Non-dimensionalisation and scaling

After a mathematical model of a continuous physical system, which may consist of, say, a set of differential equations and associated initial and boundary conditions, has been created, we try to obtain the solutions for this model. There are two kinds of solutions: exact analytical solutions and approximate solutions. Exact solutions can be obtained if we can solve an equation analytically, for example be able to solve a linear equation exactly. Approximate solutions can be obtained by applying some

type of approximation to an equation or a system of equations.

In order to obtain an approximate solution, sometimes, the first thing we want to do is to non-dimensionalise the system. Since practically useful models are often very difficult to analyse rigorously, the only way to simplify the model is to apply some kind of asymptotic reduction, based on the idea that we can neglect certain terms which are small compared with others in the system.

In general, after the process of non-dimensionalisation, we end up with an equation or equations with dimensionless variables, rather than equations with a large number of physical parameters and variables all with dimensional units. The art of non-dimensionalisation lies in the choice of scales. There is no standard way to do the scaling - the main principle is to balance the terms in the equation by choosing self-consistent scales, since the purpose is to make the largest dimensionless parameter numerically of order one in the attained properly scaled equations. Note that the process of rescaling may be necessary if the scaling causes inconsistency of the differential equation. Normally, to check for the consistency of the system, we use the approximate solution just obtained to evaluate the neglected terms, so as to ensure that they are indeed relatively small.

In practice, it is not always possible to choose all the dimensionless parameters to be $O(1)$, but it is usually best to try and choose the largest dimensionless parameter to be $O(1)$. For a more detailed reference on scaling refer to [15] and [16].

1.4 Outline of thesis

This thesis investigates analytical methods applicable to mathematical models arising from biosensor research and is motivated by a collaboration with the National Centre for Sensor Research (NCSR) and the Biomedical Diagnostics Institute (BDI) at Dublin City University. Several models of varying complexity are proposed in answer to experimental problems, usually concerned with optimising design parameters for biosensors. One main concern is to simplify the models as much as possible, without the loss of important information from the original problem.

Chapter 1 provides some background material which includes the motivation for studying biosensors as well as an elementary description of their structure and functionality. This chapter also includes a simple introduction to chemical kinetics and describes antibody-antigen interactions (which are fundamental to bioaffinity devices) and enzyme-substrate systems, which form the basis of biocatalytic devices.

Chapter 2 reviews the well-known Michaelis-Menten kinetics scheme for enzyme-substrate reactions together with a detailed mathematical analysis, which uses dynamical systems and perturbation theory methods. A comparison is given between the classical formulation, which is used in most mathematical models of enzyme-substrate interactions in the literature, and a generalised formulation which eliminates a standard simplifying assumption of irreversibility in the model. This chapter also introduces the concept of a bi-enzyme cascade reaction, which is the basis for the problem studied in Chapter 4, together with its mathematical formulation.

In Chapter 3 we give examples and analyse problems where modelling of transport phenomena only affect the transient behaviour of the system and has no effect on the final steady states of the species involved. It is often the case that the equilibrium values are the only piece of information required for the solution of a practical problem (although, sometimes, time to reach equilibrium is the real issue) and in such situations it is important to identify the conditions under which a complex partial differential equations model can be replaced with a simpler one. Such problems as these are related to immunosensors, a class of bioaffinity devices, and involve mathematical models of antibody-antigen interactions. We analyse three types of immunoassays: the direct assay, the competitive assay (which are analysed with and without diffusion effects) and the sandwich assay.

Chapter 4 studies a flow injection analysis of a bi-enzyme electrode, with the aim of finding the ratio of the two enzymes involved which yields the highest current amplitude. A detailed comparison of three mathematical models (each neglecting different aspects of the biosensor functionality) is given, and the best modelling strategy under various physical conditions is investigated.

Finally, a summary of the work from the previous chapters is given, and further suggestions on modelling biosensor problems are made.

Chapter 2

Enzyme-Substrate Kinetics: A Mathematical Analysis of The Michaelis-Menten Model

This chapter introduces the Michaelis-Menten model, one of the most widely used mathematical models in biochemical kinetics. This simple model is expressed as a system of ordinary differential equations which is analysed using dynamical systems and perturbation theory methods. The model is compared with a generalised kinetic scheme in which the second step of the reaction is reversible. Finally, the last section of this chapter provides an introduction to cascade schemes consisting of two catalytically linked enzyme-substrate reactions, which forms the basis of the problem presented in Chapter 4.

2.1 Standard Michaelis-Menten kinetics

2.1.1 Introduction

Enzyme reactions do not follow the law of mass action directly. The rate of the reaction only increases to a certain extent as the concentration of substrate increases. The maximum reaction rate is reached at high substrate concentrations due to enzyme saturation. This is in contrast to the law of mass action, which states that the reaction rate increases as the concentration of substrate increases (refer to [17]).

The simplest model that explains the kinetic behaviour of enzyme reactions is the classic 1913 model of Michaelis and Menten (refer to [18]) which is widely used in biochemistry for many types of enzymes. The Michaelis-Menten model is based on the assumption that the enzyme binds the substrate to form an intermediate complex which then dissociates to form the final product and release the enzyme in its original form. (This mechanism was also explained in Section 1.1.2.) The schematic representation of this two-step process is given by

$$E + S \underset{k_{-1}}{\overset{k_1}{\rightleftarrows}} C \xrightarrow{k_2} E + P, \tag{2.1}$$

where k_1, k_{-1} and k_2 are constant parameters associated with the rates of the reaction. The double arrow symbol $\rightleftarrows$ indicates that the reaction is reversible while the single arrow $\rightarrow$ indicates that the reaction is irreversible. Note that it is generally assumed that the second step of the reaction in (2.1) is irreversible. In reality, this is not always the case. Typically, reaction rates are measured under the condition that the product is continually removed, which prevents the reverse reaction of the second

step from occurring effectively. We will consider the possibility of a reversible second step of the reaction in Section 2.2.

We denote the concentrations of the chemical species in reaction (2.1) by their corresponding lower case letters, that is

$$e = [E], \quad s = [S], \quad c = [C], \quad p = [P],$$

each being functions of time, where [ ] traditionally denotes concentrations. Based on the principles of mass action and conservation of mass, the kinetic behavior of the chemical species is described by the following system of nonlinear ordinary differential equations, namely

$$\begin{cases} \dfrac{de}{dt} = -k_1 es + (k_2 + k_{-1})c & \text{(2.2a)} \\ \dfrac{ds}{dt} = -k_1 es + k_{-1} c & \text{(2.2b)} \\ \dfrac{dc}{dt} = k_1 es - (k_2 + k_{-1})c & \text{(2.2c)} \\ \dfrac{dp}{dt} = k_2 c. & \text{(2.2d)} \end{cases}$$

If the reaction is initiated at time $t = 0$ in a medium with $e = e_0$, $s = s_0$, then we require the initial conditions

$$e(0) = e_0, \quad s(0) = s_0, \quad c(0) = 0, \quad p(0) = 0.$$

Note that

$$\frac{de}{dt} + \frac{dc}{dt} = 0$$

in system (2.2), and hence $e + c = e_0$. This conservation law will be used extensively throughout our models, which expresses the fact that the enzyme only exists in two

forms during the reaction: free enzyme and complex-bound enzyme. We can obtain a second conservation law $s + c + p = s_0$ from system (2.2), from the fact that

$$\frac{ds}{dt} + \frac{dc}{dt} + \frac{dp}{dt} = 0.$$

Finally, we remark that, under certain experimental conditions, we can assume that the substrate concentration is kept constant for all times. (For example, the problem presented in Chapter 4 deals with the flow injection analysis of an enzymatic reaction, where the substrate is continually pumped into the system.) If we allow $s(t) = s_0$, for all t, system (2.2) reduces to a single equation

$$\frac{dc}{dt} = k_1(e_0 - c)s_0 - (k_2 + k_{-1})c,$$

with $c(0) = 0$ and it is easy to see that

$$\lim_{t\to\infty} c(t) = c^* \quad \text{and} \quad \lim_{t\to\infty} e(t) = e_0 - c^*,$$

where

$$c^* = \frac{e_0}{1 + \frac{K_m^1}{s_0}}.$$

In which

$$K_m^1 = \frac{k_{-1} + k_2}{k_1} \tag{2.3}$$

is the well known **Michaelis constant**. The second conservation law (involving s and p) does not hold for this system and equation (2.2d) shows that

$$\lim_{t\to\infty} p(t) = \infty,$$

although the rate of formation of product dp/dt will eventually approach an equilibrium.

2.1.2 Equilibrium and stability analysis

Note that equation (2.2d) yields the product concentration, p, once we have determined the complex concentration, c, so it can be uncoupled from the rest of the equations in system (2.2). Thus we only need to consider the first three equations of the system. Applying the conservation law $e + c = e_0$, system (2.2) reduces to only two equations, which are given in terms of the substrate concentration, s, and the complex concentration, c, namely

$$\begin{cases} \dfrac{ds}{dt} = -k_1(e_0 - c)s + k_{-1}c & \text{(2.4a)} \\ \dfrac{dc}{dt} = k_1(e_0 - c)s - (k_2 + k_{-1})c, & \text{(2.4b)} \end{cases}$$

with initial conditions

$$\begin{cases} s(0) = s_0 & \text{(2.5a)} \\ c(0) = 0. & \text{(2.5b)} \end{cases}$$

The equilibrium analysis carried out on the simplified system (2.4) gives the following equilibrium solutions for the different reactants, with

$$e^* = e_0, \quad s^* = 0, \quad c^* = 0,$$

where e^*, s^* and c^* denote the equilibrium values of e, s and c respectively. The equilibrium solution for the product concentration, p, can be obtained from the second conservation law $s + c + p = s_0$, which yields $p^* = s_0$. The long-term behaviour of these functions is illustrated in Figure 2.1, where we see that the enzyme concentration returns to its initial value while the substrate concentration is depleted and goes to zero. Also, the concentration of the complex increases rapidly during the short initial

period of the reaction (since the enzyme quickly reacts with the substrate), but then depletes and goes to zero. This figure is produced by using MAPLE, so as the rest of the figures in this thesis.

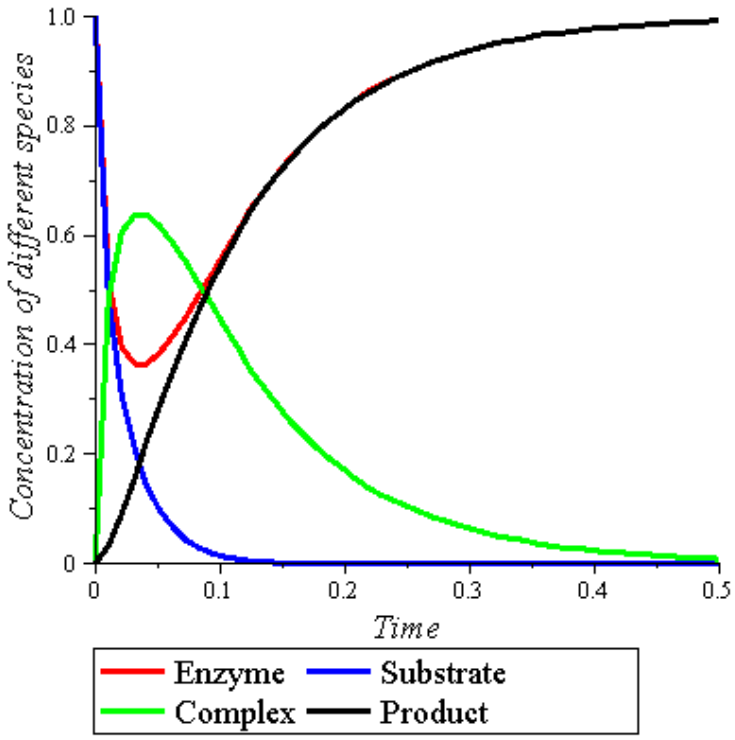

Figure 2.1 – Relative concentrations of reactants and product of the standard Michaelis-Menten kinetics. Typical values for constants used in this simulation are: $k_1 = 10^2\ m^3/mol \cdot s$, $k_{-1} = 10^{-1}\ m^3/mol \cdot s$, $k_2 = 10\ m^3/mol \cdot s$, $e_0 = 1\ mol/m^2$ and $s_0 = 1\ mol/m^3$.

How can we tell if the equilibrium point (s^*, c^*) is stable or unstable? An equilibrium is considered stable if the system always returns to it after small disturbances, and considered unstable if the system moves away from the equilibrium after small

disturbances. In general, unstable equilibrium solutions are not of much interest for practical purposes (refer to [19]).

In the stability analysis of the standard Michaelis-Menten model, we consider the simplified system (2.4), and we let

$$f(s,c) = -k_1(e_0 - c)s + k_{-1}c, \tag{2.6}$$

$$g(s,c) = k_1(e_0 - c)s - (k_2 + k_{-1})c. \tag{2.7}$$

Then the partial derivatives of equations (2.6) and (2.7) are calculated and evaluated at the equilibrium state to form the Jacobian matrix

$$\begin{pmatrix} \frac{\partial f(s^*,c^*)}{\partial s} & \frac{\partial f(s^*,c^*)}{\partial c} \\ \frac{\partial g(s^*,c^*)}{\partial s} & \frac{\partial g(s^*,c^*)}{\partial c} \end{pmatrix} = \begin{pmatrix} -k_1(e_0 - c^*) & k_{-1} + k_1 s^* \\ k_1(e_0 - c^*) & -k_1 s^* - k_2 - k_{-1} \end{pmatrix}$$

which yields the characteristic equation

$$\lambda^2 + (k_1(e_0 - c^* + s^*) + k_2 + k_{-1})\lambda + k_1 k_2(e_0 - c^*) = 0.$$

From this quadratic equation, we can easily see that the two eigenvalues λ_1 and λ_2 satisfy the conditions

$$\lambda_1 + \lambda_2 = -(k_1(e_0 - c^* + s^*) + k_2 + k_{-1}) < 0,$$

and

$$\lambda_1 \lambda_2 = k_1 k_2(e_0 - c^*) > 0,$$

since $e_0 - c^* > 0$. The fact that the sum of the two eigenvalues is negative, and their product is positive implies that we have two negative eigenvalues. The equilibrium

solution of the standard Michaelis-Menten model is therefore, linearly stable.

We can also show that the equilibrium point $(s^*, c^*) = (0, 0)$ is globally stable, and hence attracts all the phase plane trajectories of system (2.4). We start by showing that the positive quadrant

$$\Gamma = \left\{(s, c) \in R^2 : s \geq 0, c \geq 0\right\}$$

is a positive invariant region for system (2.4) (which means that trajectories entering this region cannot leave it in forward time). Hence, a solution with a positive initial condition will stay positive for all $t \geq 0$. This is easily done if we show that the flow points inwards on all boundaries of the region Γ. In particular, we have to check that

$$\frac{ds}{dt} \geq 0, \quad \text{when} \quad s = 0, \quad c \geq 0,$$

and

$$\frac{dc}{dt} \geq 0, \quad \text{when} \quad c = 0, \quad s \geq 0.$$

These conditions can be easily verified in system (2.4). Then we construct a Lyapunov function for the system as

$$V : \Gamma \subset R^2 \to R, \quad V(s, c) = s + c. \tag{2.8}$$

As described in [20], a Lyapunov function must satisfy the following properties:

1. $V(s, c) > 0$ for all $(s, c) \neq (s^*, c^*)$ and $V(s^*, c^*) = 0$;

2. $\dot{V}(s, c) < 0$ for all $(s, c) \neq (s^*, c^*)$.

The first property follows easily from the positivity of s and c proved above, while the second property can be established by noting from system (2.4) that

$$\dot{V}(s,c) = \dot{s} + \dot{c} = -k_2 c < 0, \text{ if } c \neq c^* = 0.$$

Thus, the conditions above imply that the equilibrium point (s^*, c^*) is globally asymptotically stable.

2.1.3 The quasi-steady-state approximation

In the original Michaelis-Menten model (refer to [18]), it was assumed that the substrate concentration, s, is assumed to be in instantaneous equilibrium with the enzyme-substrate complex concentration, c, which gives

$$k_1 e s = k_{-1} c.$$

Then by using the initial condition $e + c = e_0$, we find that

$$c = \frac{e_0 s}{K_s + s},$$

where $K_s = k_{-1}/k_1$. If we let v denote the velocity of the reaction, then the rate at which the product is formed is given by

$$v = \frac{dp}{dt} = k_2 c = \frac{k_2 e_0 s}{K_s + s} = \frac{v_{max} s}{K_s + s},$$

where

$$v_{max} = k_2 e_0 \tag{2.9}$$

is the maximum reaction velocity, attained when all the enzyme is bounded with the substrate (refer to [17]).

An alternative analysis of an enzymatic reaction was proposed by Briggs and Haldane in [21], and forms the basis for most modern descriptions of enzyme reactions. Their assumption is that the rates of formation and breakdown of the complex are essentially equal at all times, except at the beginning of the reaction, when the formation of the complex is very fast. Thus, we have $dc/dt \approx 0$. It is simple to determine the velocity of the reaction with this assumption (refer to [17]). Thus, from (2.4b) we obtain the complex concentration, c, in terms of the substrate concentration, s, as

$$c = \frac{k_1 e_0 s}{k_{-1} + k_2 + k_1 s} = \frac{e_0 s}{K_m^1 + s}. \tag{2.10}$$

For a detailed explanation, refer to [22], [23] and [24].

This gives an expression for c but it does not satisfy the initial conditions specified before, namely $c(0) = 0$ and $s(0) = s_0$, as we get

$$c(0) = \frac{e_0 s_0}{s_0 + K_m^1} \neq 0.$$

However, equation (2.10) is a reasonable approximation of the equilibrium value of the complex concentration which is sufficient for many experimental situations, but crucially not for all.

If we insert equation (2.10) into equation (2.4a), we obtain

$$\frac{ds}{dt} \approx -k_2 c = -\frac{k_2 e_0 s}{K_m^1 + s}. \tag{2.11}$$

Since the enzyme is traditionally considered to be present in small amounts compared with the substrate the assumption is that the substrate concentration effectively does

not change during this initial transient stage. In this case, the (approximate) dynamics are governed by equation (2.11) with the initial condition $s(0) = s_0$. This is known as the **quasi-steady-state approximation**.

The quasi-steady-state approximation gives an expression for the velocity of the reaction which is useful for practical applications. Equation (2.11) implies that

$$v = \frac{dp}{dt} = -\frac{ds}{dt} = \frac{k_2 e_0 s}{K_m^1 + s} = \frac{v_{max} s}{K_m^1 + s}, \tag{2.12}$$

where v_{max} and K_m^1 are defined in equations (2.9) and (2.3) respectively. The Michaelis constant K_m^1 can be easily determined from experimental data if we notice that, setting

$$s = K_m^1,$$

equation (2.12) implies

$$v = \frac{v_{max}}{2}.$$

This allows us to interpret K_m^1 as the substrate concentration at which the velocity of the reaction is half-maximal and it indicates how efficiently an enzyme selects its substrate and converts it to product. The lower the value of K_m^1, the more effective the enzyme is at low substrate concentrations and K_m^1 is unique for each enzyme-substrate pair. Consequently, K_m^1 values are useful for comparing the activities of two enzymes that act on the same substrate or for assessing the ability of different substrates to be recognised by a single enzyme. For practical purposes, it is also useful to know how fast the enzyme operates after it has selected and bound its corresponding substrate; that is, how fast does the complex proceed to the product

and free enzyme? This property is characterised by the catalytic constant

$$k_{cat} = \frac{v_{max}}{e_0},$$

and in the Michaelis-Menten scheme, we have

$$k_{cat} = k_2.$$

Thus, k_{cat} is the rate constant of the reaction when the enzyme is saturated with substrate (i.e., when $c \approx e_0$, $v_0 \approx v_{max}$, where v_0 is the initial velocity of the reaction); we have already seen this relationship in equation (2.9). k_{cat} is also known as the enzyme's **turnover number** because it is the number of catalytic cycles that each active site undergoes per unit time. It is a first-order rate constant and therefore has units of s^{-1} (refer to [17]).

Solving equation (2.11) with the initial condition $s(t) = s_0$ we obtain an implicit solution for s, namely

$$s(t) + K_m^1 \ln s(t) = -k_2 e_0 t + s_0 + K_m^1 \ln s_0. \tag{2.13}$$

In what follows, we show that an explicit solution for s can also be found in terms of the **Lambert W function** [1]. This function is defined as the inverse of the function f where

$$f : C \to C,\ f(w) = we^w.$$

The Lambert W function satisfies

$$z = W(z)e^{W(z)},\ \forall\ z \in C \tag{2.14}$$

[1] **Lambert W function**, which is named after Johann Heinrich Lambert, is also called the **Omega function** or **product log**.

and by implicit differentiation, we can also show that W satisfies the differential equation

$$z(1+W)\frac{dW}{dz} = W, \text{ for } z \neq -\frac{1}{e}$$

or

$$\frac{dW}{dz} = \frac{W}{z(1+W)}. \tag{2.15}$$

Now we need to write equation (2.11) into a form similar to (2.15). We let $s = SK_m^1$, then substitute it into (2.11) to obtain

$$K_m^1 \frac{dS}{dt} = -\frac{k_2 e_0 S}{S+1},$$

which gives

$$(S+1)\frac{dS}{dt} = -\frac{k_2 e_0 S}{K_m^1}. \tag{2.16}$$

Now if we let $S(t) = W(z(t))$ and substitute this into (2.16), we obtain

$$(W(z)+1)\frac{dW}{dz}z^{'}(t) = -\frac{k_2 e_0}{K_m^1}W(z).$$

Also, from equation (2.15), we get

$$z^{'}(t) = -\frac{k_2 e_0}{K_m^1}z(t),$$

for which the general solution is

$$z(t) = e^{-\frac{k_2 e_0}{K_m^1}t + C},$$

where C is an arbitrary constant. Hence,

$$s = SK_m^1 = K_m^1 W(z(t)) = K_m^1 W\left(e^{-\frac{k_2 e_0}{K_m^1}t + C}\right). \tag{2.17}$$

Then, by using the initial condition $s(0) = s_0$, we obtain

$$W^{-1}(\frac{s_0}{K_m^1}) = e^C. \tag{2.18}$$

If we let $z = W^{-1}(s_0/K_m^1)$, and together with equation (2.14), we get

$$W^{-1}(\frac{s_0}{K_m^1}) = \frac{s_0}{K_m^1} e^{\frac{s_0}{K_m^1}}. \tag{2.19}$$

Now equate equations (2.18) and (2.19) to obtain

$$e^C = \frac{s_0}{K_m^1} e^{\frac{s_0}{K_m^1}}. \tag{2.20}$$

Substituting equation (2.20) into (2.17), we obtain

$$s(t) = K_m^1 W\left(\frac{s_0}{K_m^1} e^{\frac{s_0 - k_2 e_0 t}{K_m^1}}\right).$$

We can now use the solution obtained for s to find explicit solutions for c, e and p as follows:

$$c(t) = \frac{e_0 s}{s + K_m^1} = \frac{e_0 W\left(\frac{s_0}{K_m^1} e^{\frac{s_0 - k_2 e_0 t}{K_m^1}}\right)}{1 + W\left(\frac{s_0}{K_m^1} e^{\frac{s_0 - k_2 e_0 t}{K_m^1}}\right)}, \tag{2.21}$$

$$e(t) = e_0 - c = \frac{e_0}{1 + W\left(\frac{s_0}{K_m^1} e^{\frac{s_0 - k_2 e_0 t}{K_m^1}}\right)},$$

$$p(t) = s_0 - s - c = s_0 - W\left(\frac{s_0}{K_m^1} e^{\frac{s_0 - k_2 e_0 t}{K_m^1}}\right)\left(K_m^1 + \frac{e_0}{1 + W\left(\frac{s_0}{K_m^1} e^{\frac{s_0 - k_2 e_0 t}{K_m^1}}\right)}\right).$$

The exact solution obtained for the complex concentration, c, is plotted in Figure 2.2, and is compared with a numerical solution obtained by integrating system (2.4). The reason we are interested in plotting the complex concentration, c, is due to that the amperometric signal is measured as the time evolution of dp/dt (the rate of

formation of the product) on the electrode. As remarked before, the quasi-steady-state assumption does not lead to a mathematically correct solution for c, due to its failure to satisfy the initial condition $c(0) = 0$. This assumption is, however, widely used in biochemistry to approximate the reaction rate after the initial transient period is over.

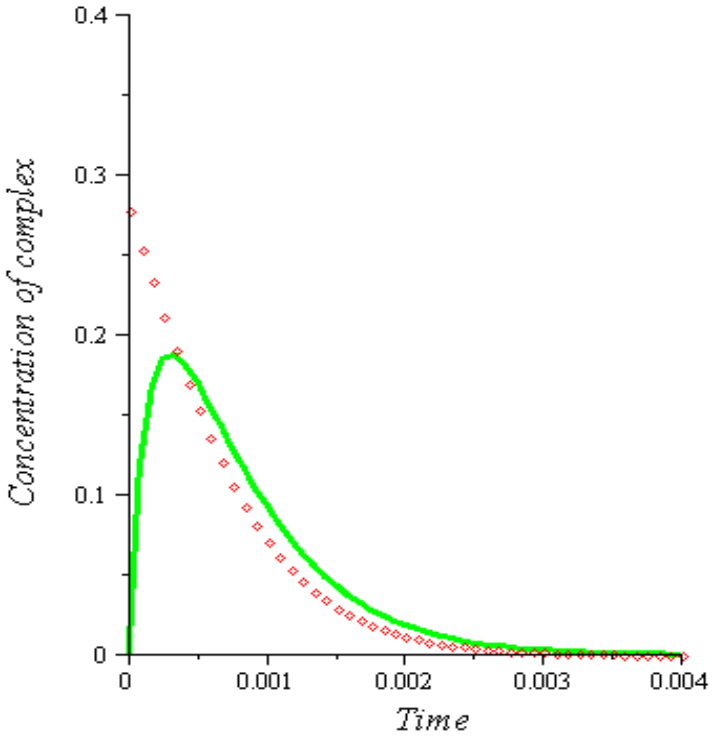

Figure 2.2 – Numerical solution of the Michaelis-Menten model (2.4) (continuous green line) versus the exact solution of the quasi-steady-state approximation of equation (2.21) (red points).

2.1.4 Perturbation analysis

The quasi-steady-state approximation $dc/dt \approx 0$ needs to be justified mathematically by non-dimensionalising system (2.4) and by identifying the effect a small parameter has on the system. The standard dimensionless variables in modelling enzyme-substrate kinetics are

$$\bar{e} = \frac{e}{e_0}, \quad \bar{s} = \frac{s}{s_0}, \quad \bar{c} = \frac{c}{e_0}, \quad \bar{p} = \frac{p}{s_0}, \quad \bar{t} = \frac{t}{t_0}, \quad \text{where} \quad t_0 = \frac{1}{k_1 e_0},$$

(refer to, for example [25]), which lead to the non-dimensional system

$$\begin{cases} \dfrac{ds}{dt} = -(1-c)s + \alpha c & \text{(2.22a)} \\ \varepsilon \dfrac{dc}{dt} = (1-c)s - kc, & \text{(2.22b)} \end{cases}$$

for simplicity, bars are omitted on all the non-dimensional variables. The values of the new parameters introduced by the non-dimensionalisation are:

$$\alpha = \frac{k_{-1}}{k_1 s_0}, \quad \varepsilon = \frac{e_0}{s_0} \ll 1, \quad k = \frac{K_m^1}{s_0}. \tag{2.23}$$

In non-dimensional form, the initial conditions are:

$$e(0) = 1, \quad s(0) = 1, \quad c(0) = 0, \quad p(0) = 0,$$

and the conservation law is:

$$e + c = 1.$$

It is often assumed that the parameter ε is small as a reflection of the fact that the remarkable catalytic effectiveness of enzymes means that very small concentrations are required in order to convert the substrate, hence, $e_0 \ll s_0$. System (2.22) is a

singularly perturbed initial value problem and we now see that the quasi-steady-state approximation consists of neglecting the term $\varepsilon dc/dt$ in the second equation. However, in doing so we are basically ignoring the boundary layer which exists near $t = 0$ (a region where $c(t)$ grows very fast) and the quasi-steady-state approximation only gives us the outer solution. A rigorous asymptotic analysis of this boundary layer will be carried out in Section 2.2.3 for the reversible Michaelis-Menten model.

A different choice of non-dimensionalisation is introduced in [26], where it is argued that, since there are practical situations in which e_0/s_0 may not be negligible, a more appropriate choice for the small parameter ε should follow by requiring that:

1. The duration of the pre-steady-state period t_c is much shorter than the characteristic time for substrate change, t_s.

2. The relative change $|\Delta s/s_0|$ in the substrate concentration during the pre-steady-state period is small.

The authors of [26] makes the approximation $s \approx s_0$ in equation (2.4b), which yields the solution

$$c(t) = \widehat{c}\left(1 - e^{\kappa t}\right),$$

where

$$\widehat{c} = \frac{e_0 s_0}{K_m^1 + s_0},\ \kappa = k_1(s_0 + K_m^1).$$

This gives the estimate $t_c \approx 1/\kappa$. The duration of the second timescale, t_s, is approximated by the formula

$$t_s \approx \frac{s_{max} - s_{min}}{|s'(t)|_{max}} = \frac{K_m^1 + s_0}{k_2 e_0}.$$

Hence, the condition $t_c \ll t_s$ yields

$$\frac{k_2 e_0}{k_1} \ll (s_0 + K_m^1)^2.$$

A stronger inequality can be obtained from condition 2 above by writing

$$\left|\frac{\Delta s}{s_0}\right| \approx \frac{t_c}{s_0}\left|s^{'}(t)\right|_{max} = \frac{e_0}{K_m^1 + s_0},$$

and hence

$$e_0 \ll K_m^1 + s_0.$$

The new choice for the small parameter of this problem should therefore be

$$\widehat{\varepsilon} = \frac{e_0}{K_m^1 + s_0} \ll 1,$$

and, choosing the non-dimensional variables

$$\bar{s} = \frac{s}{s_0}, \quad \bar{c} = \frac{c}{\widehat{c}}, \quad \bar{t} = \frac{t}{t_c},$$

gives the boundary layer problem which is governed by the equations

$$\begin{cases} \dfrac{d\bar{s}}{d\bar{t}} = \widehat{\varepsilon}\left(-\bar{s} + \dfrac{\widehat{c}}{e_0}\bar{c}\bar{s} + \dfrac{k_{-1}\widehat{c}}{k_1 e_0 s_0}\bar{c}\right) & \text{(2.24a)} \\ \dfrac{d\bar{c}}{d\bar{t}} = \dfrac{t_c k_1 s_0 e_0}{\widehat{c}}\bar{s} - t_c k_1 s_0 \bar{c}\bar{s} - t_c(k_2 + k_{-1})\bar{c}, & \text{(2.24b)} \end{cases}$$

with $\bar{s}(0) = 1$, $\bar{c}(0) = 0$. After the transition period is over, we introduce a new dimensionless time by putting

$$\widetilde{t} = \frac{t}{t_s},$$

and the resulting outer problem is

$$\begin{cases} \dfrac{d\bar{s}}{d\widetilde{t}} = -t_s k_1 e_0 \bar{s} + t_s k_1 \widehat{c}\bar{c}\bar{s} + \dfrac{t_s k_{-1}\widehat{c}}{s_0}\bar{c} & \text{(2.25a)} \\ \widehat{\varepsilon}\dfrac{d\bar{c}}{d\widetilde{t}} = \dfrac{t_s k_1 s_0 e_0}{\widehat{c}}\bar{s} - t_s k_1 s_0 \widehat{c}\bar{c}\bar{s} - t_s(k_2 + k_{-1})\bar{c}. & \text{(2.25b)} \end{cases}$$

A lengthy perturbation theory analysis is provided in [26], so no further details will be given here.

2.2 Reversible Michaelis-Menten kinetics

The typical Michaelis-Menten reaction scheme (2.1) assumes that the complex dissociation step is irreversible. In reality, there will be some degree of reversibility in product formation in many chemical reactions. Thus, a more realistic model for the Michaelis-Menten kinetics would be

$$E + S \underset{k_{-1}}{\overset{k_1}{\rightleftarrows}} C \underset{k_{-2}}{\overset{k_2}{\rightleftarrows}} E + P, \tag{2.26}$$

where k_{-2} is another reaction rate constant. The dynamics of the system are described by the following system of nonlinear differential equations by using the law of mass action:

$$\begin{cases} \dfrac{de}{dt} = -k_1 es + (k_2 + k_{-1})\, c - k_{-2} ep & \text{(2.27a)} \\ \dfrac{ds}{dt} = -k_1 es + k_{-1} c & \text{(2.27b)} \\ \dfrac{dc}{dt} = k_1 es - (k_2 + k_{-1})\, c + k_{-2} ep & \text{(2.27c)} \\ \dfrac{dp}{dt} = k_2 c - k_{-2} ep. & \text{(2.27d)} \end{cases}$$

The same conservation laws and initial conditions apply here as for the standard Michaelis-Menten model in Section 2.1.1.

2.2.1 Equilibrium and stability analysis

In system (2.27), by using the conservation laws $e + c = e_0$ and $s + c + p = s_0$, the system can be reduced to the following two independent equations in terms of s and c, namely

$$\begin{cases} \dfrac{ds}{dt} = -k_1 (e_0 - c) s + k_{-1} c & \text{(2.28a)} \\ \dfrac{dc}{dt} = k_1 (e_0 - c) s - (k_2 + k_{-1}) c + k_{-2} (e_0 - c) (s_0 - c - s). & \text{(2.28b)} \end{cases}$$

At equilibrium, we obtain the quadratic equation in terms of c from system (2.28) as

$$c^2 - \left(\frac{k_2}{k_{-2}} + e_0 + s_0 + \frac{k_{-1}}{k_1} \right) c + e_0 s_0 = 0. \tag{2.29}$$

Note that, unlike the standard Michaelis-Menten model, there are now two possible values for the equilibrium solution of c. If we let c_1 and c_2 denote the two roots of equation (2.29), we have the relations

$$c_1 + c_2 = \frac{k_2}{k_{-2}} + e_0 + s_0 + \frac{k_{-1}}{k_1} > 0, \text{ and } c_1 c_2 = e_0 s_0 > 0.$$

Thus, we conclude that equation (2.29) has two positive roots, and it can be easily seen that $c_1 < e_0 < c_2$. Hence, the root that is less than e_0 is in fact the only possible value for the equilibrium solution. However, solving equation (2.29) directly yields awkward formulae for the equilibrium values of c, s and p, and so, in Section 2.2.3, we are going to discuss an asymptotic approximation of this equilibrium solution and its dependence on the system parameters. Figure 2.3 shows the long-term behaviour of the species in the reversible model.

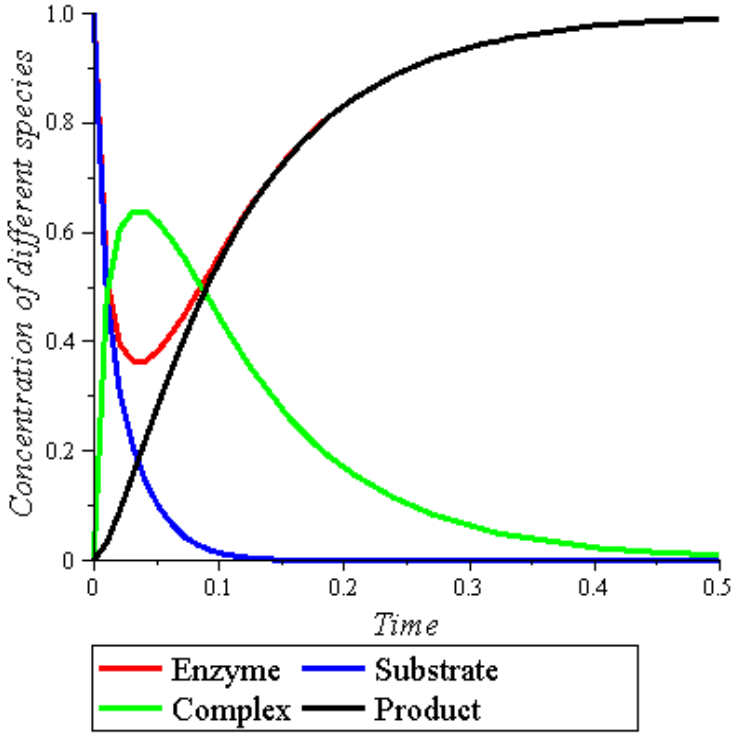

Figure 2.3 – Relative concentrations of reactants and product of the reversible Michaelis-Menten kinetics. Typical values for constants used in this simulation are: $k_1 = 10^2\ m^3/mol \cdot s$, $k_{-1} = 10^{-1}\ m^3/mol \cdot s$, $k_2 = 10\ m^3/mol \cdot s$, $k_{-2} = 10^{-2}\ m^3/mol \cdot s$, $e_0 = 1\ mol/m^2$ and $s_0 = 1\ mol/m^3$.

In the reversible Michaelis-Menten model, even without specifying explicit expressions for the equilibrium values c^*, e^*, s^* and p^*, we can still carry out the linear stability analysis of the equilibrium values. The stability analysis is carried out on system (2.28), and by using the same technique as was used in Section 2.1.2, we obtain the Jacobian matrix

$$\begin{pmatrix} -k_1\,(e_0 - c^*) & k_{-1} + k_1 s^* \\ (k_1 - k_{-2})\,(e_0 - c^*) & 2k_{-2}c^* - k_{-2}\,(e_0 + s_0 - s^*) - k_1 s^* - k_2 - k_{-1} \end{pmatrix}$$

which yields the following characteristic equation

$$\lambda^2 + \left((k_1 + k_{-2})e^* + k_{-2}p^* + k_1 s^* + k_2 + k_{-1}\right)\lambda$$

$$+e^*\left(k_1 k_{-2} e^* + k_1 k_{-2} p^* + k_1 k_2 + k_{-1}k_{-2} + k_1 k_{-2} s^*\right) = 0.$$

If we let λ_1 and λ_2 denote the two eigenvalues, by using the conservation laws $e_0 - c^* = e^*$ and $s_0 - s^* - c^* = p^*$ at equilibrium, we obtain

$$\lambda_1 + \lambda_2 = -\left((k_1 + k_{-2})e^* + k_{-2}p^* + k_1 s^* + k_2 + k_{-1}\right) < 0,$$

and

$$\lambda_1\lambda_2 = e^*\left(k_1 k_{-2} e^* + k_1 k_{-2} p^* + k_1 k_2 + k_{-1}k_{-2} + k_1 k_{-2} s^*\right) > 0.$$

Therefore, we can see again the two eigenvalues are both negative. This implies that the equilibrium solution of the reversible Michaelis-Menten model is linearly stable. Global stability can also be established by using a Lyapunov function similar to that of Section 2.1.2.

2.2.2 Non-dimensional model and approximate values of the equilibrium solution

We use the same dimensionless quantities as were used in the standard Michaelis-Menten model in Section 2.1.4 and obtain the following non-dimensional form of the reversible Michaelis-Menten model, where bars are again omitted for simplicity,

$$\begin{cases} \dfrac{ds}{dt} = -(1-c)\,s + \alpha c & \text{(2.30a)} \\ \varepsilon \dfrac{dc}{dt} = (1-c)\,s - kc + \lambda\,(1-c)\,(1-s-\varepsilon c)\,, & \text{(2.30b)} \end{cases}$$

where α, ε and k are the same as defined in equation (2.23) and

$$\lambda = \frac{k_{-2}}{k_1} \ll 1.$$

The system is supplemented by the non-dimensional initial conditions

$$e(0) = 1, \quad s(0) = 1, \quad c(0) = 0, \quad p(0) = 0,$$

and the non-dimensional conservation laws

$$\begin{cases} e + c = 1 & \text{(2.31a)} \\ s + \varepsilon c + p = 1. & \text{(2.31b)} \end{cases}$$

In this section, we are going to find an approximate equilibrium value for c as an asymptotic expansion in terms of λ; refer to [27] for details of the asymptotic methods. At equilibrium, c can be determined by the equation obtained from system (2.30) as

$$\lambda c^2 + \left(\frac{\alpha - k}{\varepsilon} - \lambda \left(\frac{1+\alpha}{\varepsilon} + 1 \right) \right) c + \frac{\lambda}{\varepsilon} = 0. \tag{2.32}$$

The initial assumption is that the solution has a particular form of expansion, namely

$$c \approx c_0 + \lambda c_1 + \cdots \tag{2.33}$$

where $\approx$ signifies asymptotic equivalence. Substituting equation (2.33) into (2.32), one finds that

$$\lambda(c_0 + \lambda c_1 + \cdots)^2 + \left(\frac{\alpha - k}{\varepsilon} - \lambda \left(\frac{1+\alpha}{\varepsilon} + 1 \right) \right) (c_0 + \lambda c_1 + \cdots) + \frac{\lambda}{\varepsilon} = 0.$$

The first problem to solve comes from the terms which are constant, this is because these equations are supposed to hold for small λ and therefore we require it to hold as $\lambda \to 0$. At $O(1)$, this gives

$$c_0 \frac{\alpha - k}{\varepsilon} = 0,$$

which gives

$$c_0 = 0.$$

Next, at $O(\lambda)$:

$$\varepsilon c_0^2 - c_0(1 + \alpha + \varepsilon) + c_1(\alpha - k) + 1 = 0,$$

we obtain

$$c_1 = \frac{1}{k - \alpha},$$

since $c_0 = 0$. This process used to find c_0 and c_1 can be continued to systematically construct the other terms of the asymptotic expansion. The approximation we have calculated so far is

$$c^* \approx \frac{\lambda}{k - \alpha} + \cdots$$

The approximate equilibrium values for the others reactants and product can be obtained from the system of equations and the conservation laws, which gives

$$\begin{cases} s^* = \dfrac{\alpha c^*}{1 - c^*} \approx \dfrac{\alpha \lambda}{k - \alpha} \\ e^* = 1 - c^* \approx 1 - \dfrac{\lambda}{k - \alpha} \\ p^* = 1 - s^* - \varepsilon c^* \approx 1 - \lambda \dfrac{\alpha + \varepsilon}{k - \alpha}. \end{cases}$$

Note that these equilibrium values can be easily obtained by solving the quadratic

equation (2.32) then expand it in terms of ε. The reason we used asymptotic expansion instead is to show a standard procedure to obtain approximate equilibrium values for models of this type. We can see that, unlike in the irreversible model, the substrate and complex concentrations are not depleted but tend to very small values, $s^*, c^* = O(\lambda)$; slightly different values are obtained for e^* and p^* as well. Note that when $\lambda = 0$ (i.e., $k_{-2} = 0$), we obtain

$$\begin{cases} c^* = 0 \\ s^* = 0 \\ e^* = 1 \\ p^* = 1, \end{cases}$$

which are the non-dimensional equilibrium values of the standard Michaelis-Menten model as shown in Section 2.1.2.

In conclusion, the standard Michaelis-Menten model and the reversible Michaelis-Menten model give qualitatively similar results. The only difference consists in slightly different values for the steady-states (such as, for example, $c^* = 0$ in the standard model, while $c^* = O(\lambda)$ in the reversible model). For later analysis in this thesis, we will always work with the standard model, as these small variations are not worth the inconvenience of dealing with an extra term and having to specify another experimental constant k_{-2}.

2.2.3 Boundary layer analysis

In system (2.30), typically $e_0 \ll s_0$ which implies $\varepsilon \ll 1$. To be precise, suppose that k and α are $O(1)$ while $\varepsilon \ll 1$. Then the term $\varepsilon dc/dt$ is small if dc/dt is $O(1)$ and can therefore be neglected, which is the quasi-steady-state assumption. However, it is a singular approximation, as we cannot satisfy both initial conditions, and we can expect a boundary layer near $t = 0$ where dc/dt is large and $\varepsilon dc/dt$ cannot be neglected. The procedure for establishing this result is the method known as **matched asymptotic expansions** (refer to [28] and [29]). This method is carried out in the following three steps.

Step 1: Outer solution

To solve system (2.30) approximately, we assume the solution can be expanded in powers of ε. In other words, we let

$$s \approx s_{out}^0 + \varepsilon s_{out}^1 + \cdots \tag{2.36}$$

and

$$c \approx c_{out}^0 + \varepsilon c_{out}^1 + \cdots \tag{2.37}$$

Insert equations (2.36) and (2.37) into system (2.30), and by equating powers of ε, we obtain the following sequence of equations for the successive terms: at $O(1)$, we obtain

$$\begin{cases} \dfrac{ds_{out}^0}{dt} = -\left(1 - c_{out}^0\right) s_{out}^0 + \alpha c_{out}^0 & \text{(2.38a)} \\ 0 = (1 - c_{out}^0)s_{out}^0 - kc_{out}^0 + \lambda(1 - c_{out}^0)(1 - s_{out}^0), & \text{(2.38b)} \end{cases}$$

and therefore

$$c_{out}^0 = \frac{s_{out}^0 + \lambda(1 - s_{out}^0)}{k + s_{out}^0 + \lambda(1 - s_{out}^0)}. \tag{2.39}$$

Substitute equation (2.39) into equation (2.38a) to obtain

$$\frac{ds^0_{out}}{dt} = -s^0_{out} + (s^0_{out} + \alpha)\frac{s^0_{out} + \lambda(1 - s^0_{out})}{k + s^0_{out} + \lambda(1 - s^0_{out})},$$

which gives

$$\frac{ds^0_{out}}{dt} = \frac{-s^0_{out}k + \alpha(s^0_{out}(1 - \lambda) + \lambda)}{k + s^0_{out}(1 - \lambda) + \lambda}. \tag{2.40}$$

This separable differential equation is easily solved to give

$$\begin{aligned}\frac{k(\alpha - k - (1 + \alpha)\lambda)}{(\alpha - \alpha\lambda - k)^2} \ln((\alpha - \alpha\lambda - k)s^0_{out} + \alpha\lambda) \\ + \frac{1 - \lambda}{\alpha - \alpha\lambda - k} s^0_{out} = t + A,\end{aligned} \tag{2.41}$$

where A is the constant of integration which will be determined later.

Step 2: Rescaling the problem: the boundary layer

If we now substitute equation (2.41) into (2.39) we get an expression for the complex concentration, c, but this does not satisfy the initial condition on c, since there are two timescales involved in the system; one is the timescale near $t = 0$ and the other one is the long timescale when the substrate concentration changes significantly.

To deal with this problem, in order to bring out the new balances in the equation, it is appropriate to introduce a rescaling of the time by

$$t = \varepsilon\tau.$$

System (2.30) then becomes

$$\begin{cases} \dfrac{ds}{d\tau} = \varepsilon(-(1 - c)s + \alpha c) & \text{(2.42a)} \\ \dfrac{dc}{d\tau} = (1 - c)s - kc + \lambda(1 - c)(1 - s - \varepsilon c). & \text{(2.42b)} \end{cases}$$

To obtain the solutions for c and s, the appropriate expansions for the boundary layer solutions are now

$$s \approx s_{in}^0 + \varepsilon s_{in}^1 + \cdots \tag{2.43}$$

and

$$c \approx c_{in}^0 + \varepsilon c_{in}^1 + \cdots \tag{2.44}$$

Substituting equations (2.43) and (2.44) into system (2.42), we obtain

$$\begin{cases} \dfrac{d(s_{in}^0 + \varepsilon s_{in}^1 + \cdots)}{d\tau} = \varepsilon(-(1 - (c_{in}^0 + \varepsilon c_{in}^1 + \cdots))(s_{in}^0 + \varepsilon s_{in}^1 + \cdots) + \alpha(c_{in}^0 + \varepsilon c_{in}^1 + \cdots)) \\ \dfrac{d(c_{in}^0 + \varepsilon c_{in}^1 + \cdots)}{d\tau} = (1 - (c_{in}^0 + \varepsilon c_{in}^1 + \cdots))(s_{in}^0 + \varepsilon s_{in}^1 + \cdots) - k(c_{in}^0 + \varepsilon c_{in}^1 + \cdots) \\ \qquad +\lambda(1 - (c_{in}^0 + \varepsilon c_{in}^1 + \cdots))(1 - (s_{in}^0 + \varepsilon s_{in}^1 + \cdots) - \varepsilon(c_{in}^0 + \varepsilon c_{in}^1 + \cdots)). \end{cases}$$

Again by equating powers of ε, at $O(1)$, we obtain

$$\frac{ds_{in}^0}{d\tau} = 0,$$

implying that

$$s_{in}^0 = B,$$

where B is an arbitrary constant of integration. With initial condition $s_{in}^0(0) = 1$, we get $B = 1$. Thus $s_{in}^0 = 1$, and

$$\frac{dc_{in}^0}{d\tau} = (1 - c_{in}^0)(s_{in}^0) - kc_{in}^0 + \lambda(1 - c_{in}^0)(1 - s_{in}^0),$$

which gives

$$\frac{dc_{in}^0}{d\tau} + (1 + k)c_{in}^0 = 1,$$

and therefore

$$c_{in}^0 = \frac{1}{1+k}(1 - e^{-(1+k)\tau}). \tag{2.46}$$

Note that when $\tau = 0$, $c_{in}^0 = 0$.

Step 3: Matching

It remains to determine the constant A in the approximation of the boundary layer solution. The important point here is that both the inner and outer expansions are approximations of the same system. Therefore, in the transition region between the inner and outer layers we should expect that the two expansions give the same result. This is accomplished by requiring that the value of s_{in}^0 as one exits the boundary layer (i.e., as $\tau \to \infty$) is equal to the value of s_{out}^0 as one enters the boundary layer (i.e., as $t \to 0$). Imposing this condition yields

$$\lim_{t\to 0}[s_{out}^0(t), c_{out}^0(t)] = \left[1, \frac{1}{1+k}\right] = \lim_{\tau\to\infty}[s_{in}^0(\tau), c_{in}^0(\tau)],$$

which gives

$$A = \frac{1-\lambda}{\alpha - \alpha\lambda - k} + \frac{k(\alpha - \alpha\lambda - k - \lambda)}{(\alpha - \alpha\lambda - k)^2}\ln(\alpha - k),$$

and equation (2.41) becomes

$$\frac{1-\lambda}{\alpha - \alpha\lambda - k}(s_{out}^0 - 1) + \frac{k(\alpha - \alpha\lambda - k - \lambda)}{(\alpha - \alpha\lambda - k)^2}\ln\left(s_{out}^0 - \frac{\alpha\lambda}{\alpha - k}(s_{out}^0 - 1)\right) = t. \tag{2.47}$$

Note that when $\lambda = 0$ (i.e., $k_{-2} = 0$), equation (2.47) simplifies to

$$s_{out}^0 + k\ln s_{out}^0 = 1 + (\alpha - k)t,$$

which corresponds to the solution obtained for the classical model in [25]. The boundary layer expansion is supposed to describe the solution in the immediate vicinity of

the endpoint $t = 0$. It is therefore not unreasonable to expect that the outer solution applies over the remainder of the interval, with the assumption that there are no other layers.

To summarise, in order to proceed with the systematic singular perturbation, we first look for the outer solution of the system in the form of regular series expansions. At $O(1)$, the sequence of equations are:

$$\begin{cases} \dfrac{ds^0_{out}}{dt} = -(1 - c^0_{out})s^0_{out} + \alpha c^0_{out} \\ 0 = (1 - c^0_{out})s^0_{out} - kc^0_{out} + \lambda(1 - c^0_{out})(1 - s^0_{out}), \end{cases}$$

and at $O(\varepsilon)$, we have

$$\begin{cases} \dfrac{ds^1_{out}}{dt} = c^1_{out}s^0_{out} - (1 - c^0_{out})s^1_{out} + \alpha c^1_{out} \\ \dfrac{dc^0_{out}}{dt} = -c^1_{out}s^0_{out} + (1 - c^0_{out})s^1_{out} - kc^1_{out} - \lambda((1 - c^0_{out})(s^1_{out} + c^0_{out}) + c^1_{out}(1 - s^0_{out})), \end{cases}$$

which are valid for $t > 0$; the solutions involve undetermined constants of integration, one at each order, which have to be determined by matching these solutions as $t \to 0$ with the singular solutions as $\tau \to \infty$.

On the other hand, the sequence of equations for the singular part of the solution, valid for $0 \leq \tau \leq 1$ are: at $O(1)$,

$$\begin{cases} \dfrac{ds^0_{in}}{d\tau} = 0 \\ \dfrac{dc^0_{in}}{d\tau} = (1 - c^0_{in})(s^0_{in}) - kc^0_{in} + \lambda(1 - c^0_{in})(1 - s^0_{in}), \end{cases}$$

and at $O(\varepsilon)$, we have

$$\begin{cases} \dfrac{ds_{in}^1}{d\tau} = -(1-c_{in}^0)s_{in}^0 + \alpha c_{in}^0 \\ \dfrac{dc_{in}^1}{d\tau} = -c_{in}^1 s_{in}^0 + (1-c_{in}^0)s_{in}^1 - kc_{in}^1 - \lambda((1-c_{in}^0)(s_{in}^1+c_{in}^0) + c_{in}^1(1-s_{in}^0)), \end{cases}$$

and so on.

The solutions of these equations must satisfy the initial conditions at $t = 0$. Since in most biological applications $0 < \varepsilon \ll 1$, we only need to evaluate the $O(1)$ terms of the solutions as shown in this section. In Figure 2.4, we show the inner solution (c_{in}^0 from (2.46)), outer solution (c_{out}^0 from (2.47) and (2.39)) and the exact solution (obtained from (2.29)) of the reversible Michaelis-Menten model. For a detailed explanation of the technique used in this section, refer to [15], [28] and [29].

2.3 Cascade reactions

This section introduces the concept of a cascade reaction and discusses some notation and elementary dynamical properties of systems describing cascade reactions. Such systems will be studied in more detail in Chapter 4.

A cascade reaction is a sequence of biochemical reactions which have the property that the product of one reaction is a reactant in the following reaction. We will focus, in particular, on a cascade scheme which consists of two enzyme-substrate reactions

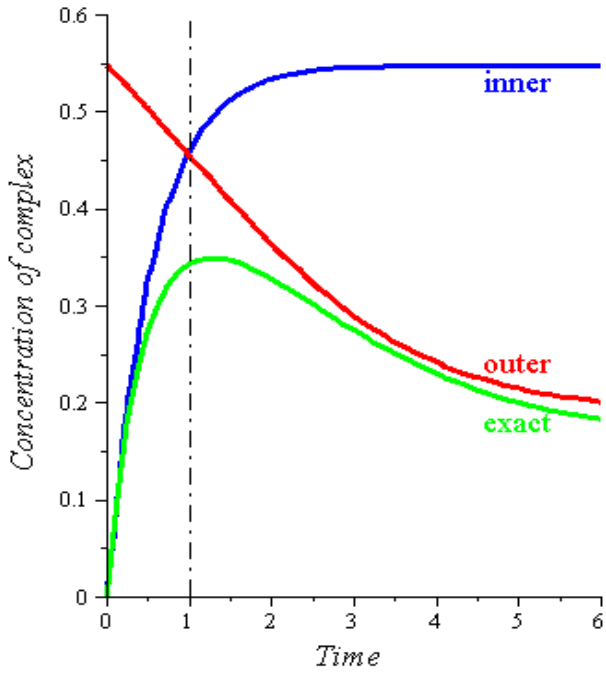

Figure 2.4 – Inner, outer and exact solution of reversible Michaelis-Menten kinetics. Typical values for constants used in this simulation are: $k_1 = 4 \times 10^2\ m^3/mol \cdot s$, $k_{-1} = 10\ m^3/mol \cdot s$, $k_2 = 3.2 \times 10^2\ m^3/mol \cdot s$, $k_{-2} = 75\ m^3/mol \cdot s$, $e_0 = 1\ mol/m^2$ and $s_0 = 1\ mol/m^3$.

described by the Michaelis-Menten kinetic models

$$E_1 + S_1 \underset{k_{-1}}{\overset{k_1}{\rightleftarrows}} C_1 \xrightarrow{k_2} E_1 + S_2, \qquad E_2 + S_2 \underset{k_{-3}}{\overset{k_3}{\rightleftarrows}} C_2 \xrightarrow{k_4} E_2 + P, \tag{2.52}$$

where E_1 is the first enzyme, E_2 is the second enzyme, S_1 is the first substrate, S_2 is the second substrate in the second reaction and also the product of the first reaction, C_1 and C_2 are the complexes and P is the final product, while k_1, k_{-1}, k_2, k_3, k_{-3} and k_4 are constant parameters which represent the rate of the reactions. As in Chapter 1, we denote the concentrations of the chemical species in reactions (2.52)

by their corresponding lower case letters, i.e.,

$$e_1 = [E_1], \quad e_2 = [E_2], \quad s_1 = [S_1], \quad s_2 = [S_2], \quad c_1 = [C_1], \quad c_2 = [C_2], \quad p = [P].$$

The initial conditions are:

$$e_1(0) = e_1^0, \quad e_2(0) = e_2^0, \quad s_1(0) = s_0, \quad s_2(0) = 0, \quad c_1(0) = 0, \quad c_2(0) = 0, \quad p(0) = 0,$$

where e_1^0 and e_2^0 are constants. The differential equations governing the evolution of these concentrations are:

$$\begin{cases} \dfrac{de_1}{dt} = -k_1 e_1 s_1 + (k_2 + k_{-1}) c_1 & \text{(2.53a)} \\ \dfrac{de_2}{dt} = -k_3 e_2 s_2 + (k_4 + k_{-3}) c_2 & \text{(2.53b)} \\ \dfrac{ds_1}{dt} = -k_1 e_1 s_1 + k_{-1} c_1 & \text{(2.53c)} \\ \dfrac{ds_2}{dt} = k_2 c_1 - k_3 e_2 s_2 + k_{-3} c_2 & \text{(2.53d)} \\ \dfrac{dc_1}{dt} = k_1 e_1 s_1 - (k_2 + k_{-1}) c_1 & \text{(2.53e)} \\ \dfrac{dc_2}{dt} = k_3 e_2 s_2 - (k_4 + k_{-3}) c_2 & \text{(2.53f)} \\ \dfrac{dp}{dt} = k_4 c_2. & \text{(2.53g)} \end{cases}$$

Note that the conservation laws for this system are:

$$\begin{cases} e_1 + c_1 = e_1^0 & \text{(2.54a)} \\ e_2 + c_2 = e_2^0 & \text{(2.54b)} \\ s_1 + c_1 + s_2 + c_2 + p = s_0. & \text{(2.54c)} \end{cases}$$

Chapter 4 deals with an experimental problem involving a cascade reaction of the type (2.52), in which the two enzymes are immobilised on an electrode at the bottom

of a flow cell as shown in Figure 2.5. It is assumed that the two enzymes fully cover the surface of the electrode and it is only the total concentration, e, that can be measured experimentally, rather than the individual concentrations, e_1^0 and e_2^0.

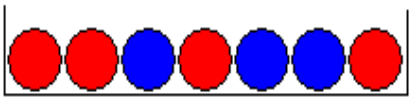

Figure 2.5 – Enzyme immobilisation.

Hence, we let

$$e = e_1^0 + e_2^0, \text{ and } \zeta = \frac{e_1^0}{e_2^0}, \tag{2.55}$$

which gives

$$e_1^0 = \frac{e\zeta}{1+\zeta}, \text{ and } e_2^0 = \frac{e}{1+\zeta}.$$

From the two conservation laws given by equations (2.54a) and (2.54b), and taking into account the fact that the product is uncoupled from all the other chemical reactants, we can reduce system (2.53) to the following four equations,

$$\begin{cases} \dfrac{ds_1}{dt} = -k_1(e_1^0 - c_1)s_1 + k_{-1}c_1 & \text{(2.56a)} \\ \dfrac{ds_2}{dt} = k_2c_1 - k_3(e_2^0 - c_2)s_2 + k_{-3}c_2 & \text{(2.56b)} \\ \dfrac{dc_1}{dt} = k_1(e_1^0 - c_1)s_1 - (k_2 + k_{-1})c_1 & \text{(2.56c)} \\ \dfrac{dc_2}{dt} = k_3(e_2^0 - c_2)s_2 - (k_4 + k_{-3})c_2. & \text{(2.56d)} \end{cases}$$

The concentrations of all the reactants and product are plotted in Figure 2.6.

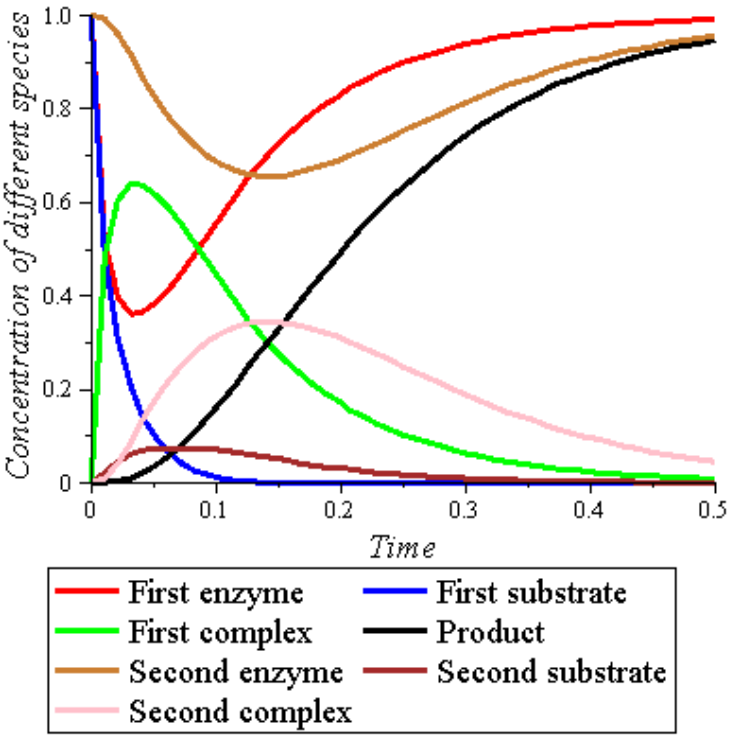

Figure 2.6 – Relative concentrations of reactants and product of the cascade reactions. Typical values for constants used in this simulation are: $k_1 = 10^2\ m^3/mol \cdot s$, $k_{-1} = 10^{-1}\ m^3/mol \cdot s$, $k_2 = 10\ m^3/mol \cdot s$, $k_3 = 10^2\ m^3/mol \cdot s$, $k_{-3} = 10^{-1}\ m^3/mol \cdot s$, $k_4 = 10\ m^3/mol \cdot s$, $e_0 = 1\ mol/m^2$ and $s_0 = 1\ mol/m^3$.

In order to gain a better insight into system (2.56), we introduce the following non-dimensional variables

$$\bar{s_1} = \frac{s_1}{s_0}, \quad \bar{s_2} = \frac{s_2}{s_0}, \quad \bar{c_1} = \frac{c_1}{e}, \quad \bar{c_2} = \frac{c_2}{e}, \quad \bar{t} = \frac{t}{t_0},$$

where $t_0 = 1/(k_1 s_0)$. This gives the non-dimensional system (the bars have been omitted);

$$\begin{cases} \dfrac{ds_1}{dt} = \varepsilon_1 \left(\dfrac{k_{-1}}{k_1 s_0} c_1 - \left(\dfrac{\zeta}{1+\zeta} - c_1 \right) s_1 \right) & \text{(2.57a)} \\ \dfrac{ds_2}{dt} = \varepsilon_1 \left(\dfrac{k_2}{k_1 s_0} c_1 - \dfrac{k_3}{k_1} \left(\dfrac{1}{1+\zeta} - c_2 \right) s_2 + \dfrac{k_{-3}}{k_1 s_0} c_2 \right) & \text{(2.57b)} \\ \dfrac{dc_1}{dt} = \left(\dfrac{\zeta}{1+\zeta} - c_1 \right) s_1 - \dfrac{K_m^1}{s_0} c_1 & \text{(2.57c)} \\ \dfrac{dc_2}{dt} = \dfrac{k_3}{k_1} \left(\dfrac{1}{1+\zeta} - c_2 \right) s_2 - \dfrac{K}{s_0} c_2, & \text{(2.57d)} \end{cases}$$

where

$$\varepsilon_1 = \frac{e}{s_0}, \quad K_m^1 = \frac{k_{-1} + k_2}{k_1}, \quad K = \frac{k_{-3} + k_4}{k_1}, \tag{2.58}$$

with non-dimensional initial conditions

$$s_1(0) = 1, \quad s_2(0) = 0, \quad c_1(0) = 0, \quad c_2(0) = 0.$$

It is easy to see that the equilibrium points of system (2.57) are given by

$$s_1^* = 0, \quad s_2^* = 0, \quad c_1^* = 0, \quad c_2^* = 0, \quad e_1^* = \frac{\zeta}{1+\zeta}, \quad e_2^* = \frac{1}{1+\zeta},$$

where s_1^*, s_2^*, c_1^*, c_2^*, e_1^* and e_2^* denote the equilibrium values of s_1, s_2, c_1, c_2, e_1 and e_2 respectively. The product concentration, p, as given by the original system (2.53) also reaches an equilibrium point which we can determine after non-dimensionalising the conservation law (2.54c), giving $p^* = s_0/e$. We note that, if we had used the reversible form of the Michaelis-Menten scheme (2.26) as studied in Section 2.2, the equilibrium values for the substrates and complexes would have depended on ζ, the initial ratio of the two participating enzymes, which is potentially more useful as it contains more information about the physical system. A similar result is obtained in Chapter 4 when the glucose concentration (s_1) is assumed to be maintained constant at the reaction site.

2.4 Summary

This chapter introduced the mathematical framework for the classical Michaelis-Menten kinetics scheme for enzyme-substrate reactions. This extensively studied model was used here as an illustration for how the law of mass action allows chemical kinetics processes to be expressed in terms of differential equations.

Numerous mathematical studies of the Michaelis-Menten model exist in the literature. For example, we reviewed an elementary singular perturbation analysis which shows that the initial rapid formation of enzyme-substrate complex can be modelled as a boundary layer near the origin. In this framework, the quasi-steady-state assumption (which is widely used in enzyme kinetics for estimating the reaction velocity) is shown to correspond to the outer solution approximation (refer to, for example, [25]). We also analysed a commonly used simplifying assumption made in the context of the Michaelis-Menten kinetic mechanism, namely that the second step of this reaction (the complex dissociation) is irreversible. We found that this simplification leads to qualitatively similar dynamical behaviour to the full reversible model and therefore its usage in mathematical modelling is completely justified. Finally, we introduce cascade reactions involving catalytically linked enzymes which were modelled as two coupled Michaelis-Menten schemes. A simple mathematical formulation in the form of an ordinary differential equations system was given as a preliminary step towards the more detailed analysis presented in Chapter 4.

Chapter 3

Modelling Antibody-Antigen Interactions

In this chapter we construct and analyse mathematical models for antibody-antigen reactions, which are important for understanding bioaffinity devices. We consider three types of immunoassays: the direct assay, the competitive assay (which are analysed with and without diffusion effects) and the sandwich assay.

3.1 The direct assay

This section studies the kinetics of the binding reaction between an antigen and an antibody, with and without modelling of transport effects. This simple reaction is rarely used on its own for diagnostic purposes but lies at the heart of every immunosensing device and so we must study it first.

3.1.1 Simplified model for the direct assay

We start our study of the direct antibody-antigen interactions by ignoring transport of species and concentrating on the kinetics of the reaction. This will result in a simple system of ordinary differential equations model and our aim here is to provide a formula for the equilibrium values of all reactants and products as well as their dependence on initial conditions.

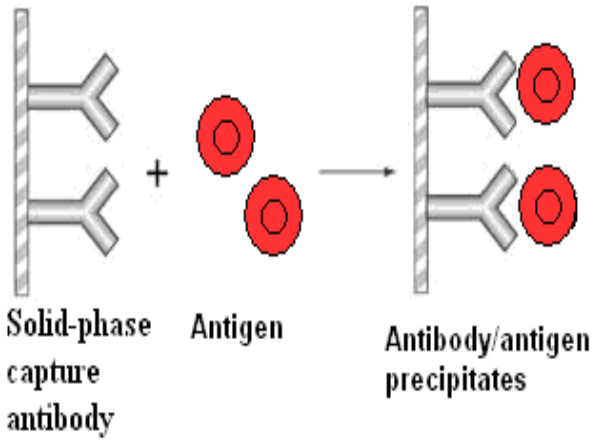

Figure 3.1 – Antibody-antigen interactions.

The antibody-antigen interaction shown in Figure 3.1 can be expressed by the following reaction equation symbolically,

$$A + B \underset{k_-}{\overset{k}{\rightleftarrows}} C, \tag{3.1}$$

where A represents antigen, B represents antibody, and C represents the product of antigen and antibody. Reaction (3.1) has a forward (association) reaction rate of k and a backward (dissociation) reaction rate of k_-, where the forward reaction rate is very

large (around 1000 times bigger than the reaction rate constant k_1 in the Michaelis-Menten kinetics) while the backward reaction is very slow and is therefore often neglected. This fact reflects the high affinity between antigen and its corresponding antibody. We denote the concentration of the chemical species in reaction (3.1) by their corresponding lower case letters, namely

$$a = [A], \quad b = [B], \quad c = [C].$$

The dynamics of the system is described by the following system of ordinary differential equations

$$\begin{cases} \dfrac{da}{dt} = -kab + k_- c & \text{(3.2a)} \\ \dfrac{db}{dt} = -kab + k_- c & \text{(3.2b)} \\ \dfrac{dc}{dt} = kab - k_- c, & \text{(3.2c)} \end{cases}$$

with initial conditions $a(0) = a_0$, $b(0) = b_0$ and $c(0) = 0$, where a_0 and b_0 are constants. Note that in system (3.2),

$$\frac{da}{dt} + \frac{dc}{dt} = 0 \quad \text{and} \quad \frac{db}{dt} + \frac{dc}{dt} = 0;$$

these together with the initial conditions give the associated conservation laws,

$$\begin{cases} a + c = a_0 & \text{(3.3a)} \\ b + c = b_0. & \text{(3.3b)} \end{cases}$$

The ratio k/k_- can be determined experimentally and from the equilibrium condition as

$$\frac{k}{k_-} = \frac{c^*}{a^* b^*}.$$

To non-dimensionalise the system, we introduce the following variables

$$\bar{a} = \frac{a}{b_0}, \quad \bar{b} = \frac{b}{b_0}, \quad \bar{c} = \frac{c}{b_0}, \quad \bar{t} = \frac{t}{t_0},$$

where $\bar{a}$, $\bar{b}$, $\bar{c}$, $\bar{t}$ denote the dimensionless variables, with $t_0 = 1/(kb_0)$. Note that we divide the concentrations of all species by the initial concentration of antibody, b_0, as we will be interested in experimental situations in which a_0 varies and can even take a zero value. Moreover, b_0 is usually known and kept constant throughout the experiment. We obtain the following system of equations, where bars are omitted on all the non-dimensional variables for simplicity,

$$\begin{cases} \dfrac{da}{dt} = -ab + \mu c & \text{(3.4a)} \\ \dfrac{db}{dt} = -ab + \mu c & \text{(3.4b)} \\ \dfrac{dc}{dt} = ab - \mu c, & \text{(3.4c)} \end{cases}$$

with non-dimensional initial conditions $a(0) = \psi$, $b(0) = 1$, $c(0) = 0$, and conservation laws

$$\begin{cases} a + c = \psi & \text{(3.5a)} \\ b + c = 1, & \text{(3.5b)} \end{cases}$$

where

$$\mu = \frac{k_-}{kb_0}, \quad \psi = \frac{a_0}{b_0}. \tag{3.6}$$

Note that $\mu \ll 1$, since the backward reaction is assumed to be much slower than the forward reaction; also, as soon as the experiment is set up, b_0 is fixed, due to the immobilisation of the antibody.

Based on the non-dimensional conservation laws in (3.5), we can reduce system (3.4) down to a single equation in terms of c, namely

$$\frac{dc}{dt} = (\psi - c)(1 - c) - \mu c.$$

Then the equilibrium value for c is given by the quadratic equation

$$c^2 - (1 + \psi + \mu)c + \psi = 0, \tag{3.7}$$

where, from (3.5b), we must select the root which satisfies the condition $c < 1$, which is

$$c = \frac{1}{2}\left(1 + \psi + \mu - \sqrt{(1 + \psi + \mu)^2 - 4\psi}\right). \tag{3.8}$$

This solution is equivalent to that obtained in [30], where a spatially extended model is considered. Note also that if $\mu \ll 1$, the leading order approximation for c is given by

$$c = \frac{1}{2}\left(\psi + 1 - |\psi - 1|\right),$$

which gives different results depending on whether $\psi > 1$ or $\psi < 1$.

In what follows, we derive approximate formulas for the equilibrium values of a, b and c using regular perturbation expansions. Such approximations will allow for a more clear interpretation of these results within the experimental framework. We assume the parameter μ is small and write

$$c = c_0 + \mu c_1 + \mu^2 c_2 + \cdots \tag{3.9}$$

Substituting the expansion (3.9) into equation (3.7), we find that

$$(c_0 + \mu c_1 + \mu^2 c_2 + \cdots)^2 - (1 + \psi + \mu)(c_0 + \mu c_1 + \mu^2 c_2 + \cdots) + \psi = 0. \tag{3.10}$$

Collecting coefficients of like powers of μ, at $O(1)$, we obtain

$$c_0^2 - (1+\psi)c_0 + \psi = 0,$$

which gives

$$c_0 = 1 \text{ or } c_0 = \psi.$$

At $O(\mu)$, we get

$$2c_0c_1 - (1+\psi)c_1 - c_0 = 0,$$

which gives

$$c_1 = \frac{1}{1-\psi} \text{ when } c_0 = 1, \text{ or } c_1 = \frac{\psi}{\psi - 1} \text{ when } c_0 = \psi.$$

This process used to find c_0 and c_1 can be continued to systematically construct the other terms of the asymptotic expansion. The approximation we have calculated so far is

$$c = 1 + \frac{\mu}{1-\psi} + \cdots \tag{3.11}$$

or

$$c = \psi + \frac{\mu\psi}{\psi - 1} + \cdots \tag{3.12}$$

Now since that the solution of c is less than 1 ($c < a_0$ for the dimensional variables), we have to consider these solutions with regard to the following three cases:

- When $\psi > 1$, we choose the solution

$$c = 1 + \frac{\mu}{1-\psi} + \cdots;$$

- When $\psi < 1$, we choose the solution

$$c = \psi + \frac{\mu\psi}{\psi - 1} + \cdots;$$

- When $\psi = 1$, we cannot choose either of the two solutions obtained in equations (3.11) and (3.12), since the two solutions do not allow $\psi = 1$ (we cannot have a zero denominator). Thus, to obtain the solution in this case, we start the asymptotic analysis again with $\psi = 1$ substituted into equation (3.7), which yields

$$c^2 - (2 + \mu)c + 1 = 0. \tag{3.13}$$

It is now more appropriate to use the expansion

$$c = c_0 + \sqrt{\mu}c_1 + \mu c_2 + \mu\sqrt{\mu}c_3 + \cdots \tag{3.14}$$

since we can clearly see that there is an $\sqrt{\mu}$ term contained in equation (3.8), and thus we obtain

$$(c_0 + \sqrt{\mu}c_1 + \mu c_2 + \mu\sqrt{\mu}c_3 + \cdots)^2 - (2 + \mu)(c_0 + \sqrt{\mu}c_1 + \mu c_2 + \mu\sqrt{\mu}c_3 + \cdots) + 1 = 0.$$

Again, by collecting terms in powers of $\sqrt{\mu}$, at $O(1)$, we obtain

$$c_0^2 - 2c_0 + 1 = 0,$$

giving

$$c_0 = 1.$$

At $O(\sqrt{\mu})$, we obtain

$$2c_0c_1 - 2c_1 = 0,$$

which means that c_1 cannot be determined here. At $O(\mu)$, we obtain

$$c_1^2 + 2c_0c_2 - 2c_2 - c_0 = 0,$$

giving

$$c_1 = 1 \text{ or } c_1 = -1.$$

Again, this process used to find c_0 and c_1 can be continued to systematically construct the other terms of the asymptotic expansion. The approximation we have calculated so far is

$$c = 1 - \sqrt{\mu} + \cdots$$

or

$$c = 1 + \sqrt{\mu} + \cdots$$

where $c = 1 + \sqrt{\mu} + \cdots$ cannot be a solution, since $c < 1$.

We now present a summary of the equilibrium values for the antigen, antibody and product in all three cases discussed above.

Case 1: When $a_0 > b_0$ (i.e., $\psi > 1$), the equilibrium solutions are

$$\begin{cases} a = \psi - 1 + \dfrac{\mu}{\psi - 1} + \cdots & \text{(3.15a)} \\ b = \dfrac{\mu}{\psi - 1} + \cdots & \text{(3.15b)} \\ c = 1 - \dfrac{\mu}{\psi - 1} + \cdots & \text{(3.15c)} \end{cases}$$

Case 2: When $a_0 < b_0$ (i.e., $\psi < 1$), the equilibrium solutions are

$$\begin{cases} a = \dfrac{\mu\psi}{1 - \psi} + \cdots & \text{(3.16a)} \\ b = 1 - \psi + \dfrac{\mu\psi}{1 - \psi} + \cdots & \text{(3.16b)} \\ c = \psi - \dfrac{\mu\psi}{1 - \psi} + \cdots & \text{(3.16c)} \end{cases}$$

Case 3: When $a_0 = b_0$ (i.e., $\psi = 1$), the equilibrium solutions are

$$\begin{cases} a = \sqrt{\mu} + \cdots & \text{(3.17a)} \\ b = \sqrt{\mu} + \cdots & \text{(3.17b)} \\ c = 1 - \sqrt{\mu} + \cdots & \text{(3.17c)} \end{cases}$$

In particular, the equilibrium value of the product is

$$c = \begin{cases} 1 - \dfrac{\mu}{\psi - 1} + \cdots, & \text{if } \psi < 1 \\ \psi - \dfrac{\mu\psi}{1 - \psi} + \cdots, & \text{if } \psi > 1 \\ 1 - \sqrt{\mu} + \cdots, & \text{if } \psi = 1. \end{cases} \tag{3.18}$$

We note that the asymptotic expansions derived above are not uniformly valid as they fail within an $O(\mu)$ region about $\psi = 1$. (It is easy to see that within this region, the term $\mu/(\psi - 1)$ becomes $O(1)$). Since b_0 is kept constant, we can view c in equation (3.18) as a function of the initial (non-dimensional) antigen concentration $\psi = a_0/b_0$ and this dependence is plotted in Figure 3.2, together with the exact solution for c given by equation (3.8). The region of non-uniformity for the asymptotic solution is clearly visible in the figure. However, real immunoassay devices generally work under the condition $a_0 > b_0$ ($\psi > 1$) and in this region we have a uniform approximation. The calibration curve would then consist of the increasing right-hand branch of the red graph in Figure 3.2(a). We note that, if $|\psi - 1| > O(\mu)$, then use of the approximation expression (3.18) might offer better insight into the behaviour

of the solution for $\mu \ll 1$, especially for chemistry researchers.

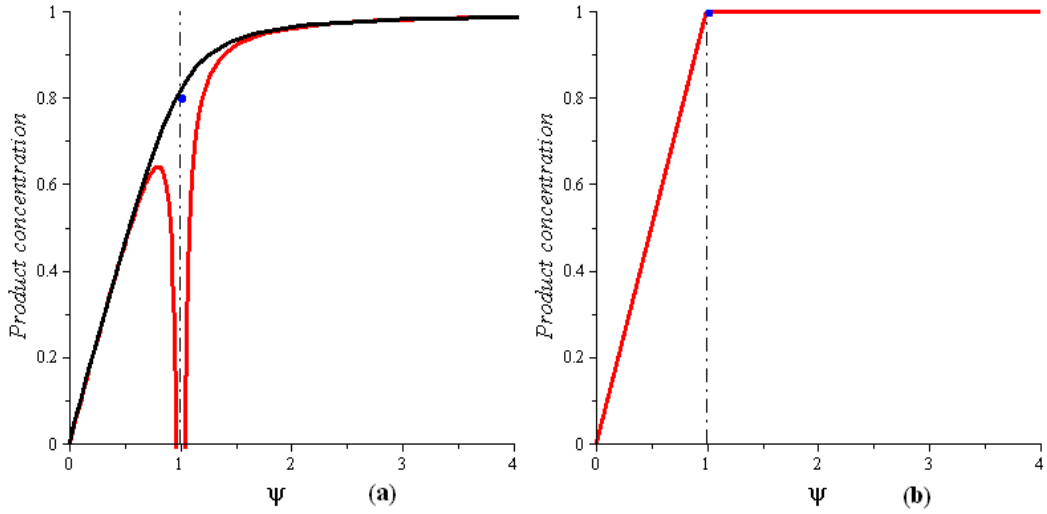

Figure 3.2 – Product concentration as a function of the initial (non-dimensional) antigen concentration ψ. Black curve correspond to the exact solution of c given by equation (3.8), red curves and the blue dot correspond to the approximate solution of c given by equations (3.18). Typical values for constants used in this simulation are: $b_0 = 2$, $k = 100$, $k_- = 8$ in (a) and $k_- = 0$ in (b).

As was expected, the steady states of system (3.4) depend on whether $a_0 > b_0$ or $a_0 < b_0$ (antigen or antibody predominates). If, for example, the concentration of antigen is greater than that of antibody (Case 1), we see from (3.15) that, reverting back to dimensional variables, $b \approx 0$, $c \approx b_0$ and $a \approx a_0 - b_0$, which is intuitively clear. (In other words, the antibody is almost depleted and the concentration of product approaches that of the original antibody concentration.) Note also that, if we ignore the backward reaction and let $\mu = 0$, the steady states in this case become: $b^* = 0$,

$c^* = b_0$ and $a^* = a_0 - b_0$. Similar interpretations are also easily obtained for the solutions in Cases 2 and 3.

3.1.2 Diffusion model for the direct assay

This subsection covers a spatially extended model of direct antibody-antigen interactions, where the two species are contained within a small cell (which we represent mathematically as a one-dimensional spatial domain). More specifically, we consider the case when the antibody is immobilised on a surface while the antigen is free to diffuse before the interaction between the two species. The resulting model is closely related to the work in [30] and [31], where it was presented as a simplified description (ignoring competitive effects) of a Fluorescence Capillary-Fill Device, a type of pregnancy test studied in [32]. We mention some of the mathematical results obtained in [30] and [31], but the emphasis of this section is on obtaining an exact formula for the equilibrium states of reactants and products and comparing these results to those of the simplified model in Section 3.1.1.

The time evolution of the antigen concentration can be described by the diffusion equation

$$\frac{\partial a(x,t)}{\partial t} = D\frac{\partial^2 a(x,t)}{\partial x^2},\ x \in (0,d),\ t \geq 0,$$

where $x = 0$ represents the free surface of the cell and $x = d$ is the bottom of the cell where the antibody is immobilised, with initial condition

$$a(x,0) = a_0.$$

The boundary conditions are:

$$\frac{\partial a(0,t)}{\partial x} = 0,$$
$$D\frac{\partial a(d,t)}{\partial x} = k_{-}c(t) - ka(d,t)(b_0 - c(t)),$$

at the top and bottom of the solution respectively, together with the conservation law

$$\int_0^d a(x,t)dx + c(t) = a_0 d, \quad t \geq 0,$$

where D is the diffusion coefficient for antigen, which has units of m^2/s. The concentration a_0 has units of $moles/m^3$, while b_0 has units of $moles/m^2$. To non-dimensionalise the system, we introduce the following variables

$$\bar{x} = \frac{x}{d}, \quad \bar{t} = \frac{Dt}{d^2}, \quad \bar{a}(\bar{x},\bar{t}) = \frac{da(x,t)}{b_0}, \quad \text{and} \quad \bar{c}(\bar{t}) = \frac{c(t)}{b_0},$$

then we obtain the non-dimensional system as shown below (bars on non-dimensional variables are omitted for simplicity),

$$\begin{cases} \dfrac{\partial a(x,t)}{\partial t} = \dfrac{\partial^2 a(x,t)}{\partial x^2} & \text{(3.19a)} \\ a(x,0) = \psi_1 & \text{(3.19b)} \\ \dfrac{\partial a(0,t)}{\partial x} = 0 & \text{(3.19c)} \\ \dfrac{\partial a(1,t)}{\partial x} = \gamma(\mu_1 c(t) - a(1,t)(1-c(t))) & \text{(3.19d)} \\ c(t) + \displaystyle\int_0^1 a(x,t)dx = \psi_1, & \text{(3.19e)} \end{cases}$$

where $x \in (0,1)$ and we define

$$\psi_1 = \frac{a_0 d}{b_0}, \quad \gamma = \frac{dkb_0}{D}, \quad \mu_1 = \frac{k_{-}d}{kb_0}. \tag{3.20}$$

Next, we are going to analyse system (3.19) as $t \to \infty$. At equilibrium,

$$\frac{\partial a(x,t)}{\partial t} = 0, \tag{3.21}$$

which gives

$$\frac{\partial^2 a(x,t)}{\partial x^2} = 0 \tag{3.22}$$

from equation (3.19a). Then integrating equation (3.22) twice, we obtain

$$a^*(x) = B, \tag{3.23}$$

where $a^*(x)$ denotes the equilibrium value of $a(x,t)$, and B is the constant of integration. From equation (3.19d) together with equation (3.23), we get

$$\mu_1 c^* - B(1 - c^*) = 0; \tag{3.24}$$

also, from equation (3.19e), we get

$$c^* + B = \psi_1, \tag{3.25}$$

where c^* represents the equilibrium value of $c(t)$. Then if we solve the system formed by equations (3.24) and (3.25), we obtain the equilibrium solution of the product concentration as

$$c^* = \frac{1}{2}\left(1 + \mu_1 + \psi_1 - \sqrt{(1 + \mu_1 + \psi_1)^2 - 4\psi_1}\right). \tag{3.26}$$

Note that the steady-state given above for the diffusion system is identical to the equilibrium value obtained in equation (3.8) for the spatially-independent case, if we allow for the slight differences in the definitions of μ_1, ψ_1 (see equation (3.20)) and μ, ψ (see equation (3.6)).

In what follows, we obtain an equivalent formulation of the diffusion system (3.19) in the form of a nonlinear Volterra integro-differential equation. We follow the approach suggested in [30] and use Laplace transforms as shown below.

If we take the Laplace transform of equation (3.19a) with respect to t, we get

$$L_t\left[\frac{\partial a(x,t)}{\partial t}\right] = L_t\left[\frac{\partial^2 a(x,t)}{\partial x^2}\right],$$

giving

$$\int_0^\infty \frac{\partial a(x,t)}{\partial t} t e^{-st}\partial t = \int_0^\infty \frac{\partial^2 a(x,t)}{\partial x^2} e^{-st}\partial t,$$

and therefore

$$\int_0^\infty e^{-st}\partial a(x,t) = \frac{\partial^2}{\partial x^2}\int_0^\infty a(x,t)e^{-st}\partial t,$$

so that

$$\left[e^{-st}a(x,t)\right]_0^\infty - \int_0^\infty a(x,t)(-s)e^{-st}\partial t = \frac{\partial^2}{\partial x^2}\widehat{a}(x,s),$$

and finally,

$$-a(x,0) + s\int_0^\infty a(x,t)e^{-st}\partial t = \frac{\partial^2}{\partial x^2}\widehat{a}(x,s).$$

Now, by using equation (3.19b), we obtain

$$\frac{\partial^2}{\partial x^2}\widehat{a}(x,s) - s\widehat{a}(x,s) + \psi_1 = 0, \tag{3.27}$$

where $\widehat{a}(x,s)$ represents the Laplace transform of the function $a(x,t)$ with respect to t. It can be seen that the non-homogeneous second-order linear equation (3.27) has the general solution

$$\widehat{a}(x,s) = Me^{\sqrt{s}x} + Ne^{-\sqrt{s}x} + \frac{\psi_1}{s}, \tag{3.28}$$

where M and N are functions of s. Partially differentiate equation (3.28) to get

$$\frac{\partial \widehat{a}(x,s)}{\partial x} = M\sqrt{s}e^{\sqrt{s}x} - N\sqrt{s}e^{-\sqrt{s}x},$$

which gives

$$\frac{\partial \widehat{a}(0,s)}{\partial x} = M\sqrt{s} - N\sqrt{s}, \tag{3.29}$$

and taking the Laplace transform of (3.19c) with respect to t to obtain

$$L_t\left[\frac{\partial a(0,t)}{\partial x}\right] = L_t\left[0\right],$$

which gives

$$\frac{\partial \widehat{a}(0,s)}{\partial x} = 0.$$

Thus, equation (3.29) becomes

$$M\sqrt{s} - N\sqrt{s} = 0,$$

which gives

$$M = N,$$

and therefore

$$\frac{\partial \widehat{a}(x,s)}{\partial x} = N\sqrt{s}\left(e^{\sqrt{s}x} - e^{-\sqrt{s}x}\right). \tag{3.30}$$

Also, equation (3.28) gives

$$\widehat{a}(x,s) - \frac{\psi_1}{s} = N\left(e^{\sqrt{s}x} + e^{-\sqrt{s}x}\right). \tag{3.31}$$

Dividing equation (3.31) by (3.30) yields

$$\frac{\widehat{a}(x,s) - \frac{\psi_1}{s}}{\frac{\partial \widehat{a}(x,s)}{\partial x}} = \frac{e^{\sqrt{s}x} + e^{-\sqrt{s}x}}{\sqrt{s}\left(e^{\sqrt{s}x} - e^{-\sqrt{s}x}\right)} = F(x,s),$$

which gives

$$\widehat{a}(x,s) = F(x,s)\frac{\partial \widehat{a}(x,s)}{\partial x} + \frac{\psi_1}{s}. \tag{3.32}$$

Now, take the inverse Laplace transform of (3.32) to obtain

$$L_t^{-1}\left[\widehat{a}(x,s)\right] = L_t^{-1}\left[F(x,s)\frac{\partial \widehat{a}(x,s)}{\partial x}\right] + L_t^{-1}\left[\frac{\psi_1}{s}\right],$$

which gives

$$a(x,t) = L_t^{-1}\left[F(x,s)\right] * L_t^{-1}\left[\frac{\partial \widehat{a}(x,s)}{\partial x}\right] + \psi_1,$$

(by the convolution theorem for Laplace transform). We let

$$\tilde{f}(x,t) = L_t^{-1}[F(x,s)] \tag{3.33}$$

to obtain

$$a(x,t) = \tilde{f}(x,t) * \frac{\partial a(x,t)}{\partial x} + \psi_1,$$

and hence

$$a(1,t) = \int_0^t f(t-s)\frac{\partial a(1,s)}{\partial x}ds + \psi_1, \tag{3.34}$$

where $f(t) = \tilde{f}(1,t)$. Substituting equation (3.34) into (3.19d), we get

$$\frac{\partial a(1,t)}{\partial x} = \gamma\left(\mu_1 c(t) - (1-c(t))\left(\int_0^t f(t-s)\frac{\partial a(1,s)}{\partial x}ds + \psi_1\right)\right). \tag{3.35}$$

Differentiating equation (3.19e) with respect to t, we obtain

$$\frac{dc(t)}{dt} + \int_0^1 \frac{\partial a(x,t)}{\partial t}dx = 0,$$

and then using equations (3.19a) and (3.19c), we get

$$\frac{dc(t)}{dt} = -\frac{\partial a(1,t)}{\partial x}, \tag{3.36}$$

which, together with (3.35) gives

$$\frac{dc(t)}{dt} = -\gamma\mu_1 c(t) + \gamma\psi_1 (1 - c(t)) + \gamma (1 - c(t)) \int_0^t f(t-s) \frac{\partial a(1,s)}{\partial x} ds. \tag{3.37}$$

Using equation (3.36), we also get

$$-\frac{dc(s)}{ds} = \frac{\partial a(1,s)}{\partial x}, \tag{3.38}$$

and, substituting equation (3.38) into (3.37) yields the following Volterra integro-differential equation, namely

$$\frac{dc(t)}{dt} = \gamma\psi_1 - \gamma(\mu_1 + \psi_1)c(t) - \gamma(1 - c(t)) \int_0^t f(t-s) \frac{dc(s)}{ds} ds, \tag{3.39}$$

where the kernel $f(t)$ can be calculated from equation (3.33), namely

$$\tilde{f}(x,t) = L_t^{-1}[F(x,s)],$$

which gives

$$\tilde{f}(x,t) = L_t^{-1} \left[\frac{1}{\sqrt{s}} \frac{1 + e^{-2\sqrt{s}x}}{1 - e^{-2\sqrt{s}x}} \right]. \tag{3.40}$$

Using the geometric series formula

$$\frac{1}{1-x} = 1 + x + x^2 + x^3 + \cdots = \sum_{n=0}^{\infty} x^n, \text{ for } |x| < 1,$$

we can write equation (3.40) as

$$\begin{aligned} \tilde{f}(x,t) &= L_t^{-1} \left[\frac{1}{\sqrt{s}} (1 + e^{-2\sqrt{s}x}) \sum_{n=0}^{\infty} e^{-2\sqrt{s}nx} \right] \\ &= L_t^{-1} \left[\frac{1}{\sqrt{\pi}} \sum_{n=0}^{\infty} \left(\sqrt{\frac{\pi}{s}} e^{-2(n+1)\sqrt{s}x} + \sqrt{\frac{\pi}{s}} e^{-2n\sqrt{s}x} \right) \right]. \end{aligned} \tag{3.41}$$

From the theory of Laplace transforms (refer to, for example [33]), we know that

$$L \left[x^{-\frac{1}{2}} e^{-\frac{a}{4x}} \right] = \sqrt{\frac{\pi}{s}} e^{-\sqrt{as}},$$

and hence, we can write equation (3.41) as

$$\tilde{f}(x,t) = \frac{1}{\sqrt{\pi t}} \sum_{n=0}^{\infty} \left(e^{-\frac{(n+1)^2 x^2}{t}} + e^{-\frac{n^2 x^2}{t}} \right) = \frac{1}{\sqrt{\pi t}} \left(1 + 2 \sum_{n=1}^{\infty} e^{-\frac{n^2 x^2}{t}} \right),$$

which gives the kernel

$$f(t) = \tilde{f}(1,t) = \frac{1}{\sqrt{\pi t}} \left(1 + 2 \sum_{n=1}^{\infty} e^{-\frac{n^2}{t}} \right). \tag{3.42}$$

We have obtained the integro-differential equation (3.39) as an equivalent formulation for system (3.19). As illustrated in [30], [31] and [34], this Volterra integro-differential equation is more amenable to both analytical and numerical studies.

In what follows, we find an approximation for $c(t)$, the product concentration, using a regular perturbation method. Consider an analytic expansion for $c(t)$ of the form

$$c(t) = c^0(t) + \varepsilon_2 c^1(t) + \cdots \tag{3.43}$$

where

$$\varepsilon_2 = \frac{1}{\psi_1} = \frac{b_0}{a_0 d}$$

as suggested in [30], which assumed that γ is order ε, with $\gamma = \gamma\psi_1\varepsilon$, $\gamma\psi_1$ and $\gamma\mu_1$ are of order 1. The non-dimensional parameter ε_2 can be considered small as the antibody sites are usually limited, and is more appropriate for the subsequent perturbation analysis than the parameter μ used previously. Substituting the expansion (3.43) into (3.39), at $O(1)$, we obtain

$$\frac{dc^0(t)}{dt} = \gamma\psi_1 - \gamma(\mu_1 + \psi_1)c^0(t), \tag{3.44}$$

which is a first-order ordinary differential equation, with initial condition $c(0) = 0$. Its solution is

$$c^0(t) = \frac{\psi_1}{\mu_1 + \psi_1}(1 - e^{-\gamma(\mu_1+\psi_1)t}). \tag{3.45}$$

Similarly, taking the $O(\varepsilon_2)$ terms, we obtain

$$\frac{dc^1(t)}{dt} = -\gamma(\mu_1 + \psi_1)c^1(t) - \gamma\psi_1(1 - c^0(t)) \int_0^t f(t-s)\frac{dc^0(s)}{ds}ds. \tag{3.46}$$

Now insert equation (3.45) into (3.46) to get

$$\begin{aligned} \frac{dc^1(t)}{dt} &= -\gamma(\mu_1 + \psi_1)c^1(t) \\ -\gamma^2\psi_1^2 \left(1 - \frac{\psi_1}{\mu_1 + \psi_1}(1 - e^{-\gamma(\mu_1+\psi_1)t})\right) &\int_0^t f(t-s)e^{-\gamma(\mu_1+\psi_1)s}ds. \end{aligned} \tag{3.47}$$

Again, (3.47) is a first-order ordinary differential equation which can be solved to obtain

$$c^1(t) = -\frac{\gamma^2\psi_1^3}{\mu_1 + \psi_1}e^{-\gamma(\mu_1+\psi_1)t} \int_0^t \int_0^u \left(\frac{\mu_1}{\psi_1}e^{\gamma(\mu_1+\psi_1)u} + 1\right) f(u-s)e^{-\gamma(\mu_1+\psi_1)s}dsdu. \tag{3.48}$$

The double integral in equation (3.48) can be simplified as follows by changing the order of integration

$$\int_0^t \int_s^t \left(\frac{\mu_1}{\psi_1}e^{\gamma(\mu_1+\psi_1)u} + 1\right) f(u-s)e^{-\gamma(\mu_1+\psi_1)s}duds.$$

Now apply the transformation of $u = v + s$, we obtain

$$\begin{aligned} &\int_0^t \int_0^{t-s} \left(\frac{\mu_1}{\psi_1}e^{\gamma(\mu_1+\psi_1)(v+s)} + 1\right) f(v)e^{-\gamma(\mu_1+\psi_1)s}dvds \\ &= \int_0^t e^{-\gamma(\mu_1+\psi_1)s} \int_0^{t-s} \left(\frac{\mu_1}{\psi_1}e^{\gamma(\mu_1+\psi_1)(v+s)} + 1\right) f(v)dvds \\ &= \int_0^t e^{-\gamma(\mu_1+\psi_1)s} \left(\frac{\mu_1}{\psi_1}e^{\gamma(\mu_1+\psi_1)s} \int_0^{t-s} e^{\gamma(\mu_1+\psi_1)v}f(v)dv + \int_0^{t-s} f(v)dv\right) ds \end{aligned}$$

$$= \frac{\mu_1}{\psi_1} \int_0^t \int_0^{t-s} e^{\gamma(\mu_1+\psi_1)v} f(v)dvds + \int_0^t e^{-\gamma(\mu_1+\psi_1)s} \int_0^{t-s} f(v)dvds,$$

and changing the order of integration again, yields

$$\frac{\mu_1}{\psi_1} \int_0^t \int_0^{t-v} e^{\gamma(\mu_1+\psi_1)v} f(v)dvds + \int_0^t \int_0^{t-v} e^{-\gamma(\mu_1+\psi_1)s} f(v)dvds$$

$$= \frac{\mu_1}{\psi_1} \int_0^t \left(\int_0^{t-v} ds \right) e^{\gamma(\mu_1+\psi_1)v} f(v)dv + \int_0^t \left(\int_0^{t-v} e^{-\gamma(\mu_1+\psi_1)s} ds \right) f(v)dv$$

$$= \frac{\mu_1}{\psi_1} \int_0^t (t-v) e^{\gamma(\mu_1+\psi_1)v} f(v)dv + \int_0^t \left(\frac{e^{-\gamma(\mu_1+\psi_1)s}}{-\gamma(\mu_1+\psi_1)} \right)_0^{t-v} f(v)dv$$

$$= \frac{\mu_1}{\psi_1} \int_0^t (t-v) e^{\gamma(\mu_1+\psi_1)v} f(v)dv + \int_0^t \frac{1}{\gamma(\mu_1+\psi_1)} \left(1 - e^{-\gamma(\mu_1+\psi_1)(t-v)}\right) f(v)dv$$

$$= \frac{1}{\gamma(\mu_1+\psi_1)} \int_0^t \left(\frac{\gamma(\mu_1+\psi_1)\mu_1}{\psi_1} (t-v) e^{\gamma(\mu_1+\psi_1)v} + 1 - e^{-\gamma(\mu_1+\psi_1)(t-v)} \right) f(v)dv.$$

Therefore,

$$c^1(t) = -\frac{\gamma\psi_1^3}{(\mu_1+\psi_1)^2} e^{-\gamma(\mu_1+\psi_1)t}$$

$$\times \int_0^t \left(\frac{\gamma(\mu_1+\psi_1)\mu_1}{\psi_1} (t-v) e^{\gamma(\mu_1+\psi_1)v} + 1 - e^{-\gamma(\mu_1+\psi_1)(t-v)} \right) f(v)dv,$$

which together with equation (3.45), gives an approximation of the function $c(t)$ that can be evaluated numerically.

3.2 The competitive assay

Competitive binding immunoassays are based on antibody-antigen interactions in which the number of antigen binding sites on the antibody is limited. The antigen and a labelled analogue are incubated together with a fixed concentration of the antibody and the signal produced will reflect the competition between the antigen and

analogue for binding to the antibody. This method requires that the antibody should have the same binding affinity for the antigen as for the labelled analogue; we also assume that the probability of binding to antibody is the same for both species.

3.2.1 Simplified model for the competitive assay

As in the previous section, we start by studying the kinetics of the chemical reactions in a competitive assay in the absence of any transport effects. The antibody-antigen interactions with competition can be expressed symbolically as

$$A + B \underset{k_-}{\overset{k}{\rightleftarrows}} C, \qquad A^{'} + B \underset{k_-}{\overset{k}{\rightleftarrows}} C^{'}, \tag{3.49}$$

where A, B and C are the same as defined in Section 3.1.1; $A^{'}$ is basically the antigen with a label attached to it called an *analogue*, and $C^{'}$ is the product formed by the antibody and analogue. We assume the two reactions have the same forward and backward rate constants of k and k_-, and we denote the concentration of all reactants and products by their corresponding lower case letters, namely

$$a = [A], \quad a^{'} = [A^{'}], \quad b = [B], \quad c = [C], \quad c^{'} = [C^{'}].$$

The dynamics of the system is described by the following system of ordinary differential equations

$$\begin{cases} \dfrac{da}{dt} = -kab + k_{-}c & \text{(3.50a)} \\ \dfrac{da^{'}}{dt} = -ka^{'}b + k_{-}c^{'} & \text{(3.50b)} \\ \dfrac{db}{dt} = -kb(a + a^{'}) + k_{-}(c + c^{'}) & \text{(3.50c)} \\ \dfrac{dc}{dt} = kab - k_{-}c & \text{(3.50d)} \\ \dfrac{dc^{'}}{dt} = ka^{'}b - k_{-}c^{'}, & \text{(3.50e)} \end{cases}$$

with initial conditions

$$a(0) = a_0, \quad a^{'}(0) = a_0^{'}, \quad b(0) = b_0, \quad c(0) = 0, \quad c^{'}(0) = 0,$$

where a_0, $a_0^{'}$ and b_0 are constants. Also, in system (3.50),

$$\begin{aligned} \frac{db}{dt} + \frac{dc}{dt} + \frac{dc^{'}}{dt} &= 0, \\ \frac{da}{dt} + \frac{dc}{dt} &= 0, \\ \frac{da^{'}}{dt} + \frac{dc^{'}}{dt} &= 0, \end{aligned}$$

which gives the following conservation laws associated with this model, namely

$$\begin{cases} b + c + c^{'} = b_0 & \text{(3.51a)} \\ a + c = a_0 & \text{(3.51b)} \\ a^{'} + c^{'} = a_0^{'}. & \text{(3.51c)} \end{cases}$$

We use a similar non-dimensionalisation strategy as in the previous section, with

$$\bar{a} = \frac{a}{b_0}, \quad \bar{a^{'}} = \frac{a^{'}}{b_0}, \quad \bar{b} = \frac{b}{b_0}, \quad \bar{c} = \frac{c}{b_0}, \quad \bar{c^{'}} = \frac{c^{'}}{b_0}, \quad \bar{t} = \frac{t}{t_0},$$

where $t_0 = 1/(kb_0)$. This yields the following system of dimensionless equations (bars are again omitted on non-dimensional variables for simplicity).

$$\begin{cases} \dfrac{da}{dt} = -ab + \mu c & (3.52a) \\ \dfrac{da^{'}}{dt} = -a^{'}b + \mu c^{'} & (3.52b) \\ \dfrac{db}{dt} = -b(a + a^{'}) + \mu(c + c^{'}) & (3.52c) \\ \dfrac{dc}{dt} = ab - \mu c & (3.52d) \\ \dfrac{dc^{'}}{dt} = a^{'}b - \mu c^{'}. & (3.52e) \end{cases}$$

The non-dimensional initial conditions are:

$$a(0) = \psi, \quad a^{'}(0) = \psi^{'}, \quad b(0) = 1, \quad c(0) = 0, \quad c^{'}(0) = 0,$$

and the non-dimensional conservation laws become

$$\begin{cases} a + c = \psi & (3.53a) \\ a^{'} + c^{'} = \psi^{'} & (3.53b) \\ b + c + c^{'} = 1, & (3.53c) \end{cases}$$

where we define

$$\psi = \frac{a_0}{b_0}, \quad \psi^{'} = \frac{a_0^{'}}{b_0}, \quad \mu = \frac{k_{-}}{kb_0}. \tag{3.54}$$

Using similar calculations to those shown in the previous section, system (3.52) together with the conservation laws (3.53) yield the following equilibrium equation for the antibody concentration, b,

$$b^2 - \left(1 - \psi - \psi^{'} - \mu\right) b - \mu = 0. \tag{3.55}$$

The exact values of the steady states for all the species are as follows:

$$\begin{cases} b = \dfrac{1}{2}\left(1-\psi-\psi^{'}-\mu+\sqrt{(1-\psi-\psi^{'}-\mu)^2+4\mu}\right) & \text{(3.56a)} \\ a = \dfrac{\psi\mu}{\mu+b} & \text{(3.56b)} \\ a^{'} = \dfrac{\psi^{'}\mu}{\mu+b} & \text{(3.56c)} \\ c = \dfrac{\psi b}{\mu+b} & \text{(3.56d)} \\ c^{'} = \dfrac{\psi^{'} b}{\mu+b}. & \text{(3.56e)} \end{cases}$$

We are now going to calculate the asymptotic approximations to these solutions as shown in (3.56), in a manner similar to the previous model. Again we start with an expansion of the form

$$b = \tilde{b_0} + \mu b_1 + \mu^2 b_2 + \cdots \tag{3.57}$$

(we have used the notation $\tilde{b_0}$ for the first term of the expansion in order to avoid confusing it with b_0, the initial antibody concentration). Then substituting equation (3.57) into (3.55), we get

$$(\tilde{b_0} + \mu b_1 + \mu^2 b_2 + \cdots)^2 - \left(1-\psi-\psi^{'}-\mu\right)(\tilde{b_0} + \mu b_1 + \mu^2 b_2 + \cdots) - \mu = 0.$$

By collecting coefficients of powers of μ, at $O(1)$, we obtain

$$\tilde{b_0}^{\,2} - \left(1-\psi-\psi^{'}\right)\tilde{b_0} = 0,$$

which gives

$$\tilde{b_0} = 0 \text{ or } \tilde{b_0} = 1-\psi-\psi^{'}.$$

At $O(\mu)$, we obtain

$$2\tilde{b_0}b_1 + \tilde{b_0} - (1-\psi-\psi^{'})b_1 - 1 = 0,$$

when $\tilde{b_0} = 0$, we get

$$b_1 = \frac{1}{\psi + \psi' - 1};$$

and when $\tilde{b_0} = 1 - \psi - \psi'$, we get

$$b_1 = \frac{\psi + \psi'}{1 - \psi - \psi'}.$$

At $O(\mu^2)$, we obtain

$$b_1^2 + 2\tilde{b_0}b_2 - (1 - \psi - \psi')b_2 + b_1 = 0,$$

and when $\tilde{b_0} = 0$ and $b_1 = 1/(\psi + \psi' - 1)$, we get

$$b_2 = -\frac{\psi + \psi'}{(\psi + \psi' - 1)^3}.$$

The solution we have calculated so far is

$$b = \mu\frac{1}{\psi + \psi' - 1} - \mu^2\frac{\psi + \psi'}{(\psi + \psi' - 1)^3} + \cdots, \quad \text{if} \quad \psi + \psi' > 1,$$

or

$$b = 1 - \psi - \psi' + \mu\frac{\psi + \psi'}{1 - \psi - \psi'} + \cdots, \quad \text{if} \quad \psi + \psi' < 1.$$

In the case where $\psi + \psi' = 1$, we cannot choose either of the two solutions, since the denominators in the solutions are equal to zero. In this case, we have to start the asymptotic analysis again with $\psi + \psi' = 1$ substituted into equation (3.55). Thus the equilibrium values for b are given by the equation

$$b^2 + \mu b - \mu = 0. \tag{3.58}$$

Again, in this case it is more appropriate to use the expansion

$$b = \tilde{b_0} + \sqrt{\mu}b_1 + \mu b_2 + \mu\sqrt{\mu}b_3 + \cdots \tag{3.59}$$

since we can clearly see that there is an $\sqrt{\mu}$ term contained in equation (3.56a). Substituting the new expansion (3.59) into equation (3.58), we obtain the equation

$$(\tilde{b_0} + \sqrt{\mu}b_1 + \mu b_2 + \mu\sqrt{\mu}b_3 + \cdots)^2 + \mu(\tilde{b_0} + \sqrt{\mu}b_1 + \mu b_2 + \mu\sqrt{\mu}b_3 + \cdots) - \mu = 0,$$

and then by collecting coefficients of powers of $\sqrt{\mu}$, at $O(1)$, yields

$$\tilde{b_0} = 0.$$

At $O(\sqrt{\mu})$, we obtain

$$2\tilde{b_0}b_1 = 0,$$

which means that b_1 cannot be determined here. At $O(\mu)$, we get

$$b_1^2 + 2\tilde{b_0}b_2 + \tilde{b_0} - 1 = 0,$$

giving

$$b_1 = 1 \text{ or } b_1 = -1, \text{ since } \tilde{b_0} = 0.$$

At $O(\mu\sqrt{\mu})$, we obtain

$$2\tilde{b_0}b_3 + 2b_1b_2 + b_1 = 0,$$

yielding

$$b_2 = -\frac{1}{2} \text{ for both solutions of } b_1.$$

Therefore, we have the solution

$$b = \sqrt{\mu} - \frac{1}{2}\mu + \cdots$$

or

$$b = -\sqrt{\mu} - \frac{1}{2}\mu + \cdots, \text{ which cannot be a solution, since } b > 0.$$

Now we need to find the solutions for a, $a^{'}$, c and $c^{'}$. From equation (3.52a) and (3.53a), we get

$$\frac{da}{dt} = -ab + \mu(\psi - a),$$

which indicates that the equilibrium value of a can be obtained from the equation

$$ab - \mu(\psi - a) = 0. \tag{3.60}$$

Here, we are going to use the same asymptotic expansion (3.59) for b, and use the expansion for a as

$$a = \tilde{a_0} + \mu a_1 + \mu^2 a_2 + \cdots \tag{3.61}$$

Insert equations (3.57) and (3.61) into (3.60) to obtain

$$(\tilde{a_0} + \mu a_1 + \mu^2 a_2 + \cdots)(\tilde{b_0} + \mu b_1 + \mu^2 b_2 + \cdots) = \mu(\psi - \tilde{a_0} - \mu a_1 - \mu^2 a_2 - \cdots).$$

To find an approximation for a, we need to consider the following three cases by considering the terms in powers of μ.

- When $\psi + \psi^{'} > 1$, we have

$$\tilde{b_0} = 0, \quad \tilde{b_1} = \frac{1}{\psi + \psi^{'} - 1}, \quad \tilde{b_2} = -\frac{\psi + \psi^{'}}{(\psi + \psi^{'} - 1)^3}.$$

At $O(1)$, we obtain

$$\tilde{a_0}\tilde{b_0} = 0,$$

which means $\tilde{a_0}$ cannot be determined here, since $\tilde{b_0} = 0$. At $O(\mu)$, we obtain

$$\tilde{a_0} b_1 + a_1 \tilde{b_0} = \psi - \tilde{a_0},$$

giving

$$\tilde{a_0} = \psi \frac{\psi + \psi^{'} - 1}{\psi + \psi^{'}}, \text{ since } \tilde{b_0} = 0 \text{ and } b_1 = \frac{1}{\psi + \psi^{'} - 1},$$

At $O(\mu^2)$, we obtain

$$\tilde{a_0}b_2 + a_1b_1 + a_2\tilde{b_0} + a_1 = 0,$$

which gives

$$a_1 = \frac{\psi}{(\psi + \psi' - 1)(\psi + \psi')}.$$

Therefore,

$$a = \psi\frac{\psi + \psi' - 1}{\psi + \psi'} + \mu\frac{\psi}{(\psi + \psi' - 1)(\psi + \psi')} + \cdots$$

- When $\psi + \psi' < 1$, we have

$$\tilde{b_0} = 1 - \psi - \psi', \quad b_1 = \frac{\psi + \psi'}{1 - \psi - \psi'}.$$

At $O(1)$, we obtain

$$\tilde{a_0}\tilde{b_0} = 0,$$

giving

$$\tilde{a_0} = 0, \text{ since } \tilde{b_0} \neq 0.$$

At $O(\mu)$, we obtain

$$\tilde{a_0}b_1 + a_1\tilde{b_0} = \psi - \tilde{a_0},$$

which gives

$$a_1 = \frac{\psi}{1 - \psi - \psi'}, \text{ since } \tilde{b_0} = 1 - \psi - \psi'.$$

Therefore,

$$a = \mu\frac{\psi}{1 - \psi - \psi'} + \cdots$$

- When $\psi + \psi' = 1$, we have

$$\tilde{b_0} = 0, \quad \tilde{b_1} = 1, \quad \tilde{b_2} = -\frac{1}{2}.$$

Note the change of power series used for a in this case. At $O(1)$, we obtain

$$\tilde{a_0}\tilde{b_0} = 0,$$

which means that $\tilde{a_0}$ cannot be determined here, since $\tilde{b_0} = 0$. At $O(\sqrt{\mu})$, we obtain

$$\tilde{a_0}b_1 + a_1\tilde{b_0} = 0,$$

which gives

$$\tilde{a_0} = 0, \text{ since } \tilde{b_0} = 0 \text{ and } b_1 = 1.$$

At $O(\mu)$, we obtain

$$\tilde{a_0}b_2 + a_1b_1 + a_2\tilde{b_0} = \psi - \tilde{a_0},$$

yielding

$$a_1 = \psi, \text{ since } \tilde{b_0} = 0 \text{ and } b_1 = 1.$$

At $O(\mu\sqrt{\mu})$, we obtain

$$\tilde{a_0}b_3 + a_1b_2 + a_2b_1 + a_3\tilde{b_0} + a_1 = 0,$$

which gives

$$a_2 = -\frac{\psi}{2}, \text{ since } b_2 = -\frac{1}{2}.$$

Therefore,

$$a \approx \sqrt{\mu}\psi - \mu\frac{\psi}{2} + \cdots$$

To summarise, the equilibrium solutions for the reactants and products in the three cases discussed above are as follows:

Case 1: When $b_0 < a_0 + a_0^{'}$ (i.e., $\psi + \psi^{'} > 1$), the equilibrium solutions are

$$\begin{cases} a = \psi - \dfrac{\psi}{\psi + \psi'} + \mu \dfrac{\psi}{(\psi + \psi' - 1)(\psi + \psi')} + \cdots & (3.62a) \\ a^{'} = \psi^{'} - \dfrac{\psi^{'}}{\psi + \psi'} + \mu \dfrac{\psi^{'}}{(\psi + \psi' - 1)(\psi + \psi')} + \cdots & (3.62b) \\ b = \dfrac{\mu}{\psi + \psi' - 1} - \mu^2 \dfrac{\psi + \psi^{'}}{(\psi + \psi' - 1)^3} + \cdots & (3.62c) \\ c = \dfrac{\psi}{\psi + \psi'} - \mu \dfrac{\psi}{(\psi + \psi' - 1)(\psi + \psi')} + \cdots & (3.62d) \\ c^{'} = \dfrac{\psi^{'}}{\psi + \psi'} - \mu \dfrac{\psi^{'}}{(\psi + \psi' - 1)(\psi + \psi')} + \cdots & (3.62e) \end{cases}$$

Case 2: When $b_0 > a_0 + a_0^{'}$ (i.e., $\psi + \psi^{'} < 1$), the equilibrium solutions are

$$\begin{cases} a = \mu \dfrac{\psi}{1 - \psi - \psi'} + \cdots & (3.63a) \\ a^{'} = \mu \dfrac{\psi^{'}}{1 - \psi - \psi'} + \cdots & (3.63b) \\ b = 1 - \psi - \psi^{'} + \mu \dfrac{\psi + \psi^{'}}{1 - \psi - \psi'} + \cdots & (3.63c) \\ c = \psi - \mu \dfrac{\psi}{1 - \psi - \psi'} + \cdots & (3.63d) \\ c^{'} = \psi^{'} - \mu \dfrac{\psi^{'}}{1 - \psi - \psi'} + \cdots & (3.63e) \end{cases}$$

Case 3: When $b_0 = a_0 + a_0^{'}$ (i.e., $\psi + \psi^{'} = 1$), the equilibrium solutions are

$$\begin{cases} a = \sqrt{\mu}\psi - \frac{1}{2}\mu\psi + \cdots & \text{(3.64a)} \\ a^{'} = \sqrt{\mu}\psi^{'} - \frac{1}{2}\mu\psi^{'} + \cdots & \text{(3.64b)} \\ b = \sqrt{\mu} - \frac{1}{2}\mu + \cdots & \text{(3.64c)} \\ c = \psi - \sqrt{\mu}\psi + \frac{1}{2}\mu\psi + \cdots & \text{(3.64d)} \\ c^{'} = \psi^{'} - \sqrt{\mu}\psi^{'} + \frac{1}{2}\mu\psi^{'} + \cdots & \text{(3.64e)} \end{cases}$$

Note that if $a_0^{'} = 0$ (i.e., labelled antigen is absent), the assay is no longer a competition system and solutions (3.62)-(3.64) reduce to the solutions (3.15)-(3.17) obtained in Section 3.1.1. Also note that the behaviour of the competitive system is qualitatively different in the three cases discussed above. Case 1 ($b_0 < a_0 + a_0^{'}$) is the case which is most relevant to experiments, since antibody sites are limited so there is a true competition between antigen and analogue. In this case, the equilibrium solutions show that antibody sites are almost depleted while antigen and analogue bind to a ratio equal to that of their initial concentrations. In Case 2 ($b_0 > a_0 + a_0^{'}$), the antibody binding sites are plentiful and so all antigen and analogue molecules will eventually bind and form products.

We now show how these results can be used for constructing calibration curves for competitive systems. The solutions of antibody-antigen interactions with competition model were considered in the case of $b_0 < a_0 + a_0^{'}$, $b_0 > a_0 + a_0^{'}$ and $b_0 = a_0 + a_0^{'}$. In a real-life testing situation, a_0 is unknown, so the analysis below is more appropriate (we assume that b_0 and $a_0^{'}$ are given).

Case I: When $b_0 \leq a_0^{'}$ (i.e., $\psi^{'} > 1$); this implies

$$b_0 < a_0 + a_0^{'} \text{ or } \psi + \psi^{'} > 1,$$

since a_0 is positive. The solution in this case is identical to the solution obtained in equation (3.62) presented above. The expression of the labelled product in terms of ψ and $\psi^{'}$ is given by

$$c^{'} = \frac{\psi^{'}}{\psi + \psi^{'}} - \mu \frac{\psi^{'}}{(\psi + \psi^{'} - 1)(\psi + \psi^{'})} + \cdots$$

We plot $c^{'}$ against ψ, as given by the proceeding formula, to get the calibration curve (red) in Figure 3.3. This is compared with the plot of the exact solution (black) given by equation (3.56e) and the two curves are in good agreement for $\mu \ll 1$. Note that, since $\psi^{'} > 1$, the asymptotic approximation in this case is uniformly valid for all values of $\psi > 0$.

Case II: When $b_0 > a_0^{'}$ (i.e., $\psi^{'} < 1$), we need to consider the following two situations;

- If $b_0 > a_0 + a_0^{'}$ then $\psi < 1 - \psi^{'}$, and the solution for $c^{'}$ is given by equation (3.63e) (Case 2 in the previous analysis);
- If $b_0 < a_0 + a_0^{'}$ then $\psi > 1 - \psi^{'}$, and the solution for $c^{'}$ is given by equation (3.62e) (Case 1 in the previous analysis).

Therefore, we conclude the solution for $c^{'}$ is given by

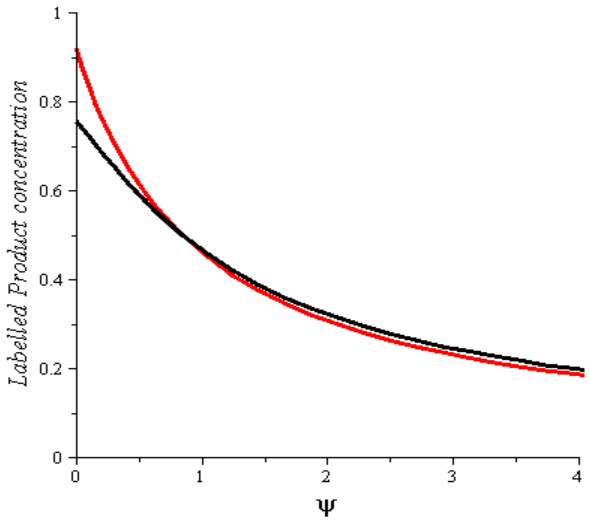

Figure 3.3 – Exact value (black) and asymptotic approximation (red) for the labelled product as functions of ψ in Case I. Typical values for constants used in this simulation are: $b_0 = 1$, $a_0^{'} = 1$, $k = 100$ and $k_{-} = 8$.

$$c^{'} = \begin{cases} \dfrac{\psi^{'}}{\psi + \psi^{'}} - \mu \dfrac{\psi^{'}}{(\psi + \psi^{'} - 1)(\psi + \psi^{'})} + \cdots , & \text{if } \psi + \psi^{'} > 1 \ (b_0 < a_0 + a_0^{'}) \\ \psi^{'} - \mu \dfrac{\psi^{'}}{1 - \psi - \psi^{'}} + \cdots , & \text{if } \psi + \psi^{'} < 1 \ (b_0 > a_0 + a_0^{'}) \\ \psi^{'} - \sqrt{\mu}\psi^{'} + \dfrac{1}{2}\mu\psi^{'} + \cdots , & \text{if } \psi + \psi^{'} = 1 \ (b_0 = a_0 + a_0^{'}). \end{cases}$$

Combining these three solution branches, we obtain the plots shown in Figure 3.4, which are shown together with the exact solution for $c^{'}$ given by equation (3.56e).

We make the same remark as in the case of direct assays, namely that the asymptotic approximation for $c^{'}$ in this case is not uniformly valid around $\psi = 1 - \psi^{'}$. Once again, the restriction $\psi + \psi^{'} > 1$ applies in most practical situations so that non-uniformity will not be relevant in this region. Note also that, when $\mu = 0$, the

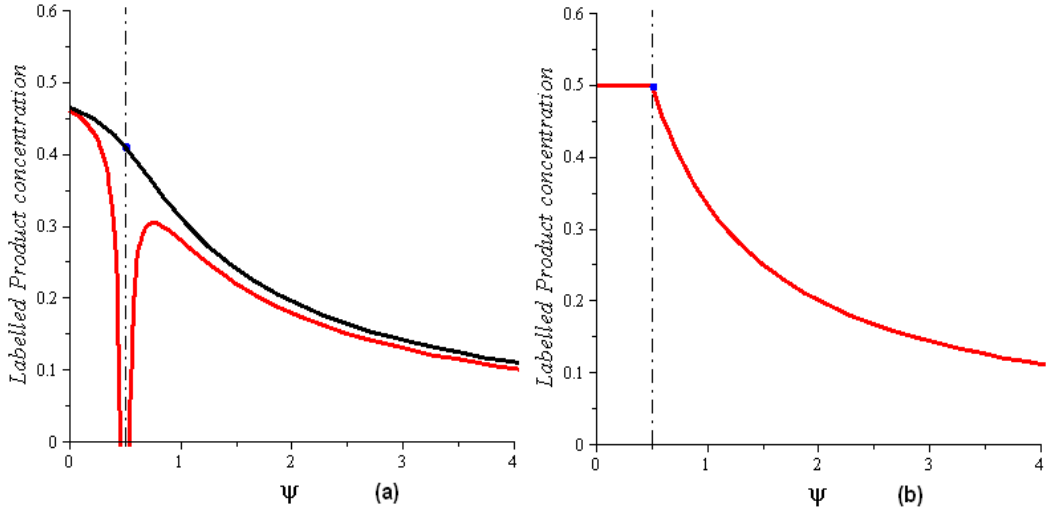

Figure 3.4 – Exact value (black) and asymptotic approximation (red) for the labelled product as functions of ψ in Case II. Typical values for constants used in this simulation are: $b_0 = 2$, $a_0^{'} = 1$, $k = 100$, $k_- = 8$ in (a) and $k_- = 0$ in (b).

asymptotic approximation is identical to equations in system (3.56).

3.2.2 Diffusion model for the competitive assay

We now consider the case when some of the reactants are free to diffuse within a small cell, modelled as a one-dimensional domain. Just as in Section 3.1.2, we assume that the antibody is immobilised to a surface (in our one-dimensional model this actually corresponds to one point) while the antigen and labelled antigen can move throughout the cell. A consistent system of equations which describes the behaviour of the relevant chemical species is given by

$$\frac{\partial a(x,t)}{\partial t} = D\frac{\partial^2 a(x,t)}{\partial x^2},$$

$$\frac{\partial a^{'}(x,t)}{\partial t} = D\frac{\partial^2 a^{'}(x,t)}{\partial x^2},$$

with $x \in (0,d)$, $t \geq 0$, and initial conditions

$$a(x,0) = a_0,$$

$$a^{'}(x,0) = a_0^{'}.$$

The boundary conditions are:

$$\begin{aligned} \frac{\partial a(0,t)}{\partial x} &= 0, \\ \frac{\partial a^{'}(0,t)}{\partial x} &= 0, \\ D\frac{\partial a(d,t)}{\partial x} &= k_{-}c(t) - ka(d,t)(b_0 - c(t) - c^{'}(t)), \\ D\frac{\partial a^{'}(d,t)}{\partial x} &= k_{-}c^{'}(t) - ka^{'}(d,t)(b_0 - c(t) - c^{'}(t)), \end{aligned} \tag{3.65}$$

together with the conservation laws

$$\int_0^d a(x,t)dx + c(t) = a_0 d, \quad t \geq 0,$$

$$\int_0^d a^{'}(x,t)dx + c^{'}(t) = a_0^{'} d, \quad t \geq 0.$$

Note that this system is a generalisation of the reaction-diffusion problem with non-local boundary conditions presented in Section 3.1.2. A similar problem was analysed in [34], as a generalisation of [30] and [31], which represented a more accurate description of the Fluorescence Capillary-Fill Device of [32]. However, the model studied here is a simpler version of the one in [34] for at least two reasons. Firstly, we have assumed (just as in Section 3.2.1) that the antibody has the same binding affinity for antigen and labelled antigen, which translated as identical sets of rate constants (k and k_{-}) for both reactions. Secondly, the model presented in [34] assumes that the

labelled antigen is initially attached to a wall and is subsequently displaced when the fluid sample is drawn by capillary action into the device. This introduces a new variable into the system discussed above, namely "the wall-bound labelled antigen" and changes the zero-flux boundary condition (3.65) into a reaction boundary condition. This approach is more suited to describing a particular type of test, the Fluorescence Capillary-Fill Device; however, we have decided to treat a more generic type of competitive immunoassay. Moreover, like in the previous section, the emphasis of our work is again on finding the equilibrium state for the products and comparing the results between the spatially restricted and diffusion models. Sometimes, time taken to achieve equilibrium is another interesting aspect.

To non-dimensionalise the system, we introduce the variables

$$\bar{x} = \frac{x}{d}, \quad \bar{t} = \frac{Dt}{d^2}, \quad \bar{a}(\bar{x}, \bar{t}) = \frac{da(x,t)}{b_0}, \quad \bar{c}(\bar{t}) = \frac{c(t)}{b_0},$$
$$\bar{a'}(\bar{x}, \bar{t}) = \frac{da'(x,t)}{b_0}, \quad \bar{c'}(\bar{t}) = \frac{c'(t)}{b_0}.$$

Then we obtain the non-dimensional system as shown below, where bars are omitted again on all of the non-dimensional variables for simplicity; these are

$$
\begin{cases}
\dfrac{\partial a(x,t)}{\partial t} = \dfrac{\partial^2 a(x,t)}{\partial x^2} & \text{(3.66a)} \\
\dfrac{\partial a^{'}(x,t)}{\partial t} = \dfrac{\partial^2 a^{'}(x,t)}{\partial x^2} & \text{(3.66b)} \\
a(x,0) = \psi_1 & \text{(3.66c)} \\
a^{'}(x,0) = \psi_2 & \text{(3.66d)} \\
\dfrac{\partial a(0,t)}{\partial x} = 0 & \text{(3.66e)} \\
\dfrac{\partial a^{'}(0,t)}{\partial x} = 0 & \text{(3.66f)} \\
\dfrac{\partial a(1,t)}{\partial x} = \gamma \left(\mu_1 c(t) - a(1,t) \left(1 - c(t) - c^{'}(t) \right) \right) & \text{(3.66g)} \\
\dfrac{\partial a^{'}(1,t)}{\partial x} = \gamma \left(\mu_1 c^{'}(t) - a^{'}(1,t) \left(1 - c(t) - c^{'}(t) \right) \right) & \text{(3.66h)} \\
c(t) + \displaystyle\int_0^1 a(x,t)dx = \psi_1 & \text{(3.66i)} \\
c'(t) + \displaystyle\int_0^1 a^{'}(x,t)dx = \psi_2, & \text{(3.66j)}
\end{cases}
$$

with $x \in (0,1)$, $t \geq 0$, and we define

$$
\psi_1 = \frac{a_0 d}{b_0}, \quad \gamma = \frac{dkb_0}{D}, \quad \mu_1 = \frac{k\_d}{kb_0}, \quad \psi_2 = \frac{a_0^{'} d}{b_0}.
$$

Next, we are going to analyse system (3.66) as $t \to \infty$. At equilibrium,

$$
\frac{\partial a(x,t)}{\partial t} = 0,
$$

giving

$$
\frac{\partial^2 a(x,t)}{\partial x^2} = 0 \tag{3.67}
$$

from equation (3.66a). Then integrating (3.67) twice and using (3.66e) gives

$$
a^*(x) = B. \tag{3.68}
$$

Similarly, we obtain

$$a^{'*}(x) = C, \tag{3.69}$$

where $a^*(x)$ and $a^{'*}(x)$ denote the equilibrium values of $a(x,t)$ and $a^{'}(x,t)$ respectively; B and C are constants of integration.

From equations (3.66f), (3.66h) together with (3.66e), (3.66g), (3.68) and (3.69), we get

$$\mu_1 c^* - B(1 - c^* - c^{'*}) = 0, \tag{3.70}$$

and

$$\mu_1 c^{'*} - C(1 - c^* - c^{'*}) = 0. \tag{3.71}$$

Also, from (3.66i) and (3.66j), we get

$$c^* + B = \psi_1, \tag{3.72}$$

and

$$c^{'*} + C = \psi_2. \tag{3.73}$$

Then if we solve the system formed by equations (3.70), (3.71), (3.72) and (3.73) together with the conservation law (3.53c), we obtain the following equilibrium solution for b^*, namely

$$b^* = \frac{1}{2}\left(1 - \mu_1 - \psi_1 - \psi_2 + \sqrt{(1 - \mu_1 - \psi_1 - \psi_2)^2 + 4\mu_1}\right). \tag{3.74}$$

Also, from equations (3.68)-(3.73), we obtain the solutions for $a^*(x)$, $a^{'*}(x)$, c^* and $c^{'*}$ as

$$\begin{cases} a^* = \dfrac{\psi_1 \mu_1}{\mu_1 + b^*} & \text{(3.75a)} \\ a^{'*} = \dfrac{\psi_2 \mu_1}{\mu_1 + b^*} & \text{(3.75b)} \\ c^* = \dfrac{\psi_1 b^*}{\mu_1 + b^*} & \text{(3.75c)} \\ c^{'*} = \dfrac{\psi_2 b^*}{\mu_1 + b^*}, & \text{(3.75d)} \end{cases}$$

which are the same solutions as shown in (3.56) obtained in Section 3.2.1 (since d/b_0 in the diffusion model is equivalent to $1/b_0$ in the non-diffusion model). Using Laplace transforms and their properties we carry out a similar calculation to that given in Section 3.1.2 and obtain the following system of Volterra integro-differential equations:

$$\begin{cases} \dfrac{dc(t)}{dt} = \gamma\psi_1 - \gamma(\mu_1 + \psi_1)c(t) - \gamma\psi_1 c^{'}(t) \\ \qquad\qquad -\gamma\left(1 - c(t) - c^{'}(t)\right)\displaystyle\int_0^t f(t-s)\frac{dc}{ds}(s)ds & \text{(3.76a)} \\ \dfrac{dc^{'}(t)}{dt} = \gamma\psi_2 - \gamma\psi_2 c(t) - \gamma\left(\mu_1 + \psi_2\right)c^{'}(t) \\ \qquad\qquad -\gamma\left(1 - c(t) - c^{'}(t)\right)\displaystyle\int_0^t f(t-s)\frac{dc^{'}}{ds}(s)ds, & \text{(3.76b)} \end{cases}$$

where $f(t)$ has the same definition as in Section 3.1.2. (see (3.42)). Note that in the absence of labelled antigen ($c^{'} = 0$), equation (3.76a) yields the result obtained for the non-competitive assay (see (3.39)).

Adding (3.76a) and (3.76b) yields

$$\begin{aligned} \frac{d(c^{'}(t) + c(t))}{dt} &= \gamma\left(1 - c(t) - c^{'}(t)\right)(\psi_1 + \psi_2) - \gamma\mu_1(c(t) + c^{'}(t)) \\ &\quad -\gamma\left(1 - c(t) - c^{'}(t)\right)\int_0^t f(t-s)\frac{d(c^{'} + c)}{ds}(s)ds, \end{aligned} \tag{3.77}$$

and, if we use the conservation law $c(t) + c^{'}(t) = 1 - b(t)$, we get

$$\frac{db(t)}{dt} = \gamma\mu_1 - \gamma(\mu_1 + \psi_1 + \psi_2)b(t) - \gamma b(t)\int_0^t f(t-s)\frac{db}{ds}(s)ds. \tag{3.78}$$

Once the solution of $b(t)$ is calculated (using, for example, the asymptotic or numerical methods detailed in [30], [31]), the product concentration $c^{'}(t)$ can be determined from equation (3.76b), which yields

$$\frac{dc^{'}(t)}{dt} = -\gamma\mu_1 c^{'}(t) + \gamma b(t)\left(\psi_2 - \int_0^t f(t-s)\frac{dc^{'}}{ds}(s)ds\right). \tag{3.79}$$

Hence, instead of solving a coupled system of integro-differential equations (3.76), we can now solve the independent equation (3.78) followed by equation (3.79). A regular perturbation analysis could be applied to (3.78) and (3.79), which is similar to the one used in Section 3.1.2 to obtain an approximation for $b(t)$ and $c^{'}(t)$.

We conclude that, our assumption of identical rate constants for antibody-antigen and antibody-analogue binding leads to a significant simplification of the problem studied in [34], whereby a coupled system of Volterra integro-differential equations was replaced by an uncoupled one. However, this simplification may not always be feasible since the label attachment may interfere with the antigen's epitope and therefore has to be considered carefully for each experimental setting.

3.3 The sandwich assay

The Sandwich assay (refer to, for example, [3]) is a type of immunoassay in which an antibody for the antigen to be assayed is immobilised to a solid surface (this

antibody is often referred to as the **capture antibody**), then the sample containing the test analyte is added and the reaction has been allowed to reach equilibrium. A second antibody, which has a radioactive or fluorescent label (and is therefore called a **tracer**) is added, sandwiching the antigen. Again, after removal of excess, the amount of bound label is measured. The signal level in this type of assay is clearly proportional to the analyte concentration in the sample, just like in the direct assay. The second antibody may be specific for a different epitope on the antigen, thus enhancing overall specificity, or for the first antibody bound to an antigen. This process is shown in Figure 3.5 and can be symbolically represented by the reactions given by (3.80)-(3.83).

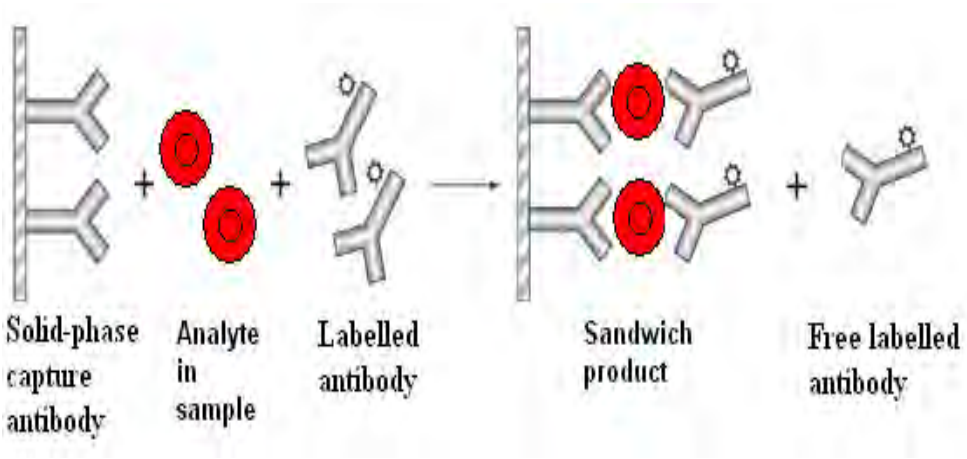

Figure 3.5 – Immunometric immunoassay.

$$A + B_1 \underset{k_{-1}}{\overset{k_1}{\rightleftarrows}} C_1, \tag{3.80}$$

$$D + B_1 \underset{k_{-1}}{\overset{k_1}{\rightleftarrows}} C_2, \tag{3.81}$$

$$A + B_2 \underset{k_{-2}}{\overset{k_2}{\rightleftarrows}} D, \tag{3.82}$$

$$C_1 + B_2 \underset{k_{-2}}{\overset{k_2}{\rightleftarrows}} C_2, \tag{3.83}$$

where A represents antigen, B_1 represents the immobilised antibody (also referred to as capture antibody), B_2 represents the labelled antibody, C_1 is the product of the antigen and immobilised antibody, C_2 is the product of C_1 and labelled antibody (also referred to as the sandwich product), and D is the product of antigen and labelled antibody. The first two reactions have a forward reaction rate of k_1 and a backward reaction rate of k_{-1}, the third and fourth reactions have a forward and backward reaction rate of k_2 and k_{-2} respectively. We have assumed that the affinity of each antibody for the corresponding antigen is the same regardless of whether the antigen is free or bound to another antibody; this simplifying assumption is not essential for the model and could easily be relaxed later. We denote the concentration of the reactants and products by their corresponding lower case letters, i.e.,

$$a = [A], \quad b_1 = [B_1], \quad b_2 = [B_2], \quad c_1 = [C_1], \quad c_2 = [C_2], \quad d = [D],$$

then the initial conditions can be represented as

$$a(0) = \alpha, \quad b_1(0) = \beta_1, \quad b_2(0) = \beta_2, \quad c_1(0) = 0, \quad c_2(0) = 0, \quad d(0) = 0,$$

where α, β_1 and β_2 are constants, such that $\alpha < \beta_1$ and $\alpha < \beta_2$ (under experimental conditions). The kinetic behavior of each reactant is given by the following system of nonlinear differential equations

$$\begin{cases} \dfrac{da}{dt} = -k_1 a b_1 + k_{-1} c_1 - k_2 a b_2 + k_{-2} d & (3.84a) \\ \dfrac{db_1}{dt} = -k_1 a b_1 + k_{-1} c_1 - k_1 b_1 d + k_{-1} c_2 & (3.84b) \\ \dfrac{db_2}{dt} = -k_2 b_2 c_1 + k_{-2} c_2 - k_2 a b_2 + k_{-2} d & (3.84c) \\ \dfrac{dc_1}{dt} = k_1 a b_1 - k_{-1} c_1 - k_2 b_2 c_1 + k_{-2} c_2 & (3.84d) \\ \dfrac{dc_2}{dt} = k_2 b_2 c_1 + k_{-2} c_2 + k_1 b_1 d - k_{-1} c_2 & (3.84e) \\ \dfrac{dd}{dt} = k_2 a b_2 - k_{-2} d - k_1 b_1 d + k_{-1} c_2, & (3.84f) \end{cases}$$

with conservation laws

$$\begin{cases} a + c_1 + c_2 + d = \alpha & (3.85a) \\ b_1 + c_1 + c_2 = \beta_1 & (3.85b) \\ b_2 + c_2 + d = \beta_2. & (3.85c) \end{cases}$$

To non-dimensionalise the system, we introduce the following variables

$$\bar{a} = \frac{a}{\beta_1}, \quad \bar{b_1} = \frac{b_1}{\beta_1}, \quad \bar{b_2} = \frac{b_2}{\beta_1}, \quad \bar{c_1} = \frac{c_1}{\beta_1}, \quad \bar{c_2} = \frac{c_2}{\beta_1}, \quad \bar{d} = \frac{d}{\beta_1}, \tag{3.86}$$

which gives the following non-dimensional system (bars are again omitted on all of the non-dimensional variables for simplicity).

$$\begin{cases} \dfrac{da}{dt} = K_{-1} c_1 + K_{-2} d - a b_1 - K^{'} a b_2 & (3.87a) \\ \dfrac{db_1}{dt} = K_{-1}(c_1 + c_2) - b_1(a + d) & (3.87b) \\ \dfrac{db_2}{dt} = K_{-2}(c_2 + d) - K^{'} b_2(a + c_1) & (3.87c) \\ \dfrac{dc_1}{dt} = a b_1 - K_{-1} c_1 - K^{'} b_2 c_1 + K_{-2} c_2 & (3.87d) \\ \dfrac{dc_2}{dt} = K^{'} b_2 c_1 + b_1 d - (K_{-1} + K_{-2}) c_2 & (3.87e) \\ \dfrac{dd}{dt} = K^{'} a b_2 - K_{-2} d - b_1 d + K_{-1} c_2, & (3.87f) \end{cases}$$

where we let

$$K_{-1} = \frac{k_{-1}}{k_1\beta_1}, \quad K_{-2} = \frac{k_{-2}}{k_1\beta_1}, \quad K^{'} = \frac{k_2}{k_1}. \tag{3.88}$$

The non-dimensional initial conditions and conservation laws are:

$$a(0) = \frac{\alpha}{\beta_1}, \quad b_1(0) = 1, \quad b_2(0) = \frac{\beta_2}{\beta_1}, \quad c_1(0) = 0, \quad c_1(0) = 0, \quad d(0) = 0, \tag{3.89}$$

and

$$\begin{cases} a + c_1 + c_2 + d = \dfrac{\alpha}{\beta_1} & \text{(3.90a)} \\ b_1 + c_1 + c_2 = 1 & \text{(3.90b)} \\ b_2 + c_2 + d = \dfrac{\beta_2}{\beta_1}. & \text{(3.90c)} \end{cases}$$

From the steady state forms of equations (3.87) and the conservation laws (3.90) we find that

$$b_1^2 + \left(\frac{\alpha}{\beta_1} - 1 + K_{-1}\right) b_1 - K_{-1} = 0,$$

$$b_2^2 + \left(\frac{\alpha - \beta_2}{\beta_1} + \frac{K_{-2}}{K'}\right) b_2 - \frac{K_{-2}\beta_2}{K'\beta_1} = 0,$$

and

$$c_2 = \frac{\frac{\beta_2}{\beta_1} b_1 + K^{'} b_2 - (1 + K^{'}) b_1 b_2}{b_1 + K_{-1} + K' b_2 + K_{-3}},$$

where

$$K_{-3} = \frac{k_{-3}}{k_1\beta_1}.$$

Therefore, it is possible to calculate the exact values of the steady states for all the species, provided that all the reaction constants and initial concentrations are accurately known. Some calibration curves, consisting of the steady states of c_2,

$c_2 + d$ and b_2 as functions of initial antigen concentration, α are plotted in Figure 3.6. The reason for plotting these species is that some antibodies have radioactive or fluorescent labels which can be measured both at the surface and in the solution. If the signal is measured at the surface, we need to plot c_2 and compare it with experimental data; however, for signals measured in the solution, it is $c_2 + d$ we are interested in. Note also that over the short initial stage of the reaction, there exists a linear response between the signal and analyte concentration.

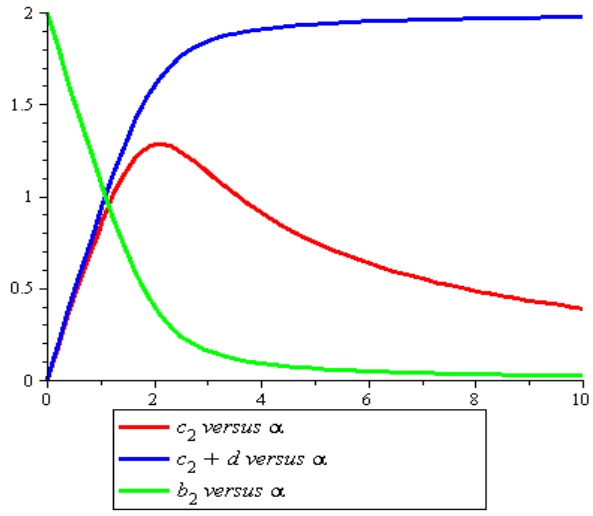

Figure 3.6 – Sandwich product c_2 (red), combined product $c_2 + d$ (blue), and unbound tracer b_2 (green) as functions of initial antigen concentration α. Typical values for constants used in this simulation are: $k_1 = 100$, $k_{-1} = 10$, $k_2 = 100$, $k_{-2} = 10$, $\beta_1 = 2$ and $\beta_2 = 2$.

The performance of a biosensor is often affected by the presence of a **non-specific** (noisy) component of the recorded signal. In the configuration described above, any

measurement of the fluorescent label in solution would inevitably include B_2, which is the amount of labelled antibody left over (or unbound) after the reaction. This is a non-specific measurement as it does not provide any information about the antigen in the sample. We have also plotted b_2, the noise, together with the "good" signals in Figure 3.6.

An alternative modelling strategy is to construct a two-step model. In the first step, we add antigen to the capture antibody and allow the reaction

$$A + B_1 \underset{k_{-1}}{\overset{k_1}{\rightleftarrows}} C_1, \tag{3.91}$$

to proceed to equilibrium. This corresponds to the direct assay model studied in Section 3.1.1, where exact and approximate formulas were obtained for the equilibrium value of C_1. After the unbound antigen is washed away, we construct a second model where the labelled antibody is introduced in the system (which does not contain any free antigen) and reacts with the product C_1 to form C_2,

$$C_1 + B_2 \underset{k_{-2}}{\overset{k_2}{\rightleftarrows}} C_2. \tag{3.92}$$

The equilibrium value of c_2 can then be obtained as a function of c_1 and hence of the initial antigen concentration, a_0. Note that this modelling strategy does not eliminate noise completely as, even after washing, the reversible nature of the reactions (3.91) and (3.92) means that small amounts of free A and C_1 will still be present in the solution. (However, in an experimental setting, washing is always practiced since it greatly reduces these amounts hence minimising non-specific interactions).

The analysis of this two-step model is similar to the one presented above and will not be given here; instead, it will be performed as part of future studies into sandwich bioassays (refer to the conclusions section). What this example illustrates is how, in a simple model, it is possible to distinguish between the specific signal and the noise and we believe that this calculation should bring valuable insight into experimental procedures.

3.4 Summary

In this chapter we analysed several modelling strategies for antibody-antigen interactions with possible applications to immunoassay design. For direct and competitive assays, we constructed two types of mathematical models: **one-point models** which describe only the reaction kinetics and **spatially extended models** which allowed for transport of one or more species to the reaction site. For both these assays (and both types of models) we were able to derive exact formulas for the equilibrium values of all reactants and construct calibration curves, which give the final product as a function of the initial analyte concentration. It was concluded that, for each of the assays considered, both modelling approaches gave identical equilibrium values and hence the biosensor response was the same regardless of whether transport effects were included in the model or not. Therefore, if the value of the equilibrium state is the only piece of information required in an experimental context we would recommend using the simpler model without diffusion. However, in many practical problems, the time taken to achieve equilibrium is also a parameter of interest and, in such cases,

we obviously cannot neglect transport. Our modelling results were found to agree with the results in [30], [31] and [34] which presented more detailed and rigorous mathematical studies of diffusion models for similar direct and competitive assays. As remarked before, the aim of our work in this chapter was to find conditions under which simpler models and studies could be used in the context of antibody-antigen interactions. The last section presented a different type of immunoassay, namely a sandwich assay, for which a simple one-point model was used in order to construct a calibration curve. This example illustrated how mathematical modelling has the potential to evaluate the ratio between specific and non-specific signals in an experimental problem and optimise biosensor performance by identifying parameter regions where the noise is minimal.

Chapter 4

Mathematical Models for Optimising Bi-enzyme Biosensors

In the previous chapter we have seen examples of problems where including diffusion of a reactant into the model only affects the transient behaviour of the system but has no effect on the final steady states of its concentration. It is often the case that the equilibrium values are the only piece of information required for the solution of a practical problem (although, sometimes, time to achieve equilibrium or size of the device is the real issue) and in such situations it is important to identify the conditions under which a complex partial differential equations model can be replaced with a simpler one.

In this chapter, we study a flow injection analysis of a bi-enzyme electrode, with the aim of **finding the ratio of the two enzymes involved which yields the highest current amplitude**. A detailed comparison is given of three mathematical

models (each neglecting different aspects of the biosensor functionality) and we try to recommend the best modelling strategy under various physical conditions. It is expected that, due to the more complex physical configuration of this system, the inclusion of diffusion effects will be important in the modelling process.

4.1 Experimental problem and modelling strategies

The problem we study here is motivated by a series of experiments conducted at the National Centre for Sensor Research (NCSR) and the Biomedical Diagnostics Institute (BDI) at Dublin City University over the past few years by a group of researchers interested in building a biosensing platform based on a bi-enzyme electrode. For more details, we refer the reader to [35], [36], and [37]. This study investigates a model biosensor system which consists of two enzymes immobilised onto an electrode modified with a conducting polymer. The first enzyme, glucose oxidase (GOX), acts as the source of the substrate for the second enzyme, horseradish peroxidase (HRP), producing hydrogen peroxide from the oxidation of glucose to gluconolactone. Horseradish peroxidase is in direct electronic communication with the electrode via the conducting polymer and facilitates the electrocatalytic reduction of hydrogen peroxide, which can be measured amperometrically at moderate reducing potentials. Cascade schemes, where an enzyme is catalytically linked to another enzyme, can produce signal amplification and therefore increase the biosensor efficiency. HRP and GOX have very

different kinetic characteristics (which have been studied extensively) and so obtaining the optimum performance of this biosensing system will depend on the correct ratio of the two enzymes.

HRP and GOX were immobilised together in one step on the polymer-modified electrode. Different solutions containing the two enzymes at different molar ratios were prepared and used to immobilise the enzymes on the electrode. (For more details of the immobilisation procedure, refer to [36] or [37].) After the immobilisation, the electrode was inserted in a flow-cell and an amperometric flow-injection analysis was carried out. Glucose standard solutions at concentrations between 0.5 and 20 mM were then passed over the electrode and the signals recorded. Figure 4.1 (reproduced with permission from [37]) shows a typical amperogram recorded after passing the glucose solutions. Figure 4.2 (also reproduced from [37]) shows a comparison between all the sensitivities of the electrodes with different molar ratios HRP/GOX. It can be clearly seen that these experiments concluded that the electrode prepared with HRP/GOX at a molar ratio of 1:1 yielded the highest sensitivity.

It is known that the GOX enzyme used in the experiments has an activity of 1.7 U/mol protein while the activity of HRP is 5.7 U/mol protein [1]. Therefore HRP is approximately three times more active than GOX and so, it was expected that a platform with a greater amount of GOX than of HRP would be most efficient. The

[1]One unit U of an enzyme is defined as the amount which catalyses the transformation of one μmol of substrate per minute. The enzyme specific activity is a measure of the purity of the enzyme preparation and is defined as the number of enzyme units per mass, U/mg or molar mass, U/mol.

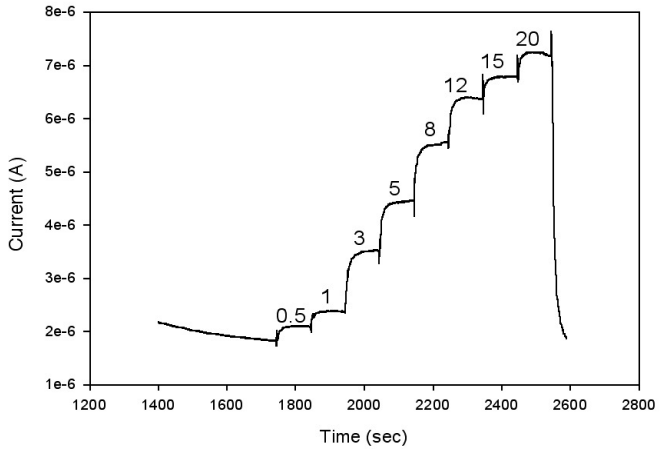

Figure 4.1 – Amperometric responses of a HRP/GOX bi-enzyme electrode to a range of glucose concentrations between 0.5 and 20 mM.

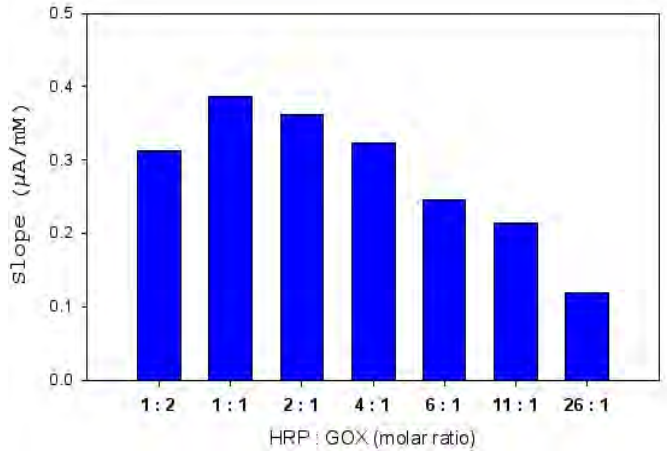

Figure 4.2 – Comparison of HRP/GOX ratio and sensitivity to glucose. The electrode prepared immobilising HRP and GOX at the molar ratio 1:1 yields the highest catalytic signals and the highest sensitivity. The glucose concentration used in this experiment was 20 mM.

fact that the electrode with HRP and GOX present at molar ratio of 1 : 1 produces the highest signals is surprising and leads to the hypothesis that other phenomena might influence the response. Several factors affect the rate at which enzymatic reactions proceed - temperature, pH, enzyme concentration, substrate concentration, and the presence of any inhibitors or activators, also the activity of HRP may be reduced disproportionately as a consequence of its immobilisation on the electrode surface, and its reliance on direct electron transfer.

In attempting to construct a mathematical model for this problem, we make the following simplifying assumptions:

1. The immobilisation mechanisms of the two enzymes are equally efficient and hence the distribution of immobilised HRP and GOX molecules on the surface of the electrode is proportional to that of the solution used.

2. Immobilisation of HRP and GOX produces a geometrically close-packed spherical monolayer which is spatially homogeneous.

3. The electron transfer process is 100% efficient, since this parameter only affects the magnitude of the signals, and not their relative responses.

A cascade reaction takes place at the electrode. Glucose oxidase catalyses the oxidation reaction of glucose to gluconic acid, with production of H_2O_2. HRP is oxidised by hydrogen peroxide and then subsequently reduced by electrons provided by the electrode, as shown in the following abbreviated reaction. These reactions may be

summarised as follows:

$$\beta\text{-D-glucose} + O_2 + H_2O \xrightarrow{\text{GOX}} \text{gluconic acid} + H_2O_2,$$

$$H_2O_2 + \text{HRP} \longrightarrow \text{Compound I} + H_2O,$$

$$\text{Compound I} + 2e^- + H^+ \longrightarrow \text{HRP} + H_2O.$$

We can see that these reactions taking place at the electrode is a biochemical cascade reaction, since the product of the first reaction feeds into the second reaction as the substrate and is then consumed. We are going to use the standard Michaelis-Menten equations (4.1) to model these reactions,

$$E_1 + S_1 \underset{k_{-1}}{\overset{k_1}{\rightleftarrows}} C_1 \xrightarrow{k_2} E_1 + S_2, \qquad E_2 + S_2 \underset{k_{-3}}{\overset{k_3}{\rightleftarrows}} C_2 \xrightarrow{k_4} E_2 + P, \tag{4.1}$$

where E_1 denotes the first enzyme GOX, E_2 denotes the second enzyme HRP, S_1 denotes the first substrate glucose, S_2 denotes the second substrate hydrogen peroxide, C_1 and C_2 are the two complexes and P is the final product. Also, k_1, k_{-1}, k_2, k_3, k_{-3} and k_4 are constant parameters which represent the rate of the reactions as in Section 1.3.

In the following sections we will present three models of varying complexity for analysing this optimisation problem. Numerical and, where possible, analytical solutions will be presented with a view to expressing the steady-state current as a function of the ratio ζ of the two immobilised enzymes and thus finding its maximum value.

The first model, the "comprehensive model" assumes that the two substrates, S_1 and S_2, are free to diffuse in the solution and consists of two diffusion equations with

the relevant nonlinear reaction-type boundary conditions. This model was proposed and solved numerically in [35]. We then jump to the other extreme and ignore all transport phenomena basically reducing the whole problem to the one-point kinetics of the cascade reaction in the second model, the "simplified model". This leads to a system of ordinary differential equations which is analysed using a combination of dynamical systems methods, perturbation techniques and numerical simulations. This model was also studied previously in [36] but the analysis presented here is more comprehensive. Finally, the third model, the "intermediate model" is proposed here for the first time and is a compromise between the two situations discussed above, where we allow one substrate (hydrogen peroxide) to diffuse but assume the other substrate (glucose) is only present at the reaction point (that is, the electrode). This leads to a simpler system in comparison with the first model, consisting of one diffusion equation with nonlinear boundary conditions.

It is perhaps instructive to give some motivations regarding the choice of these three models and discuss expectations. Based on our experience from previous chapters, we expect that the diffusion of S_1 (glucose) to the reaction site will not affect the equilibrium state except by increasing the time it takes to achieve it. So we expect there will be little difference between the first and third model. On the other hand, neglecting the diffusion of S_2 (hydrogen peroxide) in the second model is potentially more serious as this assumes that all S_2 generated in the first reaction is immediately available for the second reaction and this could affect the size of the final steady states. The three models are discussed in detail in the next three sections and comparisons between them are given at the end of the chapter.

4.2 The comprehensive model

This section reviews the model introduced in [35] (where both substrates diffuse). An additional steady-state analysis of the partial differential equations is presented which is then compared with the numerical results obtained in [35].

4.2.1 Review of the comprehensive model

In this model, the reactions (4.1) were modelled by a system of partial differential equations and boundary conditions representing convective and diffusive transport of the two substrates, glucose and hydrogen peroxide, as well as the reaction kinetics of the bi-enzyme electrode. For simplicity, the convective transport is not explicitly modelled and the flow injection is only reflected in the boundary conditions imposed at the top of the diffusion domain, $0 \leq x \leq L$. We have also assumed that diffusion is one-dimensional and x measures distance from the electrode.

In what follows, we denote the concentrations of all the chemical species mentioned in the cascade scheme (4.1) by their corresponding lower case letters (e.g., $c_1 = [C_1]$ etc.). The two substrates satisfy the following diffusion equations,

$$\frac{\partial s_1(x,t)}{\partial t} = D_1 \frac{\partial^2 s_1(x,t)}{\partial x^2}, \quad 0 \leq x \leq L, \quad t \geq 0,$$
$$\frac{\partial s_2(x,t)}{\partial t} = D_2 \frac{\partial^2 s_2(x,t)}{\partial x^2}, \quad 0 \leq x \leq L, \quad t \geq 0,$$

where D_1 and D_2 are the diffusion coefficients. At the top boundary, S_1 is in constant supply (due to the continuous glucose injection), and S_2 is assumed to be flushed away constantly, which gives the following boundary conditions

$$s_1(L,t) = s_0, \quad t \geq 0,$$

$$s_2(L,t) = 0, \quad t \geq 0.$$

At the bottom boundary, the boundary conditions reflect the fact that the diffusive flux of each substrate is equal to the corresponding reaction rate as

$$D_1 \frac{\partial s_1(0,t)}{\partial x} = k_1 e_1(t) s_1(0,t) - k_{-1} c_1(t),$$

$$D_2 \frac{\partial s_2(0,t)}{\partial x} = k_3 e_2(t) s_2(0,t) - k_2 c_1(t) - k_{-3} c_2(t),$$

together with

$$\begin{aligned}
\frac{de_1}{dt} &= -k_1 e_1(t) s_1(0,t) + (k_{-1} + k_2) c_1(t), \\
\frac{de_2}{dt} &= -k_3 e_2(t) s_2(0,t) + (k_{-3} + k_4) c_2(t), \\
\frac{dc_1}{dt} &= k_1 e_1(t) s_1(0,t) - (k_{-1} + k_2) c_1(t), \\
\frac{dc_2}{dt} &= k_3 e_2(t) s_2(0,t) - (k_{-3} + k_4) c_2(t), \\
\frac{dp}{dt} &= k_4 c_2(t).
\end{aligned}$$

In accordance with the physical problem described above, we consider the following initial conditions

$$e_1(0) = e_1^0, \quad e_2(0) = e_2^0, \quad c_1(0) = 0, \quad c_2(0) = 0, \quad p(0) = 0, \quad s_2(x,0) = 0,$$

$$s_1(x,0) = \begin{cases} s_0, & \text{if } x = L \\ 0, & \text{otherwise,} \end{cases}$$

where e_1^0, e_2^0 and s_0 are constants. We let

$$\zeta = \frac{e_1^0}{e_2^0},$$

which implies

$$e_1^0 = \frac{e\zeta}{1+\zeta}, \quad e_2^0 = \frac{e}{1+\zeta},$$

where e is the total amount of enzyme present on the electrode. We can assume that e is a constant which corresponds to full coverage of the electrode; this can be measured experimentally.

We are going to non-dimensionalise the system by introducing the following variables;

$$\bar{s_1}(\bar{x},\bar{t}) = \frac{s_1(x,t)}{s_0}, \quad \bar{s_2}(\bar{x},\bar{t}) = \frac{s_2(x,t)}{s_0}, \quad \bar{e_1}(\bar{t}) = \frac{e_1(t)}{e}, \quad \bar{e_2}(\bar{t}) = \frac{e_2(t)}{e},$$
$$\bar{c_1}(\bar{t}) = \frac{c_1(t)}{e}, \quad \bar{c_2}(\bar{t}) = \frac{c_2(t)}{e}, \quad \bar{p}(\bar{t}) = \frac{p(t)}{e}, \quad \bar{x} = \frac{x}{l}, \quad \bar{t} = \frac{t}{t_0},$$

where $t_0 = 1/(k_1 s_0)$. We then obtain the non-dimensional system

$$
\begin{cases}
\dfrac{\partial s_1(x,t)}{\partial t} = \dfrac{D_1}{k_1 s_0 l^2}\dfrac{\partial^2 s_1(x,t)}{\partial x^2} & \text{(4.2a)}\\
\dfrac{\partial s_2(x,t)}{\partial t} = \dfrac{D_2}{k_1 s_0 l^2}\dfrac{\partial^2 s_2(x,t)}{\partial x^2} & \text{(4.2b)}\\
s_1(1,t) = 1 & \text{(4.2c)}\\
s_2(1,t) = 0 & \text{(4.2d)}\\
\dfrac{\partial s_1(0,t)}{\partial x} = \dfrac{k_1 el}{D_1} e_1(t) s_1(0,t) - \dfrac{k_{-1} el}{D_1 s_0} c_1(t) & \text{(4.2e)}\\
\dfrac{\partial s_2(0,t)}{\partial x} = \dfrac{k_3 el}{D_2} e_2(t) s_2(0,t) - \dfrac{k_2 el}{D_2 s_0} c_1(t) - \dfrac{k_{-3} el}{D_2 s_0} c_2(t) & \text{(4.2f)}\\
\dfrac{de_1}{dt} = -e_1(t) s_1(0,t) + \dfrac{K_m^1}{s_0} c_1(t) & \text{(4.2g)}\\
\dfrac{de_2}{dt} = -\dfrac{k_3}{k_1} e_2(t) s_2(0,t) + \dfrac{k_{-3}+k_4}{k_1 s_0} c_2(t) & \text{(4.2h)}\\
\dfrac{dc_1}{dt} = e_1(t) s_1(0,t) - \dfrac{K_m^1}{s_0} c_1(t) & \text{(4.2i)}\\
\dfrac{dc_2}{dt} = \dfrac{k_3}{k_1} e_2(t) s_2(0,t) - \dfrac{k_{-3}+k_4}{k_1 s_0} c_2(t) & \text{(4.2j)}\\
\dfrac{dp}{dt} = \dfrac{k_4}{k_1 s_0} c_2(t), & \text{(4.2k)}
\end{cases}
$$

where the bars were dropped for convenience. An extensive numerical analysis of this system was presented in [35] where the behaviour of the enzyme ratio ζ was studied for different values of the system parameters. The time evolution of $k_4\bar{c_2}(t)$, which was taken as a measure of the amperometric signal, was calculated and the steady state value, $k_4 c_2^*$, was recorded as the current value and used for future parameter iterations. Note that the dimensional value of the current is

$$
I(t) \approx \frac{dp}{dt} = k_4 c_2(t) = e k_4 \bar{c_2}(t), \tag{4.3}
$$

hence, $k_4\bar{c_2}(t)$ can be regarded as a good measure of the amperometric signal, which should not depend on the choice of non-dimensionalisation used in the model. For

example, Figure 4.3 in [35] shows the dependence of the (steady-state) current on the GOX:HRP ratio, ζ, for different concentrations of the first substrate, glucose (s_1). The optimal ζ values (the values which yield maximum signals) are then indicated on each curve. This figure was produced using Interactive Data Language (IDL).

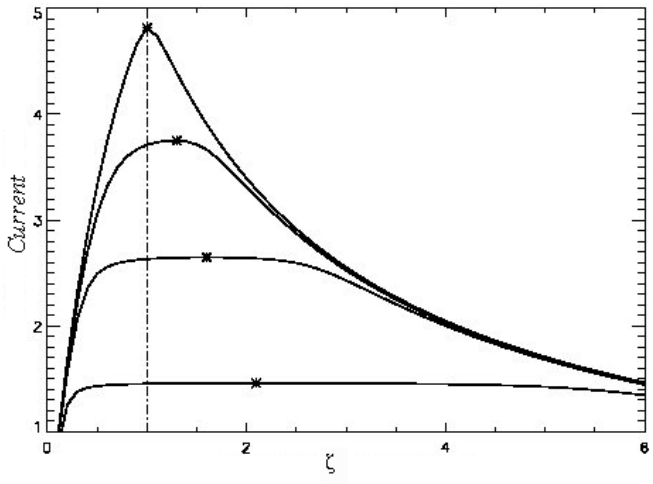

Figure 4.3 – Dependence of current on ζ for different initial concentrations of s_1. The curves correspond to $s_0 = 1, 5, 10$ and 20 mM from bottom to top. The maximum value of current is indicated on each curve.

In Figure 4.3, we note that at low glucose concentrations, varying the ratio of the immobilised enzymes has little effect on the electrode response. However, as the glucose concentration increases the optimal ratio value becomes more pronounced and converge to 1 (refer to [35]). The reason for this particular limiting value lies behind the choice of catalytic conversion constants, $k_2 = k_4$. (The value used for the simulation in [35] was $k_2 = k_4 = 10s^{-1}$.) By choosing $k_4/k_2 = 2$, a similar pattern of curves can be obtained by letting $\zeta^* \to 2$ with increasing glucose concentrations.

Figure 4.4 (also obtained in [35]) shows the dependence of the current on the GOX:HRP ratio when the relative speed of the two consecutive reactions k_4/k_2 is varied. Note again that, as the value of k_4/k_2 increases there seems to be a wider range of ζ values associated with an "optimal" biosensor response.

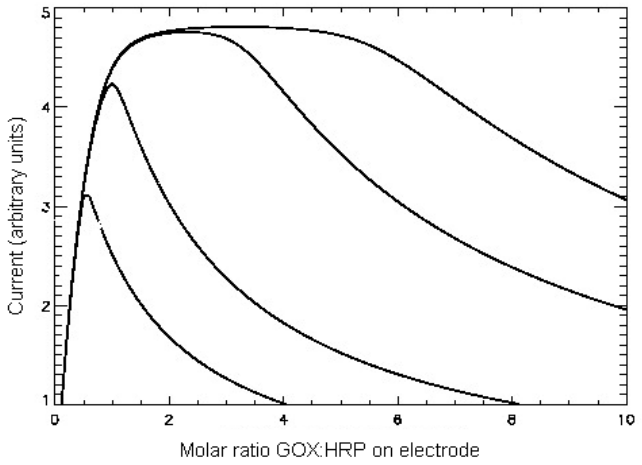

Figure 4.4 – Dependence of current on ζ (electrode GOX:HRP ratio) for different k_4/k_2 values. The lower curve corresponds to $k_4/k_2 = 0.5$ and the upper curve corresponds to $k_4/k_2 = 8$.

4.2.2 Steady-state analysis

In this section, we are going to analyse system (4.2) as $t \to \infty$. At equilibrium, equation (4.2a) gives

$$\frac{\partial s_1(x,t)}{\partial t} = 0,$$

which means

$$\frac{\partial^2 s_1(x,t)}{\partial x^2} = 0; \tag{4.4}$$

then integrating equation (4.4) twice with respect to x, we get

$$s_1^*(x) = Ax + B. \tag{4.5}$$

Similarly, from equation (4.2b), we obtain

$$s_2^*(x) = Cx + D, \tag{4.6}$$

where $s_1^*(x)$, $s_2^*(x)$ denote the equilibrium values of $s_1(x,t)$, $s_2(x,t)$ respectively, and A, B, C, D are constants of integration.

Equation (4.2c) together with equation (4.5) gives

$$s_1^*(x) = (1-B)x + B;$$

similarly equation (4.2d) together with equation (4.6) gives

$$s_2^*(x) = -Dx + D.$$

Thus, at $x = 0$, the system (4.2) can be reduced to

$$\begin{cases} 1 - B = \dfrac{k_1 el}{D_1}\left(\dfrac{\zeta}{1+\zeta} - c_1^*\right) B - \dfrac{k_{-1} el}{D_1 s_0} c_1^* & \text{(4.7a)} \\ -D = \dfrac{k_3 el}{D_2}\left(\dfrac{1}{1+\zeta} - c_2^*\right) D - \dfrac{k_2 el}{D_2 s_0} c_1^* - \dfrac{k_{-3} el}{D_2 s_0} c_2^* & \text{(4.7b)} \\ 0 = \left(\dfrac{\zeta}{1+\zeta} - c_1^*\right) B - \dfrac{K_m^1}{s_0} c_1^* & \text{(4.7c)} \\ 0 = \dfrac{k_3}{k_1}\left(\dfrac{1}{1+\zeta} - c_2^*\right) D - \dfrac{k_4 + k_{-3}}{k_1 s_0} c_2^*. & \text{(4.7d)} \end{cases}$$

Here, we have a system of four equations with four unknowns B, D, c_1^* and c_2^*, which can be reduced to the following system of two equations in term of c_1^* and c_2^*, where c_1^*, c_2^* are positive and denote the equilibrium values of $c_1(t)$, $c_2(t)$ respectively.

$$\begin{cases} (c_1^*)^2 - \left(\dfrac{D_1 s_0}{k_2 el} + \dfrac{D_1 K_m^1}{k_2 el} + \dfrac{\zeta}{1+\zeta} \right) c_1^* + \dfrac{D_1 s_0}{k_2 el} \cdot \dfrac{\zeta}{1+\zeta} = 0 & \text{(4.8a)} \\ (c_2^*)^2 - \left(\dfrac{k_2 c_1^*}{k_4} + \dfrac{D_2 K_m^2}{k_4 el} + \dfrac{1}{1+\zeta} \right) c_2^* + \dfrac{k_2 c_1^*}{k_4} \cdot \dfrac{1}{1+\zeta} = 0. & \text{(4.8b)} \end{cases}$$

System (4.8) can be easily solved to give explicit formulas for c_1^* and c_2^*; however, these formulas are lengthy, so we do not include them here, see appendix A for calculations of the explicit formulas. Note that the smaller solution is selected in both these quadratic equations, as we need

$$c_1^* \leq e_1^0 = \frac{\zeta}{1+\zeta}; \quad c_2^* \leq e_2^0 = \frac{1}{1+\zeta}.$$

We then plot the current, $k_4 c_2^*$, as a function of ζ by using MAPLE in Figure 4.5. (Parameters are not all the same as the values used in the numerical simulation of [35] as discussed in the previous section). We note again that, as we chose $k_2 = k_4$, the optimal ratio ζ^* approaches 1 for large glucose concentrations. Also, note that there is good qualitative and quantitative agreement between Figure 4.3 and Figure 4.5, as regards the behaviour of the steady state current. A comparison of the optimal GOX:HRP ratios for all three models will be given in Section 4.5. Figure 4.6 shows the current as a function of ζ when the ratio k_4/k_2 is varied; note again the similarity with the numerical result shown in Figure 4.4.

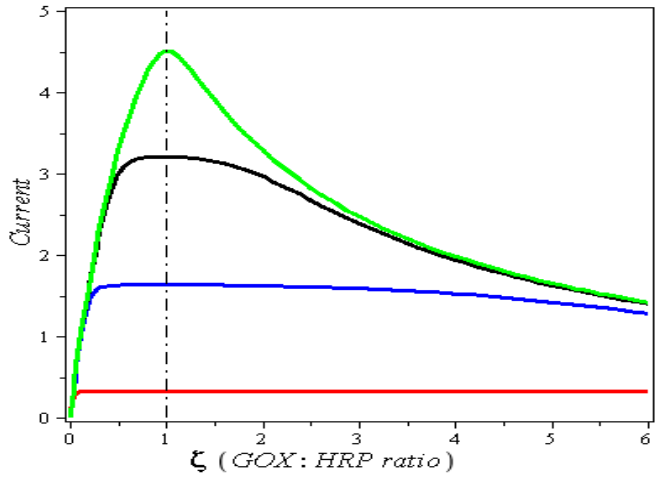

Figure 4.5 – Dependence of current on ζ as given by system (4.8). The curves correspond to $s_0 = 1, 5, 10$ and 20 mM from the bottom to top. Typical values for constants used in this simulation are: $k_1 = 10^2$, $k_{-1} = 10^{-1}$, $k_2 = 10$, $k_3 = 10^2$, $k_{-3} = 10^{-1}$, $k_4 = 10$, $e_0 = 10^{-5}$, $l = 2 \times 10^{-4}$, $D_1 = 6.7 \times 10^{-10}$ and $D_2 = 8.8 \times 10^{-10}$.

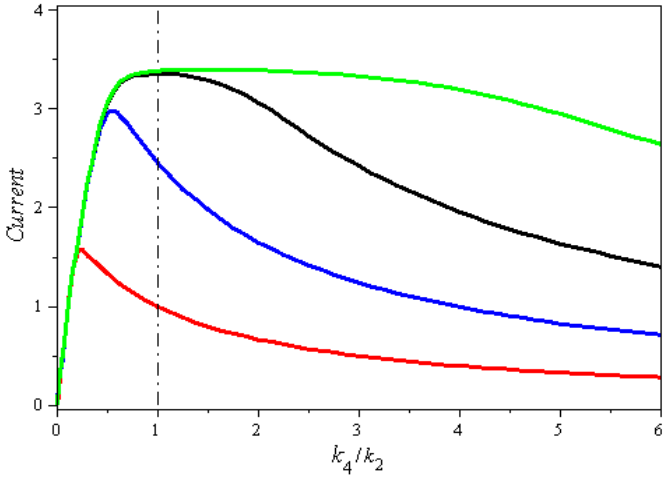

Figure 4.6 – Dependence of current on ζ as given by system (4.8). The curves correspond to $k_4/k_2 = 0.2, 0.5, 1$ and 2 from the bottom to top. Typical values for constants used in this simulation are the same as in Figure 4.5.

4.3 Simplified model

This section analyses the simple, one-point model of the cascade reaction which was introduced in [36]. A detailed stability analysis is presented here which shows that the system displays different behaviour for different values of the enzyme ratio ζ. We also use results from geometric singular perturbation theory and monotone dynamical systems in order to achieve a good understanding of this model.

4.3.1 Formation of the model

In this subsection we neglect diffusion of both substrates in the cascade reactions (4.1), and construct a one-point model. Recall that, an ordinary differential equation model for a cascade reaction was already discussed in Chapter 2. If we assume that glucose is present in constant supply at the reaction point (i.e., $s_1(t) = s_0$), the non-dimensional system (2.57) can be further simplified to the following system

$$\begin{cases} \dfrac{dc_1}{dt} = \dfrac{\zeta}{1+\zeta} - \left(1 + \dfrac{K_m^1}{s_0}\right) c_1 & \text{(4.9a)} \\ \dfrac{dc_2}{dt} = \dfrac{k_3}{k_1}\left(\dfrac{1}{1+\zeta} - c_2\right) s_2 - \dfrac{K}{s_0} c_2 & \text{(4.9b)} \\ \dfrac{ds_2}{dt} = \varepsilon_1 \left(\dfrac{k_2}{k_1 s_0} c_1 - \dfrac{k_3}{k_1}\left(\dfrac{1}{1+\zeta} - c_2\right) s_2 + \dfrac{k_{-3}}{k_1 s_0} c_2\right), & \text{(4.9c)} \end{cases}$$

with initial conditions $c_1(0) = 0$, $c_2(0) = 0$ and $s_2(0) = 0$, where the parameters ε_1, K_m^1 and K are the same as defined in equation (2.58), namely

$$\varepsilon_1 = \frac{e}{s_0}, \quad K_m^1 = \frac{k_{-1} + k_2}{k_1}, \quad K = \frac{k_{-3} + k_4}{k_1}.$$

Instead of studying the behaviour of a single reaction (defined by the initial conditions specified above), we have decided to look at the global behaviour of the dynamical system (4.9). We also anticipate that all solutions of this system will display the exact same asymptotic behaviour as $t \to \infty$.

Given the interpretation of c_1, c_2 and s_2 as concentrations, it is important to establish the positivity of solutions for this system. More precisely, we consider the positive octant

$$\Gamma = \left\{(c_1, c_2, s_2) \in R^3 \mid c_1 \geq 0, c_2 \geq 0, s_2 \geq 0\right\},$$

and prove it is a positively invariant region (which means that trajectories entering this region cannot leave it in forward time). Hence, a solution with a positive initial condition will stay positive for all $t \geq 0$. This is easily done if we show that the flow points inwards on all three boundaries of the region Γ. In particular, we have to check that

$$\begin{aligned}
\frac{dc_1}{dt} &\geq 0, \text{ on } c_1 = 0, c_2 \geq 0, s_2 \geq 0, \\
\frac{dc_2}{dt} &\geq 0, \text{ on } c_2 = 0, c_1 \geq 0, s_2 \geq 0, \\
\frac{ds_2}{dt} &\geq 0, \text{ on } s_2 = 0, c_1 \geq 0, c_2 \geq 0,
\end{aligned}$$

and these conditions can be easily verified in system (4.9). Next, we are going to find the equilibrium points of system (4.9). At equilibrium, from equations (4.9a) and

(4.9b), we obtain

$$c_1^* = \frac{\zeta}{(1+\zeta)\left(1+\frac{K_m^1}{s_0}\right)}, \tag{4.10}$$

$$c_2^* = \frac{s_2^*}{(1+\zeta)\left(s_2^*+\frac{K_m^2}{s_0}\right)}, \tag{4.11}$$

with

$$K_m^2 = \frac{k_{-3}+k_4}{k_3},$$

as defined in Chapter 2. Then from equations (4.9c), (4.10) and (4.11), we find the equilibrium value for $s_2(t)$ is,

$$s_2^* = \frac{\zeta k_2 K_m^2}{s_0\left(k_4\left(1+\frac{K_m^1}{s_0}\right)-\zeta k_2\right)}, \tag{4.12}$$

which is positive if and only if

$$\zeta < \frac{k_4}{k_2}\left(1+\frac{K_m^1}{s_0}\right).$$

We let

$$\zeta^* = \frac{k_4}{k_2}\left(1+\frac{K_m^1}{s_0}\right), \tag{4.13}$$

as we will use this parameter frequently in the remainder of this chapter. Therefore, we conclude that when $\zeta < \zeta^*$, the equilibrium values are

$$\begin{cases} c_1^* = \dfrac{k_4\zeta}{k_2\zeta^*(1+\zeta)} & \text{(4.14a)} \\ c_2^* = \dfrac{\zeta}{\zeta^*(1+\zeta)} & \text{(4.14b)} \\ s_2^* = \dfrac{\zeta K_m^2}{s_0(\zeta^*-\zeta)}, & \text{(4.14c)} \end{cases}$$

and when $\zeta > \zeta^*$, we do not have an equilibrium value for $s_2(t)$ in the positive

octant Γ. In order to better visualise the behaviour of the solution of system (4.9) starting at $(0,0,0)$, we now show that it is confined to an invariant set. We define the set Ω_1, such that

$$\Omega_1 = \left\{ (c_1, c_2, s_2) \in R^3 \mid 0 \leq c_1 \leq c_1^*, 0 \leq c_2 \leq \frac{1}{1+\zeta}, 0 \leq s_2 \leq \infty \right\}.$$

Next we are going to show the set Ω_1 is an invariant set, by showing that all the trajectories point inwards when crossing the boundary of the set Ω_1, i.e., we need to show that:

On	***Need to show***
$c_1 = 0$	$\frac{dc_1}{dt} > 0$
$c_1 = c_1^*$	$\frac{dc_1}{dt} = 0$
$c_2 = 0$	$\frac{dc_2}{dt} > 0$
$c_2 = 1/(1+\zeta)$	$\frac{dc_2}{dt} < 0$
$s_2 = 0$	$\frac{ds_2}{dt} > 0$

We can easily see that, on $c_1 = 0$, we have

$$\frac{dc_1}{dt} = \frac{\zeta}{1+\zeta} > 0.$$

On $c_1 = c_1^*$, we have

$$\frac{dc_1}{dt} = \frac{\zeta}{1+\zeta} - \left(1 + \frac{K_m^1}{s_0}\right) \frac{\zeta}{(1+\zeta)\left(1 + \frac{K_m^1}{s_0}\right)} = 0.$$

On $c_2 = 0$, we have

$$\frac{dc_2}{dt} = \frac{k_3}{k_1} \left(\frac{1}{1+\zeta}\right) s_2 > 0.$$

On $c_2 = 1/(1+\zeta)$, we have

$$\frac{dc_2}{dt} = -\frac{K}{s_0(1+\zeta)} < 0.$$

On $s_2 = 0$, we have

$$\frac{ds_2}{dt} = \varepsilon_1 \left(\frac{k_2}{k_1 s_0} c_1^* + \frac{k_{-3}}{k_1 s_0} c_2 \right) > 0,$$

since $c_1^* > 0$ and $c_2 \geq 0$. Thus, the set Ω_1 is an invariant set, and thus the solution starting at $(0,0,0)$ stays in this invariant set.

In the next three subsections, we are going to investigate in detail the long term behaviour of this solution and prove that

$$\lim_{t\to\infty} c_1(t) = c_1^*, \quad \text{for all} \quad \zeta,$$

$$\lim_{t\to\infty} c_2(t) = \begin{cases} c_2^*, & \text{if } \zeta \leq \zeta^* \\ \dfrac{1}{1+\zeta}, & \text{if } \zeta \geq \zeta^*, \end{cases}$$

$$\lim_{t\to\infty} s_2(t) = \begin{cases} s_2^*, & \text{if } \zeta < \zeta^* \\ \infty, & \text{if } \zeta \geq \zeta^*. \end{cases}$$

These results are easy to interpret in the context of the cascade reactions (4.1). If $\zeta < \zeta^*$, there is a relatively small amount of $e_1(0)$ compared to $e_2(0)$ which means that the production of s_2 in the first reaction is somehow balanced by its consumption in the second reaction and an equilibrium state can be reached. On the other hand, if $\zeta \geq \zeta^*$, the relatively large amount of $e_1(0)$ can facilitate the production of s_2 which is then not consumed fast enough in the second reaction so its concentration can grow indefinitely. (Recall that we have assumed an unlimited supply of s_1!)

We now present briefly a local stability analysis for this equilibrium point. The Jacobian matrix for system (4.9) can be constructed as follows:

$$\begin{pmatrix} \frac{\partial f_1}{\partial c_1^*} & \frac{\partial f_1}{\partial c_2^*} & \frac{\partial f_1}{\partial s_2^*} \\ \frac{\partial f_2}{\partial c_1^*} & \frac{\partial f_2}{\partial c_2^*} & \frac{\partial f_2}{\partial s_2^*} \\ \frac{\partial f_3}{\partial c_1^*} & \frac{\partial f_3}{\partial c_2^*} & \frac{\partial f_3}{\partial s_2^*} \end{pmatrix} = \begin{pmatrix} -1 - \frac{K_m^1}{s_0} & 0 & 0 \\ 0 & -\frac{k_3}{k_1}s_2^* + \frac{K}{s_0} & \frac{k_3}{k_1}\left(\frac{1}{1+\zeta} - c_2^*\right) \\ \frac{\varepsilon_1 k_2}{k_1 s_0} & \varepsilon_1\left(\frac{k_3}{k_1}s_2^* + \frac{k_{-3}}{k_1 s_0}\right) & -\frac{\varepsilon_1 k_3}{k_1}\left(\frac{1}{1+\zeta} - c_2^*\right) \end{pmatrix}$$

Then denoting the eigenvalues of the Jacobian matrix by λ_1, λ_2 and λ_3, we obtain

$$\lambda_1 = -1 - \frac{K_m^1}{s_0} < 0,$$
$$\lambda_2 + \lambda_3 = -\frac{k_3 s_0 s_2^* + k_{-3} + k_4 + \varepsilon_1 k_3 s_0\left(\frac{1}{1+\zeta} - c_2^*\right)}{k_1 s_0} < 0,$$
$$\text{and} \quad \lambda_2\lambda_3 = \frac{\varepsilon_1 k_3 k_4\left(\frac{1}{1+\zeta} - c_2^*\right)}{k_1^2 s_0} > 0;$$

this shows that we have three negative eigenvalues, which tells us the equilibrium point is locally stable. Also, a global stability analysis will be presented later in this section.

4.3.2 Slow-fast dynamics

With the notation introduced in (4.9), that system can be written as

$$\begin{cases} \dfrac{dc_1}{dt} = f_1(c_1) & \text{(4.15a)} \\ \dfrac{dc_2}{dt} = f_2(c_2, s_2) & \text{(4.15b)} \\ \dfrac{ds_2}{dt} = \varepsilon_1 f_3(c_1, c_2, s_2), & \text{(4.15c)} \end{cases}$$

where $\varepsilon_1 = e/s_0$ is a small parameter, i.e., $\varepsilon_1 \ll 1$. Posed this way, c_1 and c_2 are

fast variables, s_2 is the slow variable and t is the fast time. System (4.15) is called a **slow-fast system** (also known as **a singularly perturbed system** or **system with multiple scales**).

If we let $\tau = \varepsilon_1 t$, the system can be written in the form

$$\begin{cases} \varepsilon_1 \dfrac{dc_1}{d\tau} = f_1(c_1) & \text{(4.16a)} \\ \varepsilon_1 \dfrac{dc_2}{d\tau} = f_2(c_2, s_2) & \text{(4.16b)} \\ \dfrac{ds_2}{d\tau} = f_3(c_1, c_2, s_2). & \text{(4.16c)} \end{cases}$$

Then in system (4.16), c_1 and c_2 are still the fast variables, and s_2 is still the slow variable, but τ is the slow time. Regardless of how time is scaled, as long as $f_1(c_1) \neq 0$ and $f_2(c_2, s_2) \neq 0$, we have

$$\left|\frac{dc_1}{dt}\right| \gg \left|\frac{ds_2}{dt}\right| \quad \text{and} \quad \left|\frac{dc_2}{dt}\right| \gg \left|\frac{ds_2}{dt}\right|.$$

Thus, it is the relative rates which makes c_1 and c_2 fast and s_2 slow.

The **fast subsystem (or unperturbed system)** corresponding to system (4.15) is defined as

$$\begin{cases} \dfrac{dc_1}{dt} = f_1(c_1) & \text{(4.17a)} \\ \dfrac{dc_2}{dt} = f_2(c_2, s_2) & \text{(4.17b)} \\ \dfrac{ds_2}{dt} = 0, & \text{(4.17c)} \end{cases}$$

and the equilibrium set of system (4.17) is given by

$$f_1(c_1) = 0, \text{ which implies } c_1^* = \frac{\zeta}{(1+\zeta)\left(1+\frac{K_m^1}{s_0}\right)}, \tag{4.18}$$

$$f_2(c_2, s_2) = 0, \text{ which implies } c_2^* = \frac{s_2^*}{(1+\zeta)\left(s_2^*+\frac{K_m^2}{s_0}\right)}; \tag{4.19}$$

since ds_2/dt is identically zero (hence s_2 is constant), this set defines a one-dimensional curve of fixed points M_0, which can be thought of as a **trivially** invariant manifold. Also, using the same arguments as in Section 4.4, it can be shown that in the fast system each of these fixed points is stable. Moreover, since the eigenvalues were shown to be strictly negative, each of these equilibrium points is hyperbolic. The manifold M_0 is then said to be **normally hyperbolic** and it is these manifolds that occupy an important place in geometric singular perturbation theory (refer to [38]).

On the other hand, the **slow subsystem (or layer system)** is obtained by letting $\varepsilon_1 = 0$ in system (4.16), which gives

$$\begin{cases} 0 = f_1(c_1) & \text{(4.20a)} \\ 0 = f_2(c_2, s_2) & \text{(4.20b)} \\ \dfrac{ds_2}{d\tau} = f_3(c_1, c_2, s_2). & \text{(4.20c)} \end{cases}$$

The first two equations in system (4.20) give

$$c_1^* = \frac{\zeta}{(1+\zeta)\left(1+\frac{K_m^1}{s_0}\right)}, \tag{4.21}$$

$$c_2^* = \frac{s_2^*}{(1+\zeta)\left(s_2^*+\frac{K_m^2}{s_0}\right)}. \tag{4.22}$$

This defines a one-dimensional curve in the (c_1, c_2, s_2) space, called the **slow manifold**. Unlike the case of the fast system, there is now (slow) flow along this manifold, which is derived from equation (4.20c), and is given by

$$\frac{ds_2}{d\tau} = F(s_2) = \frac{k_2\zeta}{(1+\zeta)\left(1+\frac{K_m^1}{s_0}\right)} - \frac{(k_{-3}+k_4)\,s_2 - k_{-3}s_2}{(1+\zeta)\left(s_2+\frac{K_m^2}{s_0}\right)}.$$

Note that, by letting $F(s_2) = 0$, we obtain

$$s_2 = \frac{k_2\zeta K_m^2}{s_0\left(k_4\left(1+\frac{K_m^1}{s_0}\right) - k_2\zeta\right)},$$

so there is an equilibrium point on this slow manifold provided the same condition as before, namely $\zeta < \zeta^*$, is satisfied. Unlike regular perturbed systems, neither the slow nor fast subsystem is sufficient for understanding the behaviour of system (4.15). The dynamics of the original system are then often explained by combining the information obtained from the fast and slow systems.

4.3.3 Slow invariant manifold

The main question at this point is whether the normally hyperbolic manifold M_0 given by equations (4.18) and (4.19) obtained in the fast (unperturbed) subsystem persists for the original system (4.15) with the perturbation added. The conditions for the persistence of this manifold are given by a theorem due to Fenichel (refer to [39]), and other results in geometric singular perturbation theory (refer to [38] for a review of this theory). A rigorous analysis of the fast-slow dynamics of system (4.15) is beyond the aim of this thesis so will not be given. Instead, we use an approximation method

(refer to [41]) for the qualitative asymptotic analysis of singular differential equations by reducing the order of the differential system under consideration. The method relies on the theory of invariant manifolds, which essentially replaces the original system by another system on an invariant manifold with dimension equal to that of the slow subsystem.

Definition 1

A system of differential equations is called ***autonomous*** *if it maps into itself under arbitrary translations along the time axis. In other words a system is autonomous if its right-hand side is independent of time (refer to [40]).*

Theorem 1 (refer to [41])

A smooth surface $y = h(x, \varepsilon)$, $(x \in R^m, y \in R^n)$ *in* $R^m \times R^n$ *is a* ***slow invariant manifold*** *of the autonomous system*

$$\dot{x} = f(x, y, \varepsilon), \quad \varepsilon\dot{y} = g(x, y, \varepsilon), \tag{4.23}$$

if any trajectory $x = x(t, \varepsilon)$, $y = y(t, \varepsilon)$ *of the system* (4.23) *that has at least one point* $x = x_0$, $y = y_0$ *in common with the surface* $y = h(x, \varepsilon)$, *i.e.,* $y_0 = h(x_0, \varepsilon)$, *lies entirely in this surface, i.e.,* $y(t, \varepsilon) = h\left(x(t, \varepsilon), \varepsilon\right)$.

The motion along an invariant manifold of the system (4.23) *is governed by the equation*

$$\dot{x} = f\left(x, h(x, \varepsilon), \varepsilon\right).$$

If $x(t, \varepsilon)$ *is a solution of this equation, then the pair* $(x(t, \varepsilon), y(t, \varepsilon))$, *where* $y(t, \varepsilon) =$

$h\left(x(t,\varepsilon),\varepsilon\right)$, is a solution of the original system (4.23)*, since it defines a trajectory on the invariant manifold.*

Substituting the function $h(x,\varepsilon)$ instead of y into system (4.23) gives the following first order invariance equation for $h(x,\varepsilon)$,

$$\varepsilon\frac{\partial h}{\partial x}f\left(x,h(x,\varepsilon),\varepsilon\right)=g(x,h,\varepsilon)$$

(refer to [41]).

Now we are going to restate the slow invariant manifold defined in Theorem 1 in the notation of our system (4.16). *A smooth surface $c_1=h_1(s_2,\varepsilon_1)$ and $c_2=h_2(s_2,\varepsilon_1)$ is a slow invariant manifold of system* (4.16) *if any trajectory $s_2=s_2(t,\varepsilon_1)$, $c_1=c_1(t,\varepsilon_1)$ and $c_2=c_2(t,\varepsilon_1)$ of the system that has at least one point $s_2=s_{20}$, $c_1=c_{10}$ and $c_2=c_{20}$ in common with the surface $c_1=h_1(s_2,\varepsilon_1)$ and $c_2=h_2(s_2,\varepsilon_1)$ (i.e., $c_{10}=h_1(s_{20},\varepsilon_1)$ and $c_{20}=h_2(s_{20},\varepsilon_1)$), and lies entirely in this surface (i.e., $c_1(t,\varepsilon_1)=h_1\left(s_2(t,\varepsilon_1),\varepsilon_1\right)$ and $c_2(t,\varepsilon_1)=h_2\left(s_2(t,\varepsilon_1),\varepsilon_1\right)$).*

The motion along an invariant manifold of system (4.16) *is governed by the equation*

$$\dot{s_2}=f_3\left(s_2,h_1(s_2,\varepsilon_1),h_2(s_2,\varepsilon_1)\right).$$

Hence by substituting $h_1(s_2,\varepsilon_1)$ and $h_2(s_2,\varepsilon_1)$ instead of c_1, c_2 into system (4.16) *yields the following invariance equations,*

$$\varepsilon_1\frac{\partial h_1}{\partial s_2}f_3\left(s_2,h_1(s_2,\varepsilon_1),h_2(s_2,\varepsilon_1)\right)=f_1(c_1), \tag{4.24}$$

$$\varepsilon_1 \frac{\partial h_2}{\partial s_2} f_3\left(s_2, h_1(s_2,\varepsilon_1), h_2(s_2,\varepsilon_1)\right) = f_2(c_2, s_2). \tag{4.25}$$

To calculate an approximation to the one-dimensional slow invariant manifold, we let

$$c_1 = h_1(s_2,\varepsilon_1) = \phi_0(s_2) + \varepsilon_1\phi_1(s_2) + O(\varepsilon_1^2), \tag{4.26}$$

$$c_2 = h_2(s_2,\varepsilon_1) = \psi_0(s_2) + \varepsilon_1\psi_1(s_2) + O(\varepsilon_1^2). \tag{4.27}$$

Then if we substitute equations (4.26) and (4.27) into (4.24) and (4.25), the invariant equations become

$$\begin{aligned}\varepsilon_1 \frac{\partial \phi_0}{\partial s_2}\left(\frac{k_2}{k_1 s_0}(\phi_0(s_2)+\varepsilon_1\phi_1(s_2)) - \frac{k_3}{k_1}\left(\frac{1}{1+\zeta} - \psi_0(s_2) - \varepsilon_1\psi_1(s_2)\right)s_2 + \frac{k_{-3}}{k_1 s_0}\left(\psi_0(s_2)+\varepsilon_1\psi_1(s_2)\right)\right)\\ = \frac{\zeta}{1+\zeta} - \left(1+\frac{K_m^1}{s_0}\right)\left(\phi_0(s_2)+\varepsilon_1\phi_1(s_2)\right),\end{aligned} \tag{4.28}$$

$$\begin{aligned}\varepsilon_1 \frac{\partial \psi_0}{\partial s_2}\left(\frac{k_2}{k_1 s_0}(\phi_0(s_2)+\varepsilon_1\phi_1(s_2)) - \frac{k_3}{k_1}\left(\frac{1}{1+\zeta} - \psi_0(s_2) - \varepsilon_1\psi_1(s_2)\right)s_2 + \frac{k_{-3}}{k_1 s_0}\left(\psi_0(s_2)+\varepsilon_1\psi_1(s_2)\right)\right)\\ = \frac{k_3}{k_1}\left(\frac{1}{1+\zeta} - \psi_0(s_2) - \varepsilon_1\psi_1(s_2)\right)s_2 - \frac{K}{s_0}\left(\psi_0(s_2)+\varepsilon_1\psi_1(s_2)\right).\end{aligned} \tag{4.29}$$

Now, from equations (4.28) and (4.29), at $O(1)$, we obtain

$$\phi_0(s_2) = \frac{\zeta}{(1+\zeta)\left(1+\frac{K_m^1}{s_0}\right)},$$

$$\psi_0(s_2) = \frac{s_2}{(1+\zeta)\left(s_2+\frac{K_m^2}{s_0}\right)},$$

and at $O(\varepsilon_1)$, we obtain

$$\phi_1(s_2) = \frac{k_3 K_m^2}{k_2(1+\zeta)\left(1+\frac{K_m^1}{s_0}\right)\left(s_2+\frac{K_m^2}{s_0}\right)},$$

$$\psi_1(s_2) = \frac{k_1 K_m^2}{k_2(1+\zeta)\left(s_2+\frac{K_m^2}{s_0}\right)^2}.$$

Therefore, the approximation of the slow invariant manifold is given as

$$c_1 = h_1(s_2, \varepsilon_1) = \frac{1}{(1+\zeta)\left(\zeta + \frac{K_m^1}{s_0}\right)}\left(1 + \varepsilon_1 \frac{k_3 K_m^2}{k_2\left(s_2 + \frac{K_m^2}{s_0}\right)}\right) + O(\varepsilon_1^2), \tag{4.30}$$

$$c_2 = h_2(s_2, \varepsilon_1) = \frac{1}{(1+\zeta)\left(s_2 + \frac{K_m^2}{s_0}\right)}\left(s_2 + \varepsilon_1 \frac{k_1 K_m^2}{k_2\left(s_2 + \frac{K_m^2}{s_0}\right)}\right) + O(\varepsilon_1^2). \tag{4.31}$$

Note that, when $\varepsilon_1 = 0$, $c_1 = h_1(s_2, 0)$ and $c_2 = h_2(s_2, 0)$, equations (4.30) and (4.31) reduce to the equations of the slow manifold (4.21) and (4.22). Figure 4.7 displays a two dimensional phase diagram of the perturbed system (4.9) showing the dynamics in the variables c_2 and s_2. These graphs were obtained using the dynamical systems software XPP created by Prof. Bard Ermentrout at the University of Pittsburgh (available online at [42]). The existence of the slow manifold is clearly visible in these diagrams with an equilibrium point present in Figure 4.7(a) (if $\zeta < \zeta^*$), and no equilibrium point in Figure 4.7(b) (if $\zeta \geq \zeta^*$).

4.3.4 Dynamical systems analysis

In this section, we are going to give an alternative analysis of the system (4.9), which does not use the assumption that ε_1 is a small parameter. From equation (4.14c) we notice that the equilibrium value for s_2^* is positive if $\zeta < \zeta^*$ and negative (therefore irrelevant to our study) if $\zeta \geq \zeta^*$. Here, we are going to analyse these two cases in more detail.

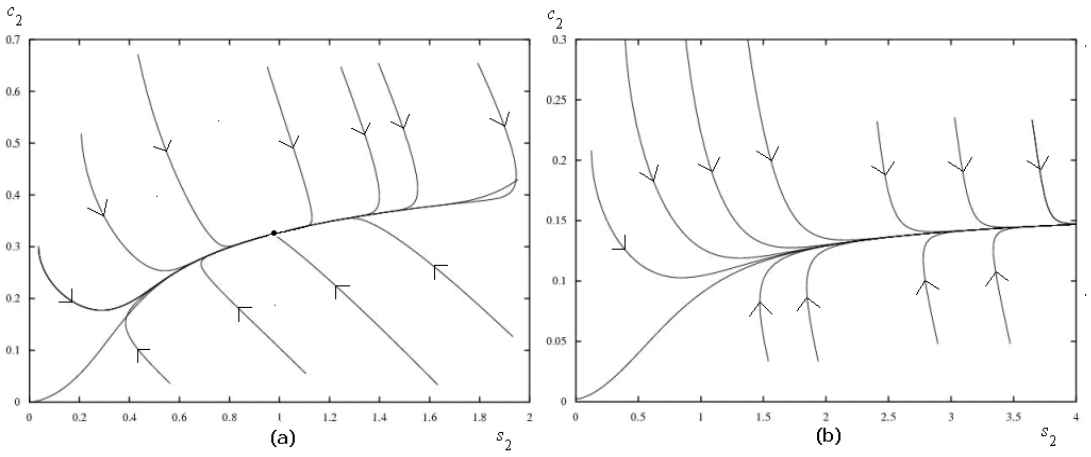

Figure 4.7 – Phase portrait of system (4.9) showing c_2 against s_2 in the cases of: (a) $\zeta < \zeta^*$, (b) $\zeta \geq \zeta^*$.

Case 1: When $\zeta < \zeta^*$, we know that in this case there is a unique equilibrium point, (c_1^*, c_2^*, s_2^*), which is positive and stable. However, the stability established previously by linear analysis is only local. That is to say, to determine whether an equilibrium of a system is stable or not, we have only considered infinitesimal perturbations around the nominal solution. This analysis is adequate for linear systems, since linear systems have identical local and global properties, but it is not adequate for non-linear systems. Therefore, in this model, the local stability does not establish that the solution starting at $(0, 0, 0)$ converges to the equilibrium point (c_1^*, c_2^*, s_2^*). To prove the equilibrium point (c_1^*, c_2^*, s_2^*) is globally stable, we are going to use LaSalle's Invariance Principle (refer to [43]) which is stated below.

Theorem 2 (LaSalle's Invariance Principle)

Consider the autonomous system

$$\dot{x} = f(x), \quad x(0) = x_0, \tag{4.32}$$

defined on the domain $D \subset R^n$. Let $\Omega \subset D$ be a compact (i.e., closed and bounded) set that is positively invariant with respect to the dynamics given by (4.32). *Let $V(\cdot)$ be a continuously differentiable function on D such that $\dot{V}(x) \leq 0$ in Ω. Let E be the set of all points in Ω where $\dot{V}(x) = 0$ and let M be the largest invariant set contained in E. Then every solution starting in Ω converges to M as $t \to \infty$.*

A set M is called an **invariant set** with respect to the dynamics (4.32) if

$$x(0) \in M, \text{ implies } x(t) \in M, \ \forall\ t \in R.$$

A set M is called **positively invariant** if

$$x(0) \in M, \text{ implies } x(t) \in M, \ \forall\ t \geq 0.$$

By definition, trajectories can neither enter nor leave an invariant set; trajectories may enter a positively invariant set; however, they just cannot leave it in forward time.

In our model, the set Ω is defined as a cube which has the origin and the equilibrium point, (c_1^*, c_2^*, s_2^*) as opposite corner points. More precisely we have

$$\Omega = \left\{(c_1, c_2, s_2) \in R^3 \mid 0 \leq c_1 \leq c_1^*, 0 \leq c_2 \leq c_2^*, 0 \leq s_2 \leq s_2^*\right\}.$$

In order to show Ω is a positively invariant set with respect to the dynamics of system (4.9), we need to show that all the flow trajectories starting in the set Ω stay in the set Ω forever.

The six faces in this cube are characterised by $c_1 = c_1^*$, $c_2 = c_2^*$, $s_2 = s_2^*$, $c_1 = 0$, $c_2 = 0$ and $s_2 = 0$. In order to show that all the trajectories point inwards through each side of the cube and do not leave it in forward time, we need to show:

On	***Need to show***
$c_1 = c_1^*$	$\frac{dc_1}{dt} \leq 0$
$c_2 = c_2^*$	$\frac{dc_2}{dt} \leq 0$
$s_2 = s_2^*$	$\frac{ds_2}{dt} \leq 0$
$c_1 = 0$	$\frac{dc_1}{dt} \geq 0$
$c_2 = 0$	$\frac{dc_2}{dt} \geq 0$
$s_2 = 0$	$\frac{ds_2}{dt} \geq 0$

From system (4.9), on the face defined by $c_1 = c_1^*$, we have

$$\frac{dc_1}{dt} = \frac{\zeta}{1+\zeta} - \left(1 + \frac{K_m^1}{s_0}\right) c_1^* = 0,$$

since $dc_1/dt = 0$ at equilibrium. This means that all trajectories starting in this plane remain in this plane. On the face defined by $c_2 = c_2^*$, we have

$$\frac{dc_2}{dt} = \frac{k_3}{k_1}\left(\frac{1}{1+\zeta} - c_2^*\right) s_2 - \frac{K}{s_0} c_2^*. \tag{4.33}$$

We also know that at equilibrium

$$\frac{k_3}{k_1}\left(\frac{1}{1+\zeta} - c_2^*\right) s_2^* - \frac{K}{s_0} c_2^* = 0; \tag{4.34}$$

subtracting equation (4.34) from (4.33) yields

$$\frac{dc_2}{dt} = \frac{k_3}{k_1}\left(\frac{1}{1+\zeta} - c_2^*\right)(s_2 - s_2^*) \leq 0,$$

since $0 \leq s_2 \leq s_2^*$ in Ω and $0 < c_2^* < 1/(1+\zeta)$. On the face defined by $s_2 = s_2^*$, we have

$$\frac{ds_2}{dt} = \varepsilon_1 \left(\frac{k_2}{k_1 s_0} c_1 - \frac{k_3}{k_1} \left(\frac{1}{1+\zeta} - c_2 \right) s_2^* + \frac{k_{-3}}{k_1 s_0} c_2 \right). \tag{4.35}$$

Similarly, we also know that at equilibrium

$$\frac{ds_2}{dt} = \varepsilon_1 \left(\frac{k_2}{k_1 s_0} c_1^* - \frac{k_3}{k_1} \left(\frac{1}{1+\zeta} - c_2^* \right) s_2^* + \frac{k_{-3}}{k_1 s_0} c_2^* \right) = 0, \tag{4.36}$$

and subtracting equation (4.36) from (4.35), we get

$$\frac{ds_2}{dt} = \varepsilon_1 \left(\frac{k_2}{k_1 s_0} (c_1 - c_1^*) + \frac{k_{-3}}{k_1 s_0} (c_2 - c_2^*) + \frac{k_3}{k_1} (c_2 - c_2^*) s_2^* \right) \leq 0,$$

since $0 \leq c_1 \leq c_1^*$, $0 \leq c_2 \leq c_2^*$ and $s_2^* \geq 0$ in Ω. On the face defined by $c_1 = 0$, we have

$$\frac{dc_1}{dt} = \frac{\zeta}{1+\zeta} > 0.$$

On the face defined by $c_2 = 0$, we have

$$\frac{dc_2}{dt} = \frac{k_3}{k_1} \frac{1}{1+\zeta} s_2 \geq 0,$$

since $0 \leq s_2 \leq s_2^*$ in Ω. On the face defined by $s_2 = 0$, we have

$$\frac{ds_2}{dt} = \varepsilon_1 \left(\frac{k_2}{k_1 s_0} c_1 + \frac{k_{-3}}{k_1 s_0} c_2 \right) \geq 0,$$

since $0 \leq c_1 \leq c_1^*$ and $0 \leq c_2 \leq c_2^*$ in Ω.

Thus, we have shown that Ω is a positively invariant set with respect to the dynamics of system (4.9). Next, we need to define the **Lyapunov function** for this model.

The Lyapunov function is simply a continuous scalar function of the state variables, with continuous partial derivatives. The original motive for the development of Lyapunov's direct method was based on the physical concept of the energy content of a system, which, in the usual dissipative case, is naturally a decreasing function of time, and this is often a fruitful source of Lyapunov functions in practice. But on the other hand, there is no reason why we should be restricted to using a function of this type, and indeed it may not be appropriate in many cases. There is, unfortunately, no completely general systematic procedure for obtaining Lyapunov functions; refer to [20] for more details on how to construct the Lyapunov functions.

In our model, the Lyapunov function is a function of the three state variables $c_1(t)$, $c_2(t)$ and $s_2(t)$ defined as

$$V(\cdot) = V(c_1(t), c_2(t), s_2(t)).$$

We let

$$V(c_1(t), c_2(t), s_2(t)) = \alpha(c_1^* - c_1) + \beta(c_2^* - c_2) + \gamma(s_2^* - s_2), \tag{4.37}$$

where α, β and γ are arbitrary constants which will be estimated in later calculations, subject to the condition that $\dot{V}(c_1(t), c_2(t), s_2(t)) \leq 0$. We have

$$\dot{V}(c_1(t), c_2(t), s_2(t)) = \frac{\partial V}{\partial c_1} \cdot \frac{\partial c_1}{\partial t} + \frac{\partial V}{\partial c_2} \cdot \frac{\partial c_2}{\partial t} + \frac{\partial V}{\partial s_2} \cdot \frac{\partial s_2}{\partial t}, \tag{4.38}$$

and since

$$\frac{\partial V}{\partial c_1} = -\alpha, \tag{4.39}$$

$$\frac{\partial V}{\partial c_2} = -\beta, \tag{4.40}$$

$$\frac{\partial V}{\partial s_2} = -\gamma, \tag{4.41}$$

we get

$$\dot{V}(c_1(t), c_2(t), s_2(t)) = -\alpha\left(\frac{\zeta}{1+\zeta} - \left(1 + \frac{K_m^1}{s_0}\right)c_1\right) - \beta\left(\frac{k_3}{k_1}\left(\frac{1}{1+\zeta} - c_2\right)s_2 - \frac{K}{s_0}c_2\right)$$
$$-\gamma\left(\varepsilon_1\left(\frac{k_2}{k_1 s_0}c_1 - \frac{k_3}{k_1}\left(\frac{1}{1+\zeta} - c_2\right)s_2 + \frac{k_{-3}}{k_1 s_0}c_2\right)\right),$$

giving

$$\dot{V}(c_1(t), c_2(t), s_2(t)) = -\frac{\alpha\zeta}{1+\zeta} + \left(\alpha + \frac{\alpha K_m^1}{s_0} - \frac{\gamma\varepsilon_1 k_2}{k_1 s_0}\right)c_1$$
$$+\left(\frac{\beta K}{s_0} + \frac{\gamma\varepsilon_1 k_{-3}}{k_1 s_0}\right)c_2 + \left(\frac{\gamma\varepsilon_1 k_3}{k_1} - \frac{\beta k_3}{k_1}\right)s_2\left(\frac{1}{1+\zeta} - c_2\right).$$

If we let

$$\frac{\gamma\varepsilon_1 k_3}{k_1} - \frac{\beta k_3}{k_1} = 0,$$

$\dot{V}(c_1(t), c_2(t), s_2(t))$ simplifies to

$$\dot{V}(c_1(t), c_2(t), s_2(t)) = -\frac{\alpha\zeta}{1+\zeta} + \frac{\alpha k_1 s_0 + \alpha(k_{-1} + k_2) - \beta k_2}{k_1 s_0}c_1 + \frac{\beta k_4}{k_1 s_0}c_2,$$

and then by letting $\alpha k_1 s_0 + \alpha(k_{-1} + k_2) - \beta k_2 = 0$, we obtain

$$\alpha = \frac{\beta k_2}{k_1 s_0 + k_{-1} + k_2},$$

which yields

$$\dot{V}(c_1(t), c_2(t), s_2(t)) = -\frac{\beta k_2 \zeta}{(k_1 s_0 + k_{-1} + k_2)(1+\zeta)} + \frac{\beta k_4}{k_1 s_0}c_2$$

$$= -\frac{\beta k_4}{k_1 s_0}\left(\frac{k_2\zeta}{k_4\left(1 + \frac{K_m^1}{s_0}\right)(1+\zeta)} - c_2\right)$$
$$= -\frac{\beta k_4}{k_1 s_0}\left(c_2^* - c_2\right).$$

Now if we take $\beta = 1$, we get

$$\dot{V}(c_1(t), c_2(t), s_2(t)) = -\frac{k_4}{k_1 s_0}(c_2^* - c_2) \leq 0,$$

since $0 \leq c_2 \leq c_2^*$ in Ω. We can see that $\dot{V}(c_1(t), c_2(t), s_2(t)) = 0$ if and only if $c_2 = c_2^*$.

Therefore, the function V defined in equation (4.37) satisfies the conditions of LaSalle's Invariance Principle if we take

$$\alpha = \frac{k_2}{k_1 s_0 + k_{-1} + k_2}, \quad \beta = 1, \quad \gamma = \frac{1}{\varepsilon_1}.$$

Now let E denote all the points in the set Ω, where $\dot{V}(c_1(t), c_2(t), s_2(t)) = 0$ (one side of the cube Ω is defined by $c_2 = c_2^*$), the largest invariant set contained in this plane is the equilibrium point (c_1^*, c_2^*, s_2^*) itself, which corresponds to the set M mentioned in the LaSalle's Invariance Principle. Thus, every solution starting in the cube Ω converges to the equilibrium point (c_1^*, c_2^*, s_2^*) as $t \to \infty$. In particular, this proves that the solution with initial conditions $c_1(0) = 0$, $c_2(0) = 0$, $s_2(0) = 0$ converges to the equilibrium point.

Case 2: When $\zeta \geq \zeta^*$, there is no equilibrium point in the positive octant where $c_1 \geq 0$, $c_2 \geq 0$ and $s_2 \geq 0$.

In this case we need to show that

$$\begin{cases} \lim\limits_{t\to\infty} c_1(t) = c_1^* = \dfrac{\zeta}{(1+\zeta)\left(1 + \frac{K_m^1}{s_0}\right)} & \text{(4.42a)} \\ \lim\limits_{t\to\infty} s_2(t) = \infty & \text{(4.42b)} \\ \lim\limits_{t\to\infty} c_2(t) = \dfrac{1}{1+\zeta}, & \text{(4.42c)} \end{cases}$$

where the first limit is easily verified since the first equation only depends on $c_1(t)$. In what follows we will use results from the theory of monotone dynamical systems (refer to [44]) to show equations (4.42b) and (4.42c) are valid.

We first define some order relations on R^n as follows. For $u, v \in R^n$, we write

$$u \leq v \;\Leftrightarrow\; u_i \leq v_i,$$

$$u < v \;\Leftrightarrow\; u_i \leq v_i,\; u \neq v,$$

$$u \ll v \;\Leftrightarrow\; u_i < v_i,$$

where $i = 1, ...n$ (refer to [45]).

Next, we define monotone and cooperative systems, following [44].

Definition 2

Consider the autonomous system of ordinary differential equations

$$x^{'} = f(x), \tag{4.43}$$

where f is continuously differentiable on an open subset $D \subset R^n$. Let $\phi_t(x)$ denotes the solution of system (4.43) *that starts at the point x at $t = 0$. The function ϕ_t will be referred to as the flow corresponding to system* (4.43).

Let $x_0, y_0 \in D$, and let $<_r$ denote any one of the relations $\leq$, $<$, $\ll$; then the dynamical system (4.43) *is said to be* ***monotone*** *if $x_0 <_r y_0$ implies that*

$\phi_t(x_0) <_r \phi_t(y_0)$, *for all* $t > 0$.

Definition 3

We say that D *is p-convex if* $tx + (1-t)y \in D$ *for all* $t \in [0,1]$ *whenever* $x, y \in D$ *and* $x \leq y$. *If* D *is a convex set then it is also p-convex. Then the system* (4.43) *is said to be a* ***cooperative system*** *if*

$$\frac{\partial f_i}{\partial x_j}(x) \geq 0, \ i \neq j, \ x \in D$$

holds on the p-convex domain D.

In our system (4.9), we let

$$D = \Omega_1 = \left\{ (c_1, c_2, s_2) \in R^3 \mid 0 \leq c_1 \leq c_1^*, 0 \leq c_2 \leq \frac{1}{1+\zeta}, 0 \leq s_2 \leq \infty \right\}.$$

Recall that the infinite rectangular box Ω_1 was shown to be a positive invariant set for system (4.9) in Section 4.3.1, and it is clearly a p-convex set. We can also easily show that

$$\begin{aligned} \frac{\partial f_1}{\partial c_2} = 0, \ \frac{\partial f_1}{\partial s_2} = 0, \\ \frac{\partial f_2}{\partial c_1} = 0, \ \frac{\partial f_2}{\partial s_2} \geq 0, \\ \frac{\partial f_3}{\partial c_1} \geq 0, \ \frac{\partial f_3}{\partial c_2} \geq 0, \end{aligned}$$

so that system (4.9) is a cooperative system, and a cooperative system generates a monotone dynamical system.

Proposition 1

If $f(x)$ is cooperative and $<_r$ is as stated in Definition 1 above, then

$$P_+ = \{x \in D \mid 0 <_r f(x)\}$$

is a positive invariant set, and any solution starting in this set is monotone so that any bounded solution here must converge to an equilibrium. (refer to [44] for the proof.)

It is easy to show that, in the case of our system, the point $(0, 0, 0)$ is in P_+, so the solution starting at the origin will be contained in P_+ for all $t > 0$. Thus, this solution is monotone but it cannot be bounded as the result above states that it would then converge to an equilibrium point inside $P_+ \subset D$. This contradicts the fact that there is no equilibrium point inside the domain D in this case. Hence, the solution starting at $(0, 0, 0)$ is unbounded, so we must have

$$\lim_{t\to\infty} s_2(t) = \infty.$$

The component $c_2(t)$ is, however, both monotone and bounded and so must converge to a finite limit. We have $dc_2/dt = 0$, which implies

$$\frac{k_3}{k_1}\left(\frac{1}{1+\zeta} - c_2\right) s_2 - \frac{K}{s_0} c_2 = 0,$$

and as

$$\lim_{t\to\infty} s_2(t) = \infty,$$

we must have

$$\lim_{t\to\infty} c_2(t) = \frac{1}{1+\zeta}.$$

4.3.5 Results

From the analysis presented in the previous subsections we conclude that the long term behaviour of system (4.9) is as follows,

$$\lim_{t\to\infty} c_1(t) = c_1^*, \quad \text{for all} \quad \zeta, \tag{4.44}$$

$$\lim_{t\to\infty} c_2(t) = \begin{cases} c_2^* = \dfrac{\zeta}{\zeta^*(1+\zeta)}, & \text{if } \zeta \le \zeta^* \quad (4.45) \\ \dfrac{1}{1+\zeta}, & \text{if } \zeta \ge \zeta^*, \quad (4.46) \end{cases}$$

$$\lim_{t\to\infty} s_2(t) = \begin{cases} s_2^*, & \text{if } \zeta < \zeta^* \quad (4.47) \\ \infty, & \text{if } \zeta \ge \zeta^*, \quad (4.48) \end{cases}$$

where c_1^*, c_2^* and s_2^* were defined in equations (4.10), (4.11) and (4.12). We plot the steady state current, $k_4 c_2(\infty)$, as a function of ζ for various values of s_0 (Figure 4.8) and k_4/k_2 (Figure 4.9). Note that the overlaying of curves in Figure 4.8 for ζ values of 1 to 6 and in Figure 4.9 for ζ values of 0 to 1, also note that from equations (4.45) and (4.46), that the optimal GOX:HRP ratio is always given by

$$\zeta^* = \frac{k_4}{k_2}\left(1 + \frac{K_m^1}{s_0}\right),$$

as $c_2(\infty)$ achieves its maximum value of $1/(1+\zeta^*)$ when $\zeta = \zeta^*$. Hence, in this simple model which ignores the diffusion of the two substrates, it is possible to obtain an explicit formula which gives the optimal value of ζ in terms of the system parameters.

Note again the agreement between the results as shown in Figure 4.8 and Figure 4.9 and the model in the previous section; further comparisons will be made in Section 4.5.

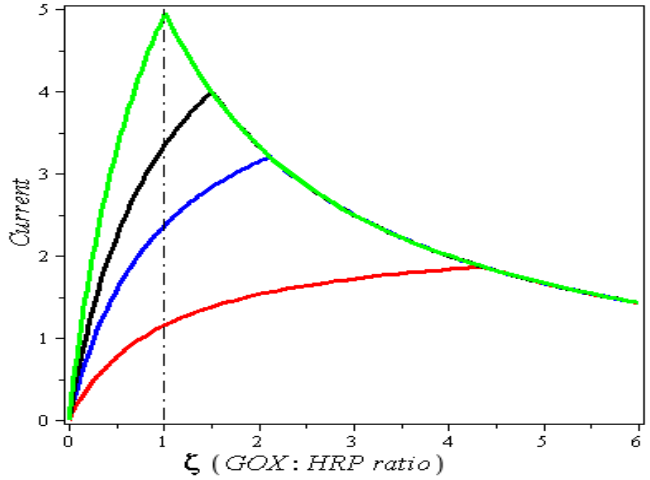

Figure 4.8 – Dependence of current on ζ for different initial concentrations of s_0. The curves correspond to $s_0 = 0.03, 0.09, 0.2$ and 5 mM from the bottom to top. Typical values for constants used in this simulation are: $k_1 = 10^2$, $k_{-1} = 10^{-1}$, $k_2 = 10$ and $k_4 = 10$.

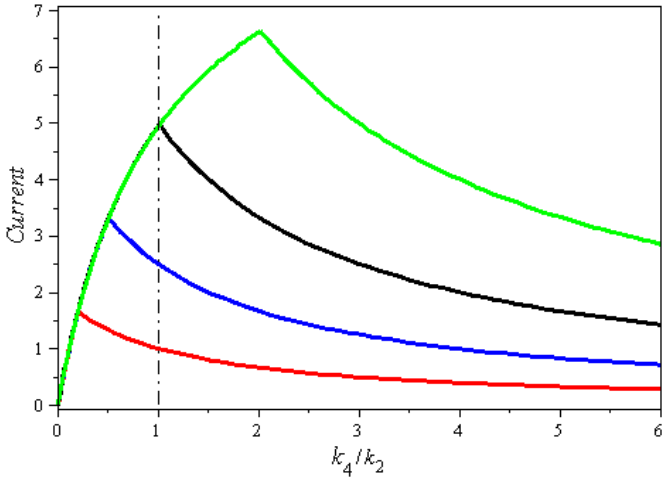

Figure 4.9 – Dependence of current on ζ for different values of k_4/k_2. The curves correspond to $k_4/k_2 = 0.2, 0.5, 1$ and 2 from the bottom to top. Typical values for constants used in this simulation are the same as in Figure 4.8.

4.4 Intermediate model

In this model, we assume the glucose (s_1) does not diffuse but is present only at the electrode boundary point, and in addition it is constant, i.e., $s_1(t) = s_0$. (In other words, s_1 is supplied continuously at the reaction site.) The second substrate is free to diffuse throughout the domain at all times during the experiment, which is reflected by the following diffusion equation

$$\frac{\partial s_2(x,t)}{\partial t} = D_1 \frac{\partial^2 s_2(x,t)}{\partial x^2}.$$

At the top layer and the electrode, we have the boundary conditions

$$s_2(L,t) = 0,$$

$$D_1 \frac{\partial s_2(0,t)}{\partial x} = k_3 e_2(t) s_2(0,t) - k_2 c_1(t) - k_{-3} c_2(t),$$

together with

$$\begin{aligned}
\frac{de_1}{dt} &= -k_1 e_1(t) s_1(t) + (k_{-1} + k_2) c_1(t), \\
\frac{de_2}{dt} &= -k_3 e_2(t) s_2(0,t) + (k_{-3} + k_4) c_2(t), \\
\frac{dc_1}{dt} &= k_1 e_1(t) s_1(t) - (k_{-1} + k_2) c_1(t), \\
\frac{dc_2}{dt} &= k_3 e_2(t) s_2(0,t) - (k_{-3} + k_4) c_2(t), \\
\frac{dp}{dt} &= k_4 c_2(t).
\end{aligned}$$

The initial conditions are:

$$e_1(0) = e_1^0, \quad e_2(0) = e_2^0, \quad s_1(0) = s_0, \quad s_2(x,0) = 0,$$

$$c_1(0) = 0, \quad c_2(0) = 0, \quad p(x,0) = 0,$$

and the conservation laws are:

$$\begin{cases} e_1(t) + c_1(t) = e_1^0 \\ \\ e_2(t) + c_2(t) = e_2^0. \end{cases}$$

We are going to non-dimensionalise the system by introducing the following variables,

$$\bar{s_2}(\bar{x}, \bar{t}) = \frac{s_2(x,t)}{s_0}, \quad \bar{e_1}(\bar{t}) = \frac{e_1(t)}{e}, \quad \bar{e_2}(\bar{t}) = \frac{e_2(t)}{e},$$

$$\bar{c_1}(\bar{t}) = \frac{c_1(t)}{e}, \quad \bar{c_2}(\bar{t}) = \frac{c_2(t)}{e}, \quad \bar{x} = \frac{x}{l}, \quad \bar{t} = \frac{t}{t_0},$$

where $t_0 = 1/(k_1 s_0)$; we then obtain the non-dimensional system

$$\begin{cases} \dfrac{\partial s_2(x,t)}{\partial t} = \dfrac{D_1}{k_1 s_0 l^2} \dfrac{\partial^2 s_2(x,t)}{\partial x^2} & \text{(4.50a)} \\ s_2(x,0) = 0 & \text{(4.50b)} \\ s_2(1,t) = 0 & \text{(4.50c)} \\ \dfrac{\partial s_2(0,t)}{\partial x} = \eta \left(s_2(0,t) \left(\dfrac{1}{1+\zeta} - c_2(t) \right) - \kappa c_1(t) - \mu c_2(t) \right) & \text{(4.50d)} \\ \dfrac{dc_1(t)}{dt} = \dfrac{\zeta}{1+\zeta} - (1+\sigma_1) c_1(t) & \text{(4.50e)} \\ \dfrac{dc_2(t)}{dt} = \rho_2 \left(s_2(0,t) \left(\dfrac{1}{1+\zeta} - c_2(t) \right) - \sigma_2 c_2(t) \right), & \text{(4.50f)} \end{cases}$$

with non-dimensional initial conditions

$$e_1(0) = \frac{\zeta}{1+\zeta}, \quad e_2(0) = \frac{1}{1+\zeta}, \quad s_2(x,0) = 0, \quad c_1(0) = 0, \quad c_2(0) = 0,$$

and conservation laws

$$\begin{cases} e_1(t) + c_1(t) = \dfrac{\zeta}{1+\zeta} \\ e_2(t) + c_2(t) = \dfrac{1}{1+\zeta}, \end{cases}$$

where

$$\zeta = \frac{e_1^0}{e_2^0}, \quad \eta = \frac{k_3 el}{D_1}, \quad \kappa = \frac{k_2}{k_3 s_0},$$
$$\mu = \frac{k_{-3}}{k_3 s_0}, \quad \rho_2 = \frac{k_3}{k_1}, \quad \sigma_1 = \frac{K_m^1}{s_0}, \quad \sigma_2 = \frac{K_m^2}{s_0}.$$

We now carry out a steady-state analysis of system (4.50), similar to the calculation carried out in Section 4.2.2. At equilibrium,

$$\frac{\partial s_2(x,t)}{\partial t} = 0,$$

which gives

$$\frac{\partial^2 s_2(x,t)}{\partial x^2} = 0. \tag{4.52}$$

Then by integrating (4.52) twice, we obtain

$$s_2^*(x) = Ax + B,$$

which gives

$$s_2^*(0) = B, \tag{4.53}$$

where $s_2^*(x)$ denotes the equilibrium value of $s_2(x,t)$, A and B are constants of integration. Also, from equation (4.50c), we obtain $A = -B$ and this condition together with equation (4.53) yields

$$s_2^*(x) = B(1-x),$$

which gives

$$\frac{\partial s_2^*(0)}{\partial x} = -B. \tag{4.54}$$

From equation (4.50e), we obtain

$$c_1^* = \frac{\zeta}{(1+\zeta)(1+\sigma_1)},$$

and, from equation (4.50f), we obtain

$$c_2^* = \frac{1}{1+\zeta}\frac{s_2^*(0)}{s_2^*(0)+\sigma_2}.$$

Also, from equations (4.50d) and (4.54), we get

$$-B = \eta\left(s_2^*(0)\left(\frac{1}{1+\zeta} - c_2^*\right) - \kappa c_1^* - \mu c_2^*\right),$$

which gives

$$(1+\zeta)B^2 + \left(\sigma_2(1+\zeta) + \eta(\sigma_2 - \mu) - \frac{\kappa\zeta\eta}{1+\sigma_1}\right)B - \frac{\kappa\zeta\eta\sigma_2}{1+\sigma_1} = 0,$$

from which, B can be easily obtained as a function of ζ, i.e., $B(\zeta)$. (Note that since the above quadratic equation has two real roots of different signs, we choose the positive root.)

Thus, the equilibrium value for the current is

$$I \approx k_4 c_2^* = \frac{k_4}{1+\zeta}\frac{B(\zeta)}{B(\zeta)+\sigma_2}.$$

The plot of the current ($k_4 c_2^*$) versus ζ for different initial concentrations of glucose is as shown in Figure 4.10; if we vary k_4/k_2 instead, we obtain the graphs in Figure 4.11.

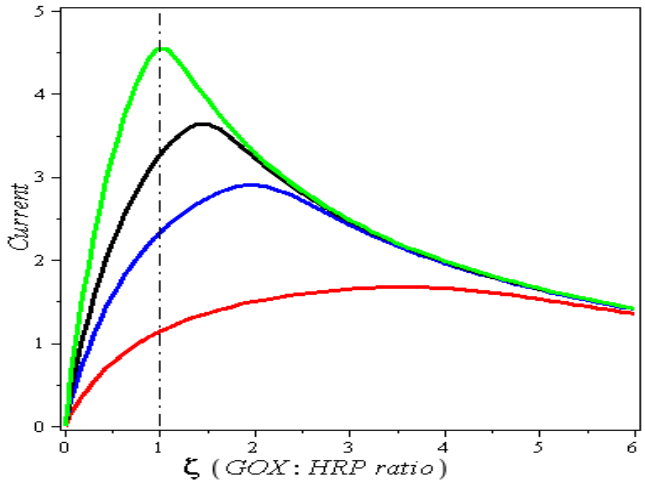

Figure 4.10 – Dependence of current on ζ for different initial concentrations of s_0. The curves correspond to $s_0 = 0.03, 0.09, 0.2$ and 5 mM from the bottom to top. Typical values for constants used in this simulation are: $k_1 = 10^2$, $k_{-1} = 10^{-1}$, $k_2 = 10$, $k_3 = 10^2$, $k_{-3} = 10^{-1}$, $k_4 = 10$, $e_0 = 10^{-5}$, $l = 2 \times 10^{-4}$ and $D_1 = 6.7 \times 10^{-10}$.

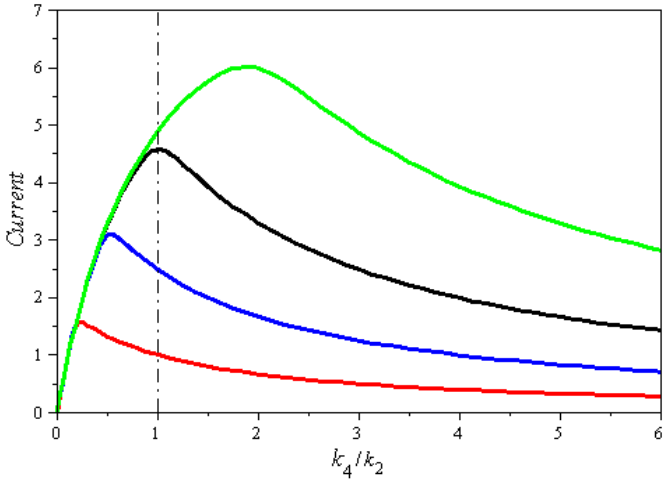

Figure 4.11 – Dependence of current on ζ for different values of k_4/k_2. The curves correspond to $k_4/k_2 = 0.2, 0.5, 1$ and 2 from the bottom to top. Typical values for constants used in this simulation are the same as in Figure 4.10.

4.5 Summary and comparisons

In this chapter, we have studied the behaviour of a bi-enzyme biosensor based on a cascade reaction, with particular emphasis placed on determining the value of the enzyme ratio which leads to optimal performance (characterised by maximum signal amplitude). Three different models were considered: the "comprehensive model" (where diffusion effects were included for both substrates, glucose and hydrogen peroxide), the "simplified model" (which concentrated on the kinetics of the two reactions and no transport was taken into account) and the "intermediate model" (which only considered the diffusion of the second substrate). As the simplified model consisted of a system of ordinary differential equations, we were able to present a detailed analytical study of its solutions (including an exact formula for the optimal GOX:HRP ratio), unlike in the other two models where the results were mostly numerical.

The dependence of the biosensor response (i.e., the measured amperometric current) as a function of ζ, the ratio of the two enzymes, is again plotted in Figure 4.12, for different values of the glucose concentration and, in Figure 4.13, for different values of k_4/k_2. To facilitate the comparison of the three models, we then plot the optimal ζ value (the value which maximises the current) as a function of the glucose concentration. The four resulting curves are as shown in Figure 4.14.

We note that the simple model and the intermediate model give identical results for the optimal enzyme ratio for all values of initial glucose concentration. The values predicted by the comprehensive model are quite different at low glucose con-

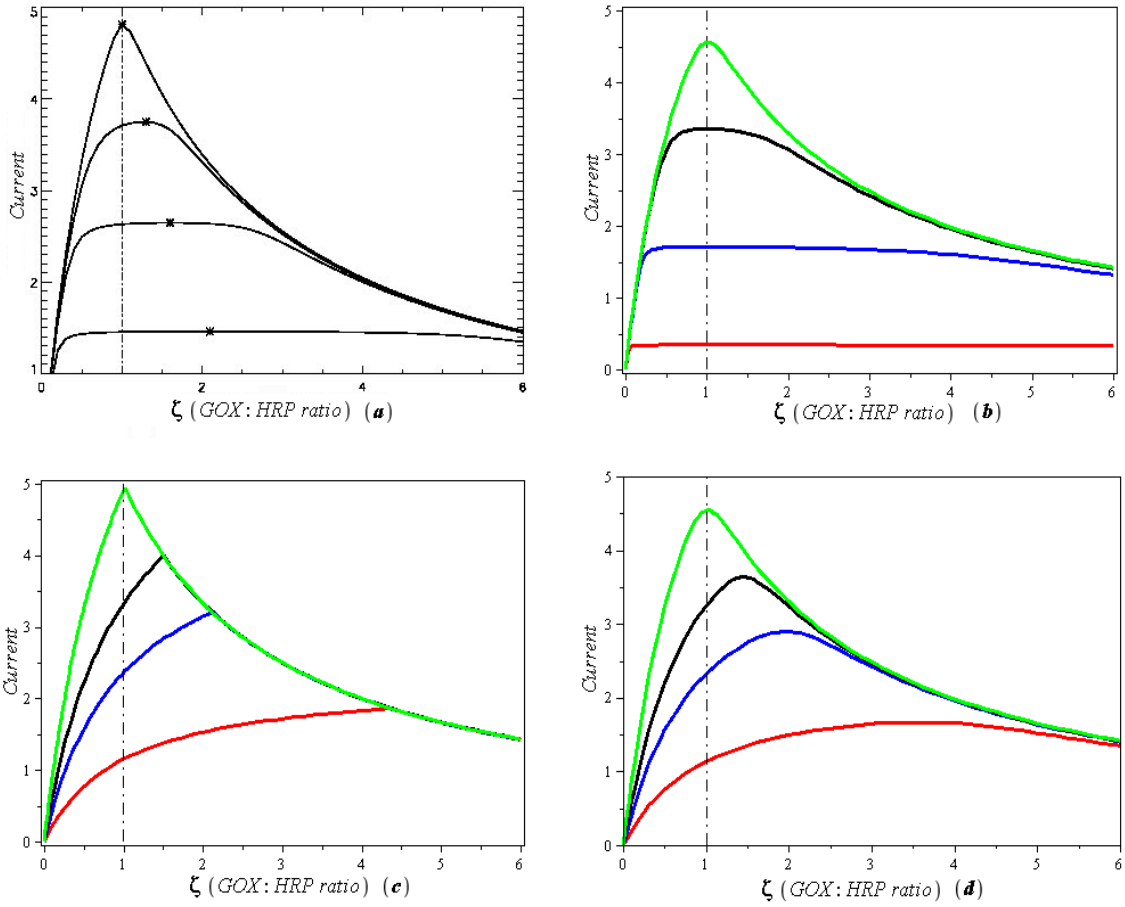

Figure 4.12 – Dependence of current on ζ for different initial concentrations of s_0. Steady-state analysis of (a) and (b) comprehensive model, (c) simplified model, and (d) intermediate model.

centrations but, again, identical at high glucose concentrations. Note that, at high glucose concentration, the optimal enzyme ratio approaches the same value regardless of the model used (This value is $\zeta^* = 1$ in our graph, as a consequence of choosing $k_2 = k_4$.). The fact that a given optimal enzyme ratio is achieved at a higher value of glucose concentration in the comprehensive model is quite obvious, since in that model the glucose is diffusing from a distant place (unlike in the other two models

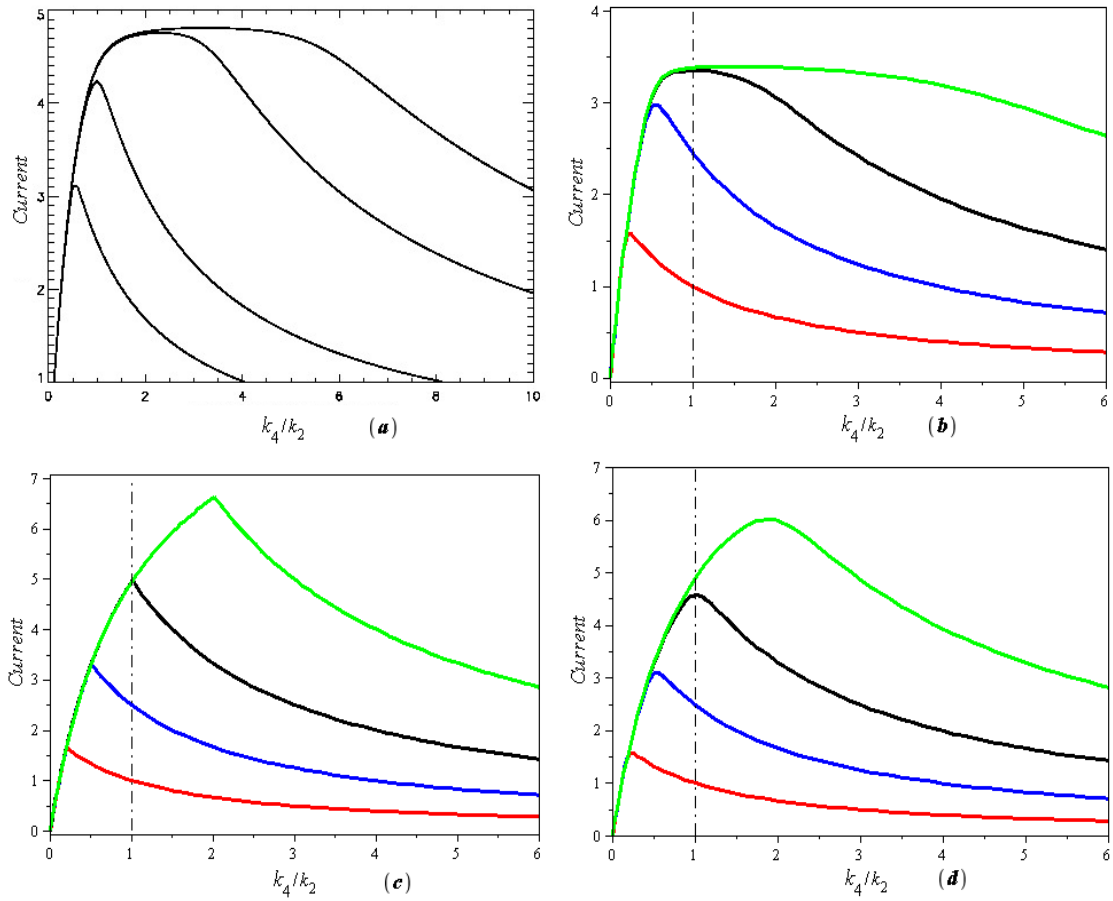

Figure 4.13 – Dependence of current on ζ for different values of k_4/k_2. Steady-state analysis of (a) and (b) comprehensive model, (c) simplified model, and (d) intermediate model.

where s_0 represents the glucose concentration at the reaction site). Also, at high glucose concentrations, we expect both enzymes to be saturated with the corresponding substrates (i.e., working at maximum capacity) and so increasing the amount of glucose will not make any difference to the biosensor performance. The three models will give the same result in this regime as the transport effects only affect the availability of substrates at the reaction site.

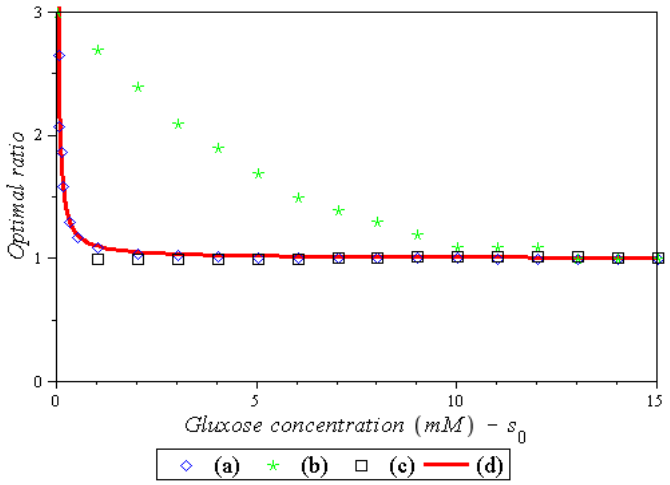

Figure 4.14 – Dependence of optimal ratio (GOX:HRP) on s_0 (glucose concentration). (a) Steady-state analysis of intermediate model, (b) Numerical analysis of comprehensive model, (c) Steady-state analysis of comprehensive model, and (d) Steady-state analysis of simplified model.

Next, we studied the dependence of the optimal enzyme ratio on a different parameter associated with our chemical system, namely k_4/k_2 which represents the ratio of the catalytic turnover numbers for the two consecutive reactions. The optimal ratio ζ was plotted against k_4/k_2 for the three models and the resulting graphs are shown in Figure 4.15. Note that, the simple model predicts a linear relationship between ζ^* and k_4/k_2, as illustrated by equation (4.13). The three models seem to give identical results at low values of k_4/k_2, but diverge when the second reaction becomes much faster than the first.

In conclusion, parameter regimes which are characterised by high glucose concentrations and low values of k_4/k_2 seem relatively indifferent to the modelling strategy

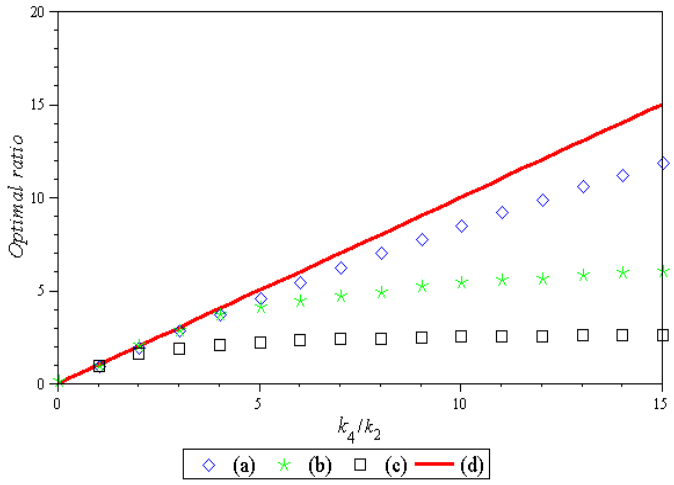

Figure 4.15 – Dependence of optimal ratio (GOX:HRP) on k_4/k_2 ratio. (a) Steady-state analysis of intermediate model, (b) Numerical analysis of comprehensive model, (c) Steady-state analysis of comprehensive model, and (d) Steady-state analysis of simplified model.

used and so we would recommend the simple model, which is the easiest to analyse. For all the other parameter regions, further understanding of the behaviour of the system is required and our results so far seem to imply that we need to investigate the relationship between diffusion rates and the speeds of the two reactions. An asymptotic analysis based on these parameters will form the subject of a future study.

Conclusions and Future Work

The motivation for this thesis was provided by a collaboration with the National Centre for Sensor Research (NCSR) and the Biomedical Diagnostics Institute (BDI) at Dublin City University involving mathematical and computational modelling of biosensors. Several experimental problems relevant to ongoing research in these centres were presented which were mostly concerned with optimising design parameters for biosensing devices. We constructed mathematical models for these problems and, using analytical methods or numerical simulations, we attempted to describe the behaviour of solutions, with a view to providing recommendations for improving experimental practice. As well as studying these practical problems directly, a large part of the thesis was dedicated to reviewing existing mathematical models relevant to biosensor design, usually involving kinetics or transport of chemical species.

A brief summary of our work is given below. In Chapter 2, we reviewed the Michaelis-Menten mathematical framework for studying the kinetics of enzyme-substrate interactions. This scheme is widely used for modelling such reactions in the biochemistry literature and numerous mathematical studies of the resulting models exist. We also investigated a generalised model corresponding to the more realistic assumption

of reversible kinetics and found it to be equivalent to the predominantly used classical scheme. Chapter 3 studied mathematical models for antibody-antigen reactions in the context of three different types of immunosensors, namely direct, competitive and sandwich assays. In the case of direct and competitive assays, we determined that the predicted biosensor response (as measured by the concentration of the steady-state products) is the same for models with or without diffusion of species. This work can therefore be used to provide simplified modelling strategies for chemistry researchers. We have also examined the connection between modelling results and experimental calibration curves as well as the possibility of tracking non-specific biosensor responses. Chapter 4 analysed and compared three different models of varying complexity, with the aim of determining the optimal enzyme ratio necessary for maximising a biosensor performance. It was concluded that the models agreed when the analyte concentration was sufficiently high and the catalytic rates of the two enzymes were assumed to be close to each other. In this parameter regime, the optimal ratio of the two enzymes was seen to be equal to 1, which agreed with experimental results. However, as detailed in the summary and comparison section of Chapter 4, we need to understand the behaviour of this system for other parameter regions and so further asymptotic and numerical studies are required, especially for the two modelling strategies which involve diffusion.

The design of biosensing devices offers a rich source of mathematical modelling problems and we hope to continue our interdisciplinary collaboration with NCSR/BDI. Some of the identified problems, whose study was already initiated and presented partially in this thesis, are listed below.

Fluorescent-based immunoassays

Such devices are currently studied within the BDI in connection with the possibility of early detection of biochemical markers for meningitis or cancer. Due to their high sensitivity, fluorescence-based bioassays are widely used in biomedical diagnostics. The most commonly used fluorescent labels are organic or inorganic molecules. However, organic and inorganic dyes are susceptible to rapid photo bleaching and quenching due to interaction with the solvent environment and molecular quenchers such as oxygen. Furthermore, while fluorescence-based detection offers high sensitivity in principle, there is often a low level of detectable fluorescence from the bioassay platform due to the relatively low surface coverage of labelled biomolecules. Hence, there is a need for brighter fluorescent labels which will increase sensitivity and lower the limit of detection (LOD) in optical bioassays, particularly in the case of low volume samples. This project was focused on modelling of a fluorescence-based sandwich immunoassay in which highly fluorescent silica nanoparticles are used as the fluorescence label instead of the conventionally used single dye label. This will complement and make a significant contribution to the ongoing BDI fluorescence-based immunoassay development programme.

Sandwich assays were briefly introduced in Chapter 3 but more theoretical and numerical studies are needed. Mathematical models of sandwich assays are relatively rare in the literature so it is hoped that further work in this area would provide significant insight into the design of these important optical bioassays.

Enzyme-channelling immunoassays

The problem studied in Chapter 4 dealt with the optimisation of a bi-enzyme electrode. This represents, however, only a first step towards modelling the theoretical and experimental platform studied by NCSR researchers which provided the initial motivation. The original experimental setting involves a combination of antibody and enzyme (HRP) immobilised on an electrode and a fluid sample containing antigen and analogue. The analogue is, in this case, antigen which is labelled with a second enzyme (GOX). The substrate of the enzyme label (i.e., glucose) is also introduced into the system and the same cascade reaction as in Chapter 4 is initiated. The main question to be answered in this context is, given the amount of enzyme-labelled antigen and the signal recorded at the electrode, what was the initial concentration of pure antigen in the sample? This competitive immunosensor was studied experimentally in [37] where it was argued that there are many advantages of coupling the immunological reaction to an enzyme-channelling scheme such as, for example, increasing the amplitude of the specific signal (obtained from labelled antigen binding to antibody) relative to the noise (given by reactions in the bulk solution). A mathematical model for this complex system was proposed in [46] and some preliminary numerical simulations were performed. We intend to take this problem a step further and attempt a theoretical analysis of the model, which would combine results obtained for competitive assays in Chapter 3 as well as cascade reactions in Chapter 4. As suggested in Section 3.3, constructing analytical and numerical techniques for tracking specific and non-specific signals should also be feasible, which should lead to improved design parameter choices and device optimisation.

Bibliography

[1] J.S. Wilson, *Sensor technology handbook, Volume 1.* Published by Elsevier Inc., 2005.

[2] A. Sadana, *Binding and Dissociation Kinetics for Different Biosensor Applications Using Fractals.* Published by Elsevier, 2006.

[3] D. Wild, *The Immunoassay Handbook.* Published by Elsevier, 2005.

[4] E. Benjamini, R. Coico and G. Sunshine, *Immunology: a short course.* Published by Wiley, 2000.

[5] B. Suzanne, *Forensic Chemistry.* Published by Upper Saddle River, N.J.: Pearson Prentice Hall, 2006.

[6] G. Williams, *Advanced Biology for you.* Published by Stanley Thornes (Publishers) Ltd, 2000.

[7] J.L. Jain, S. Jain and N. Jain, *Elementary Biochemistry.* Published by S.Chand and Company Ltd, 2007.

[8] L. Gorton, *Biosensors and Modern Biospecific Analytical Techniques.* Published by Elsevier B.V., 2005.

[9] T.M. Canh, *Biosensors.* Published by Chapman & Hall and Masson, 1993.

[10] F. Scheller and F. Schubert, *Biosensors.* Published by Akademie Verlag licensed edition for Elsevier Science Publishers B.V., 1992.

[11] R. Chang, *Physical Chemistry for the Biosciences.* Published by University Science Books, 2005.

[12] H. Gutfreund, *Kinetics for the life sciences: receptors, transmitters and catalysts.* Published by Cambridge University Press, 1995.

[13] V. Leskovac, *Comprehensive enzyme kinetics.* Published by Kluwer Academic/Plenum Publishers, New York, 2003.

[14] H. Anton, I. Bivens and S. Davis, *Calculus.* Published by Wiley, New York, 2005.

[15] C.C. Lin and L.A. Segel, *Mathematics Applied to Deterministic Problems in the Natural Sciences.* Published by SIAM, 1988.

[16] L. A. Segel, *Simplification and Scaling.* SIAM Rev., 14 (1972), pp. 547-571.

[17] J. Keener, J. Sneyd, *Mathematical Physiology.* Published by Springer-Verlag, New York, Inc., 1998.

[18] L. Michaelis and M. Menten, *Die Kinetik der Invertinwirkung.* Biochem. Z., 49(1913), pp. 333.

[19] S.H. Strogatz, *Nonlinear Dynamics and Chaos (with applications to Physics, Biology, Chemistry and Engineering.* Published by Perseus Books Publishing, L.L.C., 1994.

[20] P.A. Cook, *Nonlinear Dynamical Systems.* Published by Prentice-Hall International (UK) Ltd, 1986.

[21] G.E. Briggs and J.B.S. Haldane, *A note on the kinetics of enzyme action.* Biochem. J., 1925.

[22] A. Fersht, *Enzyme Structure and Mechanism.* Published by W.H.Freeman, New York, 1985.

[23] J. Bowen, A. Acrivos and A. Oppenheim, *Singular perturbation refinement to quasi-steady state approximation in chemical kinetics.* Chem. Engrg. Sci., 18 (1963), pp. 177-188.

[24] A. Lehninger, *Principle of Biochemistry.* Published by Worth, New York, 1982.

[25] A.C. Fowler, *Mathematical Models in the Applied Sciences.* Published by Cambridge University Press, 1997.

[26] L.A. Segel and M. Slemrod, *The Quasi-steady-state assumption: a case study in perturbation.* SIAM review, Vol. 31, No. 3, pp. 446-477, September 1989.

[27] N.G. de Bruijn, *Asymptotic Methods in Analysis.* Published by North-Holland Publishing Co., Amsterdam, 1970.

[28] S. O'Brien, *Perturbation Techniques and Asymptotics.* Ref.No.:4933 (lecture notes) University of Limerick, Limerick, Ireland.

[29] W. Eckhaus, *Matched Asymptotic Expansions and Singular Perturbations.* Published by North-Holland Publishing Co., Amsterdam, 1973.

[30] S. Jones, B. Jumarhon, S. McKee and J.A. Scott, *A mathematical model of a biosensor.* Journal of Engineering Mathematics 30: 321-337, 1996.

[31] B. Jumarhon and S. McKee, *On the Heat Equation with Nonlinear and Nonlocal Boundary Conditions.* Journal of Mathematical Analysis and Applications 190, 806-820 (1995).

[32] R. A. Badley, R. A. L. Drake, I. A. Shanks, A. M. Smith and P. R. Stephenson, *Optical biosensors for immunoassays, the fluorescence capillary-fill device.* Philos. Trans. R. Soc. Lond. Ser. B 316 (1987), 143-160.

[33] L. Debnath, *Integral Transforms and Their Applications.* Published by Boca Raton: CRC Press, 1995.

[34] M.S. de Jesus Rebelo, *Analytical and Numerical Methods for Nonlinear Volterra Integral Equations with Weakly Singular Kernel.* Ph. D thesis.

[35] D. Mackey, A.J. Killard, A. Ambrosi, M.R. Smyth, *Optimizing the ratio of horseradish peroxidase and glucose oxidase on a bienzyme electrode: Comparison of a theoretical and experimental approach.* Sensors and Actuators B122(2007) 395-402.

[36] D. Mackey and A.J. Killard, *Optimising design parameters of enzyme-channelling biosensors.* Progress in Industrial Mathematics at ECMI 2006, pp. 853–857, Springer, R. Mattheij et al. (editors), 2008.

[37] A. Ambrosi, *The application of nanomaterials in electrochemical sensors and biosensors.* Ph D. thesis, Dublin City University, 2007.

[38] T.J. Kaper, *An introduction to geometric methods and dynamical systems theory for singular perturbation problems. In Analysing Multiscale Phenomena using Singular Perturbation Methods.* Proc. Sympos. Appl. Math., 56, R.E.O'Malley and J. Cronin, eds., 1999, pp. 85-131.

[39] N. Fenichel, *Geometric singular perturbation theory for ordinary differential equations.* J. Diff. Eq., 31 (1979), pp. 53-98.

[40] V.I. Arnol'd, *Ordinary Differential Equations.* Springer-Verlag Berlin Heidelberg, 1992.

[41] V. Sobolev and E. Shchepakina, *Explicit, Implicit and parametric invariant manifolds for model reduction in chemical kinetics.* IMA Preprint Series 2243.

[42] *www.math.pitt.edu/ bard/xpp/xpp.html*

[43] H. K. Khalil, *Nonlinear Systems.* Published by Prentice-Hall, 2002.

[44] H.L. Smith, *Monotone Dynamical Systems - An introduction to the Theory of Competitive and Cooperative Systems.* Published by American Mathematical Society, 1995.

[45] M.W. Hirsch, H.L. Smith, *Monotone Dynamical Systems.* In Handbook of Differential Equations, Ordinary Differential Equations (volume 2) eds, A.Canada, P.Drabek, A.Fonda, Elsevier, Amsterdam, 2005.

[46] Y. Liu, *Mathematical and computational modelling of biosensor: a modular approach.* Ph D. thesis, Dublin Institute of Technology, 2011.

[47] J.R. Cannon, *The One-Dimensional Heat Equation.* Menlo Park; Addison-Wesley, London, 1984.

[48] N. Burgess, J. Dixon, S. Jones, and M.L. Thoma, *A Reaction-Diffusion Study of a Small Cell.* UCINA Report No. 86/2, Oxford University, 1986.

[49] D. Voet, J.G. Voet and C.W. Pratt, *Fundamentals of Biochemistry life at the molecular level.* Hoboken, N.J. Wiley; Chichester: John Wiley [distributor], 2006.

[50] A.G. Marangoni, *Enzyme kinetics: A modern approach.* Published by Hoboken, N.J.: Wiley-Interscience, 2003.

[51] M.W. Hirsch, S. Smale, R.L. Devaney, *Differential Equations, Dynamical Systems and An Introduction to Chaos.* San Diego, CA: Academic Press, 2004.

[52] A.J. Killard, S. Zhang, H. Zhao, R. John, E.I. Iwuoha, M.R. Smyth, *Development of an electrochemical flow-injection immunoassay (FIIA) for the real-time monitoring of biospecific interactions.* Anal. Chim. Acta 400 (1999) 109-119.

Appendix A

$$\begin{cases} 1 - B = \dfrac{k_1 el}{D_1}\left(\dfrac{\zeta}{1+\zeta} - c_1^*\right) B - \dfrac{k_{-1} el}{D_1 s_0} c_1^* & \text{(A.1a)} \\ -D = \dfrac{k_3 el}{D_2}\left(\dfrac{1}{1+\zeta} - c_2^*\right) D - \dfrac{k_2 el}{D_2 s_0} c_1^* - \dfrac{k_{-3} el}{D_2 s_0} c_2^* & \text{(A.1b)} \\ 0 = \left(\dfrac{\zeta}{1+\zeta} - c_1^*\right) B - \dfrac{K_m^1}{s_0} c_1^* & \text{(A.1c)} \\ 0 = \dfrac{k_3}{k_1}\left(\dfrac{1}{1+\zeta} - c_2^*\right) D - \dfrac{k_4 + k_{-3}}{k_1 s_0} c_2^*. & \text{(A.1d)} \end{cases}$$

Equation (A.1c) can be simplified in terms of B as

$$B = \frac{K_m^1 c_1^*}{\frac{\zeta}{1+\zeta} - c_1^*}, \tag{A.2}$$

then substitute (A.2) into (A.1a), we obtain

$$(c_1^*)^2 - \left(\frac{D_1 s_0}{k_2 el} + \frac{D_1 K_m^1}{k_2 el} + \frac{\zeta}{1+\zeta}\right) c_1^* + \frac{D_1 s_0}{k_2 el} \cdot \frac{\zeta}{1+\zeta} = 0. \tag{A.3}$$

Similarly, equation (A.1d) can be written in terms of D as

$$D = \frac{K_m^2 c_2^*}{\frac{1}{1+\zeta} - c_1^*}, \tag{A.4}$$

then substitute (A.4) into (A.1b), we obtain

$$(c_2^*)^2 - \left(\frac{k_2 c_1^*}{k_4} + \frac{D_2 K_m^2}{k_4 el} + \frac{1}{1+\zeta}\right) c_2^* + \frac{k_2 c_1^*}{k_4} \cdot \frac{1}{1+\zeta} = 0. \tag{A.5}$$

Hence, the system of four equations with four unknowns B, D, c_1^* and c_2^* has been reduced to the following system of two equations in term of c_1^* and c_2^*, where c_1^*, c_2^* are positive and denote the equilibrium values of $c_1(t)$, $c_2(t)$ respectively.

$$\begin{cases} (c_1^*)^2 - \left(\dfrac{D_1 s_0}{k_2 el} + \dfrac{D_1 K_m^1}{k_2 el} + \dfrac{\zeta}{1+\zeta}\right) c_1^* + \dfrac{D_1 s_0}{k_2 el} \cdot \dfrac{\zeta}{1+\zeta} = 0 & \text{(A.6a)} \\ (c_2^*)^2 - \left(\dfrac{k_2 c_1^*}{k_4} + \dfrac{D_2 K_m^2}{k_4 el} + \dfrac{1}{1+\zeta}\right) c_2^* + \dfrac{k_2 c_1^*}{k_4} \cdot \dfrac{1}{1+\zeta} = 0. & \text{(A.6b)} \end{cases}$$

System (A.6) can be easily solved to give the following explicit formulas for c_1^* and c_2^*:

$$c_1^* = \frac{\left(\frac{D_1 s_0}{k_2 el} + \frac{D_1 K_m^1}{k_2 el} + \frac{\zeta}{1+\zeta}\right) \pm \sqrt{\left(\frac{D_1 s_0}{k_2 el} + \frac{D_1 K_m^1}{k_2 el} + \frac{\zeta}{1+\zeta}\right)^2 - \frac{4 D_1 s_0}{k_2 el} \cdot \frac{\zeta}{1+\zeta}}}{2} \qquad \text{(A.7)}$$

$$c_2^* = \frac{\left(\frac{k_2 c_1^*}{k_4} + \frac{D_2 K_m^2}{k_4 el} + \frac{1}{1+\zeta}\right) \pm \sqrt{\left(\frac{k_2 c_1^*}{k_4} + \frac{D_2 K_m^2}{k_4 el} + \frac{1}{1+\zeta}\right)^2 - \frac{4 k_2 c_1^*}{k_4} \cdot \frac{1}{1+\zeta}}}{2}. \qquad \text{(A.8)}$$